Dissertation

Resource Management in Heterogeneous Computing Systems with Tasks of Varying Importance

Submitted by

Bhavesh Khemka

Department of Electrical and Computer Engineering

In partial fulfillment of the requirements

For the Degree of Doctor of Philosophy

Colorado State University

Fort Collins, Colorado

Summer 2014

Doctoral Committee:

Advisor: Anthony A. Maciejewski
Co-Advisor: H. J. Siegel

Sudeep Pasricha
Gregory A. Koenig
Patrick J. Burns

Abstract

Resource Management in Heterogeneous Computing Systems with Tasks of Varying Importance

The problem of efficiently assigning tasks to machines in heterogeneous computing environments where different tasks can have different levels of importance (or value) to the computing system is a challenging one. The goal of this work is to study this problem in a variety of environments. One part of the study considers a computing system and its corresponding workload based on the expectations for future environments of Department of Energy and Department of Defense interest. We design heuristics to maximize a performance metric created using utility functions. We also create a framework to analyze the trade-offs between performance and energy consumption. We design techniques to maximize performance in a dynamic environment that has a constraint on the energy consumption. Another part of the study explores environments that have uncertainty in the availability of the compute resources. For this part, we design heuristics and compare their performance in different types of environments.

Acknowledgements

This dissertation has been made possible by the efforts and support of many people. First and foremost, I would like to thank my advisors: Dr. Anthony A. Maciejewski and Dr. Howard J. Siegel for taking the enormous time and energy to impart an abundance of valuable lessons over countless meetings these past five years. Their knowledge, desire for perfection, patience, attention to detail, sense of humor, and wisdom have led to an amazing learning experience. I cannot thank them enough and I will always be grateful to them. I would also like to thank Dr. Sudeep Pasricha for his guidance and inputs. His constant push to model real systems as closely as possible has helped shape and direct many parts of the different research projects. Dr. Gregory A. Koenig, who has been the lead for all the research projects that were done in collaboration with Oak Ridge National Laboratory (ORNL) and the U.S. Department of Defense (DoD), has always been a caring and supportive mentor (including during my internship at ORNL). His readiness to teach and to foster my growth has been very motivating and I will always be thankful to him for that. I would like to thank Dr. Patrick Burns for critiquing this work, providing constructive feedback, and for serving on my committee.

I would like to thank the organizations that funded the different research projects of this dissertation. Without their support and resources, the research would not have been possible. Parts of the research in this dissertation were supported by the Colorado State University George T. Abell Endowment and the National Science Foundation under grant number CNS-0905339. Parts of the research in this dissertation used resources of the National Center for Computational Sciences at ORNL, supported by the Extreme Scale Systems Center at ORNL, which is supported by DoD under subcontract numbers 4000094858 and 4000108022.

Some parts of the research also used the CSU ISTeC Cray System supported by National Science Foundation under grant number CNS-0923386.

I would like to thank our collaborators at ORNL and DoD: Chris Groer, Marcia Hilton, Gene Okonski, Steve Poole, Sarah Powers, Jendra Rambharos, and Mike Wright, for their patience and willingness to have teleconference calls on a weekly basis during the past four years. Their inputs based on hands-on experience of how schedulers work in the real world has been invaluable in guiding the research. It truly has been a unique learning experience.

I am thankful to my teammate and friend, Ryan Friese, for the innumerable discussions, long brainstorming sessions, collaborative writing and code development, laughter, and last minute favors. It has been an absolute delight to work with him.

My sincere thanks to the members of the robust computing research group at CSU: Abdulla Al-Qawasmeh, Mohsen Amini, Jonathan Apodaca, Luis D. Briceño, Daniel Dauwe, Tim Hansen, Eric Jonardi, Paul Maxwell, Mark Oxley, Greg Pfister, Jerry Potter, Jay Smith, Kyle Tarplee, and Dalton Young, for their insightful and helpful suggestions and feedback regarding not only the research but also the presentation of the material throughout my Ph.D.

Many research projects in this dissertation used the CSU ISTeC Cray System for running the simulation experiments. I would like to extend thanks to the system administrators: Dr. Richard Casey, Wimroy D'Souza, and Daniel Hamp for their assistance and quick response. With their help I was able to finish my experiments sooner, and as a result perform more extensive tests and still get results in a timely manner.

I am deeply indebted to my parents, Mahesh Khemka and Kiran Khemka, for their undying love and constant support throughout my life. Their care and wisdom are beyond compare. Even though they were away during my Ph.D., memories of their support and

care kept me going: the nutritious foods in the wee hours of the morning, the many wise advices, their forward-thinking mentality always looking out for me, and the freedom and encouragement to let me pursue whatever I want. I am truly blessed to have such wonderful parents. I also want to thank my extremely caring sisters: Ritu Kedia, Raksha Rajdev, and Rakhee Divakaran for their perennial support. They have always shown me the humor in places where I see none.

Priya Naik and Karthik Kadappan have been much more than friends to me in these past five years. They have been with me through all the lowest lows with their genuine concern and encouragement and during the highs to celebrate the moment in an ever-more grander fashion. My heart-felt thanks to them for being patient and understanding with me and for their heart-warming love and support.

I would like to thank Saket Doshi and Gaurav Madiwale for all the help, for always being there, for so many fun memories, and for just being the great people they are. I am also very thankful for all the amazing friends at the Indian Students Association at CSU. My experience here would be incomplete and not as lively without them.

In closing, I would like to thank my Guru who has made everything possible, including this wonderful experience to learn and to grow. I cannot thank him enough for his guidance, blessings, patience, encouragement, love, and support.

This dissertation is typset in LaTeX using a document class designed by Leif Anderson.

DEDICATION

To the most nurturing and enlightened parents that ever lived

Table of Contents

List of Tables

List of Figures

CHAPTER 1

Introduction and Overview

High-performance computing (HPC), high-throughput computing, and many-task computing are currently used to solve a host of problems. These environments may be heterogeneous and oversubscribed. By heterogeneous we mean that different tasks may have varied execution times on the different machines. By oversubscribed we mean that the workload of tasks is large enough such that the total offered work exceeds the capacity of the system in steady state operation (or over an extended period). The process of allocating tasks to machines for execution is often referred to in the literature as "resource allocation" or "mapping," and the process of ordering the tasks' execution is referred to as "scheduling." The mapping and scheduling problem has been known, in general, to be NP-Complete [1], and therefore heuristics are commonly used to find a solution to this problem. Performing resource management in oversubscribed heterogeneous environments further complicates the problem.

In many scenarios, different tasks are of different "importance" to the enterprise computing system. In such environments, it becomes beneficial to account for the differences in the values of different tasks to make resource allocation decisions. This is particularly important in oversubscribed heterogeneous computing environments. In this dissertation, we design and analyze techniques to perform mapping and scheduling decisions in computing environments that have tasks with different "reward" or "utility" values.

In Chapter 2, we design utility functions to create a performance metric for schedulers in a dynamic oversubscribed heterogeneous computing environment. We model a computing system and its intended workload based on the expectations for future environments of

Department of Energy and Department of Defense interest. We design twelve heuristics and compare their performance. We also create additional operations to assist the heuristics in making mapping decisions. We analyze the performance of the heuristics under two different levels of oversubscription.

During 2010, global HPC systems accounted for 1.5% of total electricity use, while in the U.S., HPC systems accounted for 2.2% [2]. With the rising demand and costs of energy it becomes extremely important to make scheduling decisions in an energy-efficient manner. Chapter 3 explores the bi-objective problem of maximizing performance and minimizing energy consumption. The goal is to create a Pareto front of solutions from which the system administrator can pick a point to operate by analyzing the trade-offs between performance and energy consumption. Chapter 4 deals with energy-constrained utility maximization. We design an energy filtering technique that helps heuristics avoid mapping decisions that can lead to high energy consumption. Possible extensions for both of these works are mentioned in Chapter 6.

In many large-scale distributed computing environments, it is common for failures to randomly occur in the compute resources. These effects are estimated to worsen as we approach exa-scale. Making resource allocation decisions while being aware of such failures further complicates the scheduling problem. In Chapter 5, we explore this problem by studying and comparing the performance of different heuristics in a variety of environments. Directions for future work of this study are detailed in Chapter 6.

CHAPTER 2

Utility Functions and Resource Management[1]

2.1. Introduction

A utility function for a task describes the value of completing the execution of the task at a specific time [5–9]. Utility functions capture the time-varying importance of a task to both the user and the enterprise as a whole. In this work, the value of completing a task decays over time and so we model monotonically-decreasing utility functions. The design of utility functions needs to be flexible to capture the importance of tasks within a diverse user base. In practice, utility functions may be created through a collaboration between the user and the owner of the computing system. We design dynamic resource management techniques to maximize the total utility that can be earned by completing tasks in an oversubscribed heterogeneous distributed environment. By oversubscribed we mean that the workload is large enough that the total desired work exceeds the capacity of the system in steady state operation, i.e., over an extended period. By a heterogeneous environment we mean that the execution time of each task may vary across the suite of machines. We model this computing environment and the workload of tasks that arrive dynamically. A scheduler makes resource allocation decisions to map (assign) the incoming tasks to the machines. The total utility earned from all completed tasks captures how much useful work was done and how timely that information was to the user. The system characteristics and the workload parameters are based on environments being investigated by the Extreme Scale Systems Center (ESSC) at

[1]This work was done jointly with the Ph.D. students Luis D. Briceno and Ryan Friese. The full list of co-authors is at [3]. A preliminary version of portions of the work mentioned in this chapter appeared in [4]. This research used resources of the National Center for Computational Sciences at Oak Ridge National Laboratory, supported by the Extreme Scale Systems Center at ORNL, which is supported by the Department of Defense under subcontract numbers 4000094858 and 4000108022. This research also used the CSU ISTeC Cray System supported by NSF Grant CNS-0923386.

Oak Ridge National Laboratory (ORNL). The ESSC is part of a collaborative effort between the Department of Energy (DOE) and the Department of Defense (DoD) to perform research and deliver tools, software, and technologies that can be integrated, deployed, and used in both DOE and DoD environments.

We design a method that can be used to create utility functions by defining three parameters: priority, urgency, and utility class. The priority of a task represents the level of importance of a task to the enterprise, while urgency indicates how quickly the task loses utility. The utility class provides finer control of the shape of the utility function by partitioning it into intervals. We assume that the scheduler has experiential information about the execution time of each type of task on each type of machine. However, the scheduler does not know the arrival time, utility function, or type of each task until the task arrives.

We use two forms of dynamic heuristics to perform the resource allocation decisions. Immediate-mode heuristics schedule only the incoming task and do not have the opportunity to re-map tasks that are already in machine queues (e.g., [10–12]). Batch-mode heuristics consider a set of tasks and have the ability to re-map tasks that are enqueued and waiting to execute (e.g., [10, 11]). We create seven immediate-mode and five batch-mode heuristics, and analyze their performance using simulation experiments. To examine the effect of oversubscription on the performance of the heuristics, we simulate two levels of oversubscription. We also study the effect of heuristic variations, such as dropping tasks and altering the mapping decision frequency for the batch-scheduler.

The contributions of this chapter are: (a) a model of the planned DOE/DoD oversubscribed heterogeneous high performance computing environment, (b) the design of a metric using utility functions, based on the three parameters of priority, urgency, and utility class, to measure the performance of schedulers in an oversubscribed heterogeneous computing

environment, (c) the design of twelve heuristics to perform the scheduling operations and their evaluation over a variety of environments, and (d) the exploration and the analysis of heuristic variations, such as dropping tasks and varying the number of tasks scheduled at each batch-mode mapping event.

The remainder of the chapter is organized as follows. In Sec. 2.2, we explain our system model, including our method to design the utility functions (from the three parameters mentioned before), the characteristics of the workload, and the characteristics of the computing environment. We formally give our problem statement in Sec. 2.3, and introduce our metric to compare the performance of resource allocation heuristics. In Sec. 2.4, we describe the various heuristics we have designed and the method to drop tasks. We compare our study to other work from the literature in Sec. 2.5. We explore the design of our simulation experiments in Sec. 2.6. In Sec. 2.7, we present and analyze our simulation results. Finally, we conclude the chapter and discuss possible future directions in Sec. 2.8.

2.2. System Model

2.2.1. Utility Functions.

2.2.1.1. *Overview.* In our study, it is assumed that an enterprise computing system earns a certain amount of utility for completing each task. The amount of utility earned depends on the task and the time at which the task was completed relative to the time it arrived, and reflects its importance to the system. We use utility functions to model the time-varying benefit of completing the execution of a task. The utility functions we model are monotonically decreasing. This implies that if a task takes longer to complete, it cannot earn higher utility. We understand that there may be use cases for non-monotonically-decreasing utility functions, but they are not considered here. We design a flexible utility function for a

task that is defined by three parameters: priority, urgency, and utility class. The goal is to use a small set of parameters that the users understand and enables the users to obtain the desired utility curve. By using a combination of these parameters we can create a variety of shapes for the utility functions. These parameters were designed based on the needs of the ESSC at ORNL. We expect that these parameters will be set by the customer (submitting the job) in collaboration with the system owner and the overall system administration policies.

2.2.1.2. *Parameters.*

Priority. Priority represents the importance of the task to the organization. It sets the maximum value of a utility function. As the functions are monotonically decreasing, this is equivalent to the starting value of the utility function. Let $\pi(p)$ be the maximum utility of tasks belonging to priority level p, where $p \in \{critical, high, medium, low\}$. Each of these priority levels has a fixed value of maximum utility associated with it. Fig. 2.1a shows utility functions with different levels of priority for a fixed level of urgency (defined below). As shown in Fig. 2.1a, a task's utility does not begin to decay as soon as it arrives, because this would make the maximum utility value of a task unachievable (i.e., the task needs non-zero time to execute). In Sec. 2.6.2, we describe how we determine the length of this interval.

Urgency. The urgency of a task models the rate of decay of the utility of that task over time. It affects the "shape" of the utility function. Tasks that are more urgent will have their utility values decrease at a faster rate than less urgent tasks. In this study, we model the decay of utilities as an exponential (other functions may be used). Let $\rho(r)$ be the exponential decay rate of tasks belonging to urgency level r, where $r \in \{extreme, high, medium, low\}$. Fig. 2.1b illustrates utility functions with different urgency levels for a fixed priority level.

The urgency level of a task along with the task's average execution time control the duration for which the starting utility value of a task does not decay (see Sec. 2.6.2).

Utility Class. A utility class is used to fine-tune a utility function by dividing the function into a set of intervals with discrete characteristics. We define each interval (except the first) to have three parameters: a start time, a percentage of maximum utility at that start time, and an exponential decay rate modifier. By defining different utility classes we can devise a wide variety of utility functions. We could set a hard deadline for a task by having the utility of the task drop to zero. For our simulations, we created four utility classes and each task belongs to one of these four classes (the number of utility classes can be domain dependent).

The first element within a utility class is the set of time intervals that partition the time axis of the utility function (except the end time of the first interval). Let $t(k, c)$ be the start time of the k^{th} interval relative to the arrival time of a task belonging to utility class c.

The second element in a utility class sets the percentage of the maximum utility at the start of each of the intervals except the first. Let $\psi(k, c)$ be this percentage for the k^{th} interval, where $0 \leq \psi(k, c) \leq 1$ and $\psi(k, c) \leq \psi(k-1, c)$ for $k > 1$. Therefore, the maximum utility value in the k^{th} interval of a utility function for a task with a priority level p and utility class c is given by, $\Psi(k, c, p) = \psi(k, c) \times \pi(p)$.

The final element in a utility class c is a modifier, $\delta(k, c)$, to the exponential decay rate of the interval k, with $k > 1$ to ignore the first interval. The exponential decay rate in interval k of a utility function with urgency level r and utility class c is given by, $\Delta(k, c, r) = \delta(k, c) \times \rho(r)$. The values of this modifier are typically near 1, because the purpose of this modifier is to provide small differences in the decay rate across the intervals.

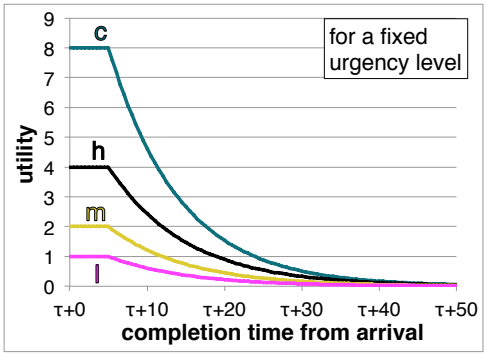

(A)

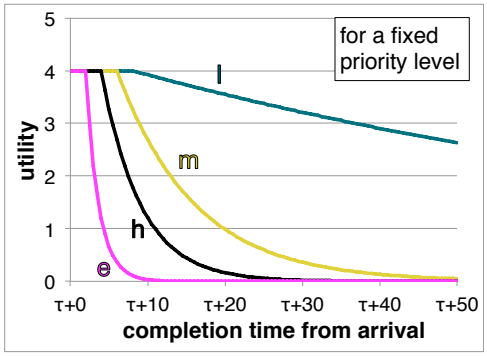

(B)

FIGURE 2.1. (a) Four utility functions with different priority levels and a fixed urgency level showing the decay in utility for a task after its arrival time τ. The curves labeled "c," "h," "m," and "l" are the curves with *critical*, *high*, *medium*, and *low* priorities, respectively. (b) Four utility functions with different urgency levels and a fixed priority level showing the decay in utility for a task after its arrival time τ. The curves labeled "e," "h," "m," and "l" are the curves with *extreme*, *high*, *medium*, and *low* urgency levels, respectively. The length of time for which the starting utility value of a task persists (does not decay) is shorter for more urgent tasks.

Fig. 2.2 shows a utility function (at a fixed priority and urgency level) partitioned into separate intervals, each with its own rate of decay and starting utility value. The last interval shows that the utility drops to zero as time tends to infinity.

2.2.1.3. *Construction of a Utility Function.* Let p be the priority level, r the urgency level, and c the utility class of a task i. The utility value $U(p, r, c, t)$ at any time t relative to the arrival time of the task, where $t(k, c) \leq t < t(k+1, c)$, is given by the following equation:

$$U(p, r, c, t) = (\Psi(k, c, p) - \Psi(k+1, c, p)) \times e^{-\Delta(k,c,r)\cdot(t-t(k,c))} + \Psi(k+1, c, p). \quad (1)$$

2.2.2. MODEL OF ENVIRONMENT. We group tasks with similar computational requirements into task types and machines with similar performance capabilities into machine types. We model a heterogeneous environment, where the execution times of different task types may vary across the different machine types. We assume we are given an Estimated Time to

Compute (ETC) matrix, where $ETC(i,j)$ is the estimated time to compute a task of type i on a machine of type j. This is a common assumption in the resource management literature [13–18]. For simulation purposes, we use a synthetic workload as described in Sec. 2.6.3, but in practice, one could use historical data to obtain such information [15, 17]. We model special-purpose and general-purpose machines. The special-purpose machine types have the ability to execute certain task types much faster than the general-purpose machine types, but may be incapable of executing other task types. Further details are in Sec. 2.6.3.

We model a dynamic environment where tasks arrive throughout a 24 hour period. The scheduler does not know the arrival time, utility function, or type of each task until the task arrives. The system is composed of dedicated compute resources with a workload large enough to create an oversubscribed environment. We assume that the tasks in the workload are independent (no inter-task communication is required) and serial (each task executes on a single machine). For scheduling purposes we do not consider the pre-emption of tasks. We do, however, allow tasks to be dropped prior to execution (see Sec. 2.4.4).

2.3. Problem Statement

Our goal is to design resource management techniques to maximize the overall system utility achieved in an oversubscribed heterogeneous environment. To solve this problem, we devise twelve heuristics to perform the scheduling operations and design a metric using utility functions to measure the performance of schedulers. Once a task arrives, we can calculate the completion time of the task based on the resource to which it is mapped. Using the completion time of task i, denoted $t_{completion}(i)$, and the task's utility function parameters (namely, $p(i), r(i)$, and $c(i)$), the utility earned by the task can be calculated using Equation 1 to obtain $U(p(i), r(i), c(i), t_{completion}(i))$. Let $\Omega(t_{end})$ be the set of tasks that have completed

execution by time t_{end}. The goal of our resource management procedures is to maximize the total utility that can be earned by the system over the 24 hour period and is computed using:

$$U_{system}(t_{end}) = \sum_{i \in \Omega(t_{end})} U(p(i), r(i), c(i), t_{completion}(i)). \quad (2)$$

2.4. Resource Management Policies

2.4.1. Overview. The scheduling problem, in general, has been shown to be NP-complete [1], and therefore it is common to use heuristics to solve this problem. Any time when a decision has to be made to assign a task to a machine we call a mapping event. The two types of dynamic heuristics (also known as online heuristics [19]) we use, immediate-mode heuristics and batch-mode heuristics, differ in the method that a mapping event is triggered and in the set of tasks that can be scheduled during a mapping event.

In immediate-mode heuristics, a mapping event occurs when a task arrives. The only exception to this is when the execution of the previous mapping event has not finished before the arrival of the next task. In that case, the trigger time for the next mapping event is delayed until the previous mapping event finishes execution. The immediate-mode heuristics assign the new task to some machine queue. Once the task is put in the machine queue it cannot be remapped. We design and evaluate seven immediate-mode heuristics.

In batch-mode heuristics, typically mapping events are triggered after fixed time intervals or a fixed number of task arrivals. If the previous mapping event has not completed execution, the trigger time of the next mapping event is delayed until the previous mapping event finishes execution. We refer to the task that is next in-line for execution on a machine queue as a pending task. We refer to the part of the machine queues that do not include the executing and the pending tasks as the virtual queues of the scheduler. Fig. 2.3 shows tasks

waiting in the virtual queues of an example system with four machines. The batch-mode heuristics make mapping decisions for both the tasks that have arrived since the last mapping event and the tasks that are waiting in the virtual queues. This set of tasks is the called the mappable tasks. The batch-mode heuristics (unlike immediate-mode heuristics) have the capability to re-map tasks in the virtual queues of scheduler. The batch-mode heuristics do not re-map pending tasks so the machine does not become idle when its executing task completes. The simulation results in Sec. 2.7 show that the batch-mode heuristics have a significant advantage because they have more information available while making a mapping decision (as they consider a set of tasks). Furthermore they can alter those decisions in the future by remapping tasks when additional information becomes available. We design and evaluate five batch-mode heuristics.

2.4.2. Immediate-mode Heuristics.

2.4.2.1. *Naive Immediate-mode Heuristics.* The first two immediate-mode heuristics do not consider the execution time estimates of different task types on machine types, nor the ready-times of the machines (the times that the machines finish execution of their already queued tasks). These heuristics are used as baseline heuristics for comparison purposes. We refer to these heuristics as the naive immediate-mode heuristics.

The Random heuristic assigns the newly arrived task to a random machine on which it can execute (i.e., not a special-purpose machine where it cannot execute). The Round-Robin heuristic assigns the incoming tasks in a round-robin fashion. The machines are listed in a randomized order and this ordering is kept fixed. The first task that arrives for a mapping event is assigned to the first machine (on which it can execute), the next incoming task is assigned to the next machine (on which it can execute), and so on.

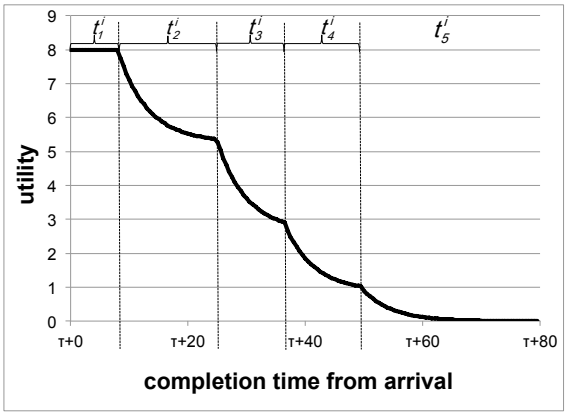

FIGURE 2.2. Utility function for a fixed priority level, urgency level, and utility class, showing the decay in utility for a task after its arrival time τ. The t^is represent the duration of the different intervals in the utility class of task i. The last interval extends to infinity.

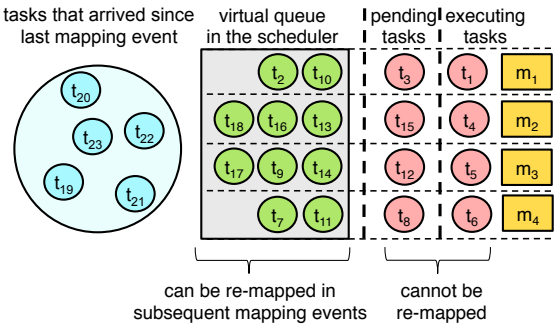

FIGURE 2.3. Machine queues of a sample system with four machines. The tasks in the executing and pending slots are not eligible to be re-mapped, whereas the tasks in the virtual queue section of the machine queues can be re-mapped. This only applies to the batch-mode heuristics.

2.4.2.2. *Smart Immdediate-mode Heuristics.* We refer to the next five heuristics as the smart immediate-mode heuristics. The results in Sec. 2.7 show that these heuristics perform better than the naive immediate-mode heuristics.

The Maximum Utility (Max Util) heuristic is based on the Minimum Completion Time heuristic from the literature [20, 21, 11, 22, 23]. The heuristic assigns a newly arrived task to the machine that would complete it soonest. We model monotonically-decreasing utility functions and, thus, the machine that completes the task the earliest is also the machine that earns the highest utility from the task. This heuristic accounts not only for the execution time of the task on machines, but also the ready-time of the machines.

The Maximum Utility-Per-Time (Max UPT) heuristic computes the utility a newly arrived task can earn on each machine divided by its execution time on that machine. It

then assigns the task to the machine that maximizes "utility earned / execution time." The reasoning behind this is to earn highest utility per time in an oversubscribed system.

We design two heuristics based on the Minimum Execution Time (MET) heuristic [20, 21, 11]. The Minimum Execution Time-Random (MET-Random) heuristic first finds the set of machines that belong to the machine type that can *execute* the newly-arrived task the fastest (ignoring machine ready time). Among those machines, it assigns the task to a random machine. The Minimum Execution Time-Max Util (MET-Max Util) heuristic also finds the set of machines belonging to the minimum *execution* time machine type for the newly arrived task, but picks the machine among them that minimizes *completion* time (which also maximizes utility).

The K-Best Types heuristic is based on the K-Percent Best heuristic, introduced in [11] and used in [24, 21, 25, 26]. The idea is to try combining the benefits of the MET heuristic and the Max Util heuristic. The K-Best Types heuristic first finds the K-best machine types that have the lowest *execution* times for the current task. Among the machines of these machine types, it then picks the machine that minimizes *completion* time (which also maximizes utility). By using different values of K, we can control the extent to which the heuristic is biased towards MET-Max Util or Max Util. We empirically determine the best value of K.

2.4.3. Batch-mode Heuristics. The Min-Min Completion Time (Min-Min Comp) heuristic is based on the concept of the two-stage Min-Min heuristic that has been widely used (e.g., [21, 27, 25, 26, 28, 10, 11, 29, 22, 23, 30]). In the first stage, the heuristic independently finds for each mappable task the machine that can complete it the soonest. In the second stage, the heuristic picks from all the task-machine pairs (of the first stage) the pair that has the earliest completion time. The heuristic assigns the task to that machine,

removes that task from the set of mappable tasks, updates the ready-time of that machine, and repeats this process iteratively until all tasks are mapped. This batch-mode heuristic is computationally efficient because it explicitly does not perform any utility calculations.

The Sufferage heuristic concept introduced in [11] and used in, for example, [31, 32, 27, 28, 25, 10, 22], attempts to assign tasks to their maximum utility machine. Ties are broken in favor of the tasks that would "suffer" the most if they did not get their maximum utility machine. In the first stage, the heuristic calculates for each mappable task a sufferage value, i.e., the difference between the best and the second-best utility values that the task could possibly earn. In the second stage, tasks are assigned to their maximum utility machines. If multiple tasks request the same machine, then the task that has the highest sufferage value is assigned to that machine. Assigned tasks are removed from the mappable tasks set, ready-times of machines updated, and the process repeated until all tasks are mapped.

The Max-Max Utility (Max-Max Util) heuristic is also a two-stage heuristic, like the Min-Min Comp heuristic. The difference is that in each stage Max-Max Util maximizes utility, as opposed to minimizing completion time. In the first stage, this heuristic finds task-machine pairs that are identical to those found in the first stage of the Min-Min Comp heuristic, because of the monotonically-decreasing utility functions. In the second stage, the decisions made by Max-Max Util may differ from those of Min-Min Comp. This is because in the second stage, the Max-Max Util heuristic picks the maximum utility choice among the different task-machine pairs, and the utility earned depends both on the completion time and the task's specific utility function.

The Max-Max Utility-Per-Time (Max-Max UPT) heuristic is similar to the Max-Max Util heuristic. The difference being that in each stage Max-Max UPT maximizes "utility earned / execution time," as opposed to maximizing utility. As mentioned before, this

heuristic attempts to maximize utility earned by a task while minimizing the time it uses computational resources. Completing tasks sooner is helpful in an oversubscribed system.

The MET-Max Util-Max UPT heuristic is similar to the Max-Max UPT heuristic with a difference in the first stage. In the first stage, this heuristic pairs each task with the minimum completion time machine among the machines that belong to its minimum execution time machine type. Therefore, for a task, this batch-mode heuristic performs utility calculations only for a subset of the machines (i.e., those machines that belong to the machine type that executes this task the fastest).

2.4.4. Dropping Low-Utility Tasks. In an oversubscribed environment, it is not possible to earn significant utility from all tasks. We introduce the ability to drop low-utility earning tasks while making mapping decisions. Dropping a task means that it will never be mapped to any machine (unless the user resubmits it). The motivation for doing this is to reduce the wait times (i.e., increase the achieved utility) of the other (higher-utility earning) tasks that are queued in the system. In practice, we expect that policy decisions will determine the extent to which this technique is applied, and that it will only be used in extreme situations. The extent of dropping is a tunable parameter that can be varied based on the system oversubscription level. The goal is to drop tasks that would earn less utility than a pre-set threshold, referred to as the dropping threshold. In this study, for each simulation, the dropping threshold is fixed at a particular value. The model can be extended to have a dropping threshold that varies based on the current or expected system load. We use different methods to drop tasks in the immediate-mode and the batch-mode heuristics.

For the immediate-mode heuristics, the decision to drop a task is made after the heuristic determines the machine queue in which to map the task. We can compute the completion time of the task on this machine and the utility that this task will earn. If the utility earned

by this task is less than the dropping threshold, we do not assign the task to the machine, and drop it from any further consideration. If the utility earned is greater than or equal to the dropping threshold, the task is placed on the machine queue as decided by the heuristic.

For the batch-mode heuristics, the decision to drop a task requires more computation because of the possibility of the task being remapped to another machine in a subsequent mapping event. Before calling the heuristic, for each mappable task, we determine the maximum possible utility that the task could earn on any machine assuming it could start execution immediately after the pending task. If this utility is less than the dropping threshold, we drop this task from the set of mappable tasks. If it is not less than the threshold, the task continues to stay in the set of mappable tasks and the batch-mode heuristic performs its allocation decisions.

In addition to the dropping operation, for the batch-mode heuristics, we implement a technique to permute tasks that are at the head of the virtual queues of the machines, but this did not improve performance. This technique is described in App. A.

2.5. Related Work

Numerous studies have proposed heuristics to solve the problem of performing resource management in dynamic heterogeneous computing environments (e.g., [26, 25, 10, 11]). Few of them, however, optimize for the total utility that the system earns. In a survey of utility function based resource management [6], the authors point out that in an oversubscribed system it is preferable to use utility accrual algorithms for performing scheduling decisions because these have the ability to pick and execute tasks that are more important to the system (earn high utility). Additional research explores developing a framework for measuring the productivity of supercomputers [33]. They propose a metric for productivity that

is the ratio of the utility earned by completing a task to the cost of doing this operation. Possible shapes for the utility-time and the cost-time curves of a task are discussed. The authors also mention the possible interpretations of "utility" and "cost." Similar to our work, they consider only monotonically-decreasing utility-time functions. Our work enhances this by parameterizing the shape of the utility functions and designing resource management techniques to maximize the aggregate utility.

Value functions (similar to utility functions) are used in systems with processes running on symmetric, shared-memory multi-processors (SMP) with one to four processing elements [5]. Each process has a value function associated with it that specifies the value earned by the system depending on when it completes execution of that process. The scheduler can consider the arrival times of tasks to make current scheduling decisions. Moreover, the processes can be periodic. This is in contrast to our model where the scheduler has no prior knowledge of the arrival time of the tasks. The paper presents two algorithms that make decisions based on value density (value divided by processing time) and shows that these algorithms perform better than scheduling algorithms that consider either only deadlines or only execution times (ignoring the utility earned). This is similar to some of our heuristics that use utility-per-time. Unlike our environment, they consider homogeneous processing elements. Other systems using similar value functions have also been examined [34, 35].

Kim et al. define tasks with three soft deadlines [25]. The actual completion time of the task is compared to the soft deadlines to obtain a deadline factor. The deadline factor is multiplied with the priority of a task to calculate the actual "value" that is earned for completing the task. Dynamic heuristics are used to maximize the total value that can be earned by mapping the tasks to machines. Although tasks can have different priorities, the degradation curve for the value of a task is always a step-curve with the steps occurring at

the soft deadlines. In our model, each task can have its own utility function shape and the utility decays exponentially. Also, we model special-purpose machine and task types, have different arrival patterns for the different kinds of tasks, and experiment with dropping low utility-earning tasks in our oversubscribed system.

The concepts of utility functions have been used in real-time systems for scheduling tasks [7, 8]. The problem of scheduling non-preemptive and mutually independent tasks on a single processor has been examined [7]. In that study, each task has a time value function that gives the task's contribution at its completion time. The goal is to order the execution of the tasks on the single processor to maximize the cumulative contribution from the tasks. Analytical methods have been used to create performance features and optimize them [8]. In that study, all jobs have the same shape for their utility functions, as opposed to our study where every task can have a different shape for its utility function. Although these papers address the maximization of total utility earned, the environment of a single processor versus our environment of a heterogeneous distributed system makes solution techniques significantly different for the two cases.

In [9], the users of a homogeneous high performance computing system can draw arbitrary shapes for utility functions for the jobs they submit. The users decide the level of accuracy in modeling the utility functions. The work in [9] uses a genetic algorithm to solve the problem of maximizing utility. The average execution time of the algorithm is 8,900 seconds. In our study, scheduling decisions are made at much smaller intervals (after a minute in the case of the batch-mode heuristics). Furthermore, we assume a heterogeneous computing system, as opposed to the homogeneous computing system that they model.

2.6. Simulation Setup

2.6.1. Overview. In this study, we simulate a heterogeneous computing environment where a workload of tasks arrive dynamically. To model the execution time characteristics of the workload, we use an Estimated Time to Compute (ETC) matrix (as described in Sec. 2.2.2). To completely describe the workload, we need to determine each task's utility function parameters, task type, and arrival time. In this section, we explain how we generate these parameters for our simulations *based on the expectations for future environments of DOE and DoD interest*.

Each experiment discussed in Sec. 2.7 has its results averaged over 50 simulation trials. Each trial has a new workload of tasks (with different utility functions, task types, and arrival times). Each trial also models a different compute environment by using different values for the entries of the ETC matrix. We now describe our method of generating these values for each of the trials.

2.6.2. Generating Utility Functions. For each task in the workload, we need to assign the three parameters to describe its utility function (i.e., priority, urgency, and utility class). As mentioned in Sec. 2.2.1.2, we have four possibilities for each of these parameters. We model four utility classes in this study because these are representative of the expected workload at ESSC. In our simulations, a task's utility class is chosen uniformly at random among the four classes modeled. Fig. 2.4 illustrates the utility functions obtained by using the four utility classes that we used in this study for a fixed priority level and a fixed urgency level. The length of the first interval during which the utility value does not decay is represented by "F" in the figure. It is dependent on the urgency level of the task as well

as the average execution time of the task. App. B gives the method for its computation. App. C gives the values used to create the four utility classes.

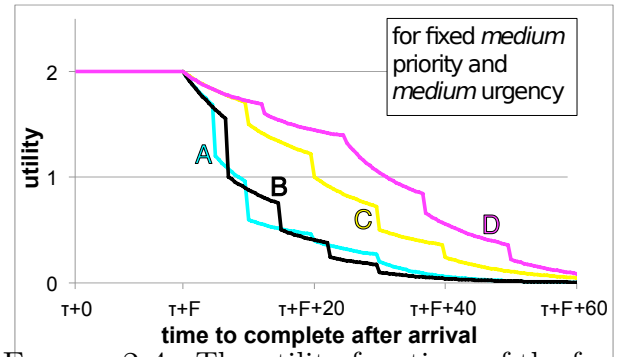

FIGURE 2.4. The utility functions of the four utility classes (A, B, C, and D) used in this study shown at fixed priority and urgency levels showing the decay in utility for a task after its arrival time τ. The duration of its first interval during which the utility value remains constant is represented by F on the x-axis.

In our simulations, the priority and urgency levels of a task are set based on a joint probability distribution that is representative of DOE/DoD environments. App. D shows this probability distribution as a matrix. The model results in most tasks having *medium* and *low* priorities with *medium* and *low* urgencies, and a few important tasks having *critical* and *high* priorities with *extreme* and *high* urgencies.

The values of maximum utility set by the various priority levels are: $\pi(critical) = 8$, $\pi(high) = 4$, $\pi(medium) = 2$, and $\pi(low) = 1$. We also experimented with a different set of values for the priority levels: $\pi(critical) = 1,000$, $\pi(high) = 100$, $\pi(medium) = 10$, and $\pi(low) = 1$. The exponential decay rates for the various urgency levels are: $\rho(extreme) = 0.6$, $\rho(high) = 0.2$, $\rho(medium) = 0.1$, and $\rho(low) = 0.01$. These priority and urgency values are based on the needs of the ESSC.

2.6.3. GENERATING ESTIMATED TIME TO COMPUTE (ETC) MATRICES. In our simulation environment, we group together tasks that have similar execution time characteristics into task types, and machines that have similar performance capabilities into machine types. We model 100 task types and 13 machine types. In our simulations, the procedure by which we assign tasks to task types is described in Sec. 2.6.4. We model an environment consisting of 100 machines, where each machine belongs to one of 13 machine types. Among these 13

machine types, 4 are special-purpose machine types while the remaining are general-purpose machine types. We model the special-purpose machine types as having the capability of executing certain task types (which are special to them) approximately ten times faster than on the general-purpose machine types. These special-purpose machine types, however, lack the ability to execute the other task types. In our environment, three to five task types were special on each special-purpose machine type.

We use techniques from the Coefficient of Variation (COV) method [36] to generate the entries of the ETC matrix. The mean value of execution time on the general-purpose and the special-purpose machine types is set to ten minutes and one minute, respectively. Complete details about our parameters for generating ETC matrices are described in App. E. The appendix also discusses how we distribute the 100 machines among the 13 machine types.

In this study, the task type of a task is not correlated to the worth of the task to the system, and therefore is not related to the utility function of the task. The task type only controls the execution time characteristics of the task.

2.6.4. Generating the Arrival Pattern of Tasks. To generate the arrival times of the tasks in the simulation, we use different arrival patterns for the special-purpose and the general-purpose task types. The goal of our arrival pattern generation is to closely model expected workloads of DOE and DoD interest. Our simulation models the arrival and mapping of tasks for a 24 hour period. Real-world oversubscribed systems rarely start with empty queues. To model this in our environment, we simulate the arrival and mapping of tasks for 26 hours, and exclude the first two hours of data from result calculations. The initial two hours serve to bring the system up to steady-state and avoid the scenario where the machine queues start with no tasks. We calculate all of our results (utility earned, average heuristic execution time, number of dropped tasks, etc.) for the duration of 24

hours (i.e., from the end of the 2^{nd} to the end of the 26^{th} hour). We also model two levels of oversubscription. In one case, approximately 33,000 tasks arrive during a 24 hour period whereas in the other case approximately 50,000 tasks arrive over that period.

Before we generate the arrival patterns for the special-purpose and the general-purpose tasks types, we first find a mean arrival rate of tasks for every task type (irrespective of special-purpose or general-purpose). We find the estimated number of tasks of each task type that will arrive during the day by sampling from a Gaussian distribution. The mean for this distribution is the ratio of the desired number of tasks to arrive (33,000 or 50,000) to the number of task types in the system. The variance is set to $1/10^{th}$ of the mean. We obtain the mean arrival rate of a task type by dividing the estimated number of tasks of this task type that are to arrive during the period by 24 hours. The mean arrival rate of each task type is used to generate arrival rate patterns (that have different arrival rates during the 24 hours), based on whether it is a special-purpose or a general-purpose task type. For the general-purpose task types, we use a sinusoidal pattern for the arrival rate. For the special-purpose task types, we use a bursty arrival rate pattern. App. F discusses how we create the arrival pattern for a general-purpose or special-purpose task type, and use this arrival rate pattern of a task type to obtain the actual number and arrival times of the tasks belonging to that task type.

2.7. Simulation Results and Analysis

2.7.1. Overview. As mentioned in the previous section, we generate 50 simulation trials for each experiment that we describe in this section. All bar charts in this section have results averaged over the 50 trials with error bars showing 95% confidence intervals. For the batch-mode heuristics, the next mapping event occurs after both of the following conditions have

been met: a time interval of one minute has passed since the last mapping event and the execution of the previous mapping event has finished. Later in this section, we show results with different methods of triggering batch-mode mapping events.

To make a fair comparison across the two levels of oversubscription, it is important to analyze the performance of a heuristic as a percentage of the maximum possible utility that could be achieved in that oversubscription level. The value of maximum utility bound that can be earned is calculated by summing the utility values achieved if all tasks were assumed to begin execution on their minimum execution time machine as soon as they arrive. We consider only tasks whose completion times are within the 24 hour period. The values of the maximum utility bound averaged across the 50 trials in the 33,000 and 50,000 tasks arriving per day cases are 65,051 and 98,708, respectively. First, we compare the performance of the various heuristics with the two levels of oversubscription. We then explore the effect of dropping tasks with different levels of dropping thresholds.

The best value of K for the K-Best Types heuristic was empirically found to be K=1 machine type in our environment. At K=1, the K-Best Types performs the same mapping decisions as the MET-Max Util heuristic. We therefore do not show the results from this heuristic in any of the bar charts.

2.7.2. Preliminary Results. Fig. 2.5 shows the performance of the different heuristics in terms of the percentage of maximum utility earned with the two levels of oversubscription. Irrespective of the oversubscription level, we observe that the naive immediate-mode heuristics always perform poorly compared to the smart immediate-mode heuristics. This is because the naive heuristics do not consider ETC information, machine ready-times, and the utility earned by a task on the various machines. The batch-mode heuristics always perform significantly better than the smart immediate-mode heuristics. This is because the

batch-mode heuristics not only consider machine ready-times, but also have the ability to schedule a set of tasks and re-map tasks that are in the virtual queues. Most of the batch-mode heuristics are able to use this to their advantage and move any high utility-earning task that may have just arrived to the front of the virtual queues in the next mapping event. With the immediate-mode heuristics, the newly-arrived high utility-earning tasks would be queued behind other tasks, and by the time they get an opportunity to execute, their utility may have decayed significantly. With the 33,000 tasks per day case, on average, the batch-mode heuristics gave an improvement of approximately 250% compared to the smart immediate-mode heuristics.

Comparing the percentage of maximum utility earned by the heuristics for the two levels of oversubscription shows that higher oversubscription makes it harder to earn the maximum possible utility. The actual utility earned by a heuristic in the 50,000 tasks per day case will typically be higher than that in the 33,000 tasks per day case. For example, the utility earned by Min-Min Comp in the 33,000 tasks per day case is 53.13% of 65,051 = 34,555, and in the 50,000 tasks per day case is 41.26% of 98,708 = 40,726. Even though for both levels of oversubscription we consider the utility earned by the system only for the 24 hour duration, the higher oversubscription rate allows a heuristic to select more higher utility earning tasks, and therefore earn higher utility.

The Max Util and Max UPT immediate-mode heuristics earn most of their utility from the special-purpose machines. This is because the special-purpose machines are able to quickly execute the tasks assigned to them (i.e., special-purpose tasks) and these machines are not oversubscribed. As a result, a task assigned to a special-purpose machine begins execution quickly and is able to earn high utility. In contrast, the general-purpose machines have long queues of tasks and therefore the tasks assigned to them usually earn very low

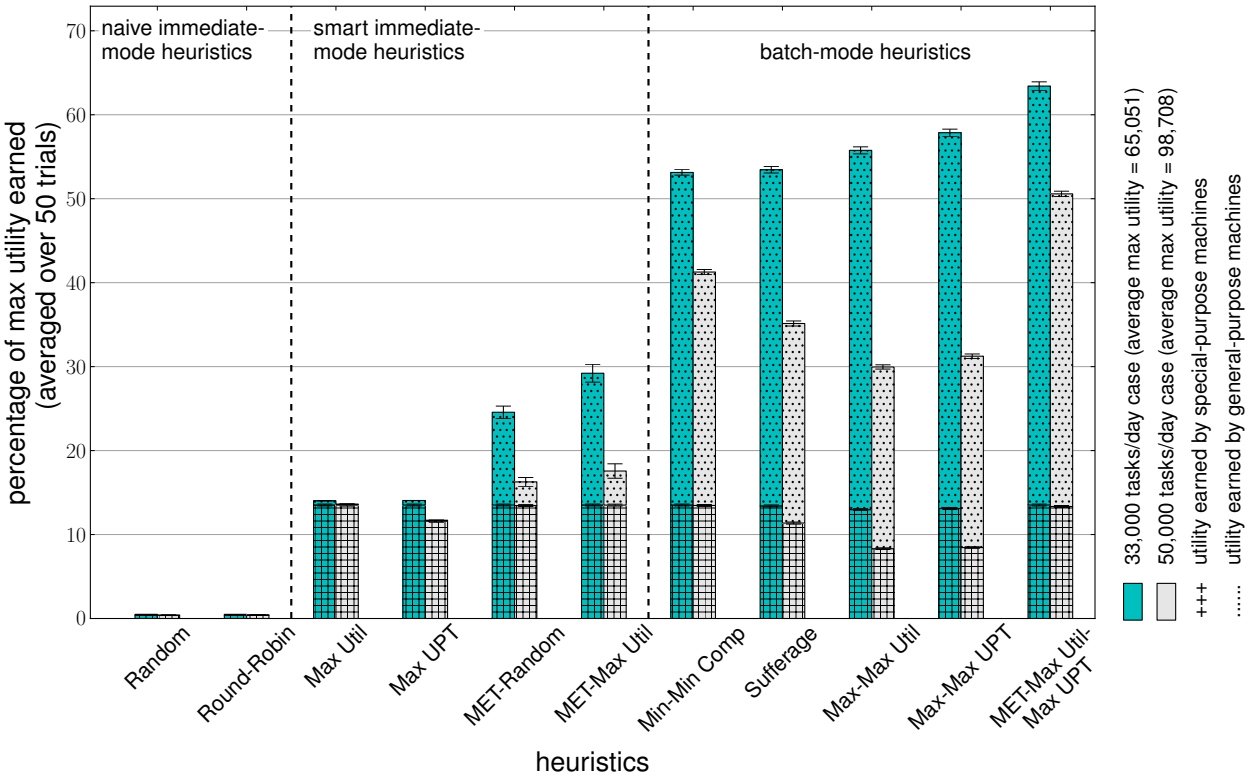

FIGURE 2.5. Percentage of maximum utility earned by all the heuristics under two levels of oversubscription: 33,000 tasks arriving within a day, and 50,000 tasks arriving within a day. No tasks were dropped in these cases. The utility earned value (as opposed to the percentage of maximum utility earned) by a heuristic in the 50,000 tasks per day case will typically be higher than that in the 33,000 tasks per day case.

utility by the time they finish execution. MET-Random and MET-Max Util alleviate this problem by assigning tasks to machines where they execute the fastest. This allows these heuristics to earn utility from the general-purpose machines as well.

The performance of many batch-mode heuristics is severely affected by the increase in the oversubscription level. The higher oversubscription results in more tasks being present in the batch during the mapping events. With an increase in the size of the batch, the batch-mode heuristics take considerably longer to perform each mapping event. This leads to triggering fewer mapping events (because a new mapping event cannot begin until the previous one completes). Fig. 2.7 shows the total number of mapping events for the batch-mode heuristics

under the two levels of oversubscription. The total number of mapping events are partitioned into two sections: those triggered at the time interval of one minute and those initiated when the execution of the previous mapping event took longer than one minute. We observe that the batch-mode heuristics (other than Min-Min Comp in 33,000 tasks per day case) have fewer mapping events being triggered than the expected amount (namely, 1,440 if they were all triggered after one minute). With fewer mapping events, it takes longer for the high utility-earning tasks to be moved up to the front of the virtual queues and the delay may cause their utility values to decay significantly. Min-Min Comp executes faster than the other batch-mode heuristics because it does not perform any explicit utility calculations. MET-Max Util-Max UPT also executes relatively quickly because it performs utility calculations only for a subset of the machines. Max-Max Util and Max-Max UPT earn very low utility in the 50,000 tasks per day case because they have only 200 mapping events being triggered during the day. In contrast to the batch-mode heuristics, the immediate-mode heuristics execute quickly, and as a result, even in the case where 50,000 tasks arrive during the day, they have approximately 50,000 mapping events with only 0.5% of those on average (250 out of 50,000) being initiated as a result of the heuristic execution of the previous mapping event taking longer than the arrival time of the next task.

Picking the minimum execution time machine type for a task is automatically providing load balancing in our environment. The MET-type heuristics (both immediate-mode and batch-mode) are performing particularly well because of the high heterogeneity modeled in our environment. If we had a variation in our environment where the workload includes many task types that perform best on a select few machines, these MET-type heuristics would assign all of those tasks only to these few machines resulting in long machine queues on these fast machines, where the wait time of a task would negate the faster execution time.

Our level of heterogeneity is modeled based on the expectations for future environments of DOE and DoD interest.

2.7.3. Results with Dropping Tasks. As mentioned in Sec. 2.4.4, we implement techniques in the immediate-mode and batch-mode heuristics to drop tasks that earn utility values less than a dropping threshold. We experiment with six levels for the dropping threshold: 0 (which is equivalent to no dropping), 0.05, 0.5, 1.5, 3, and 5. These are chosen based on our system model, including the values of maximum utility for the various priority levels, i.e., 8, 4, 2, and 1. We run simulations with all the heuristics using the six dropping thresholds for the two cases of oversubscription. In Fig. 2.6, we show the results for the 50,000 tasks per day case. The results of the 33,000 oversubscription level show similar trends, and are discussed in App. G. The heuristics significantly benefit from the dropping operation. For almost all heuristics, the utility earned increases as we increase our dropping threshold from 0 to 1.5. With a dropping threshold of 1.5, all the *low* priority tasks are dropped because their starting utility is 1. This may be undesirable in general, but for our oversubscribed system this results in the best performance. The average computation capability of our environment is such that approximately 26,000 tasks can execute in the 24-hour period (based on the average execution time of each task on each machine). Our dropping operation lets us pick the best 26,000 tasks to execute to maximize the total utility that can be earned. Based on a different system model and administrative policies one may set the specific levels of dropping thresholds differently.

The immediate-mode heuristics do not have the ability to move newly arrived high-utility earning tasks to the head of the queue because they are not allowed to remap queued tasks. The dropping operation benefits the immediate-mode heuristics by clearing the machine queues of the lower-utility-earning tasks, which allows the other queued tasks to execute

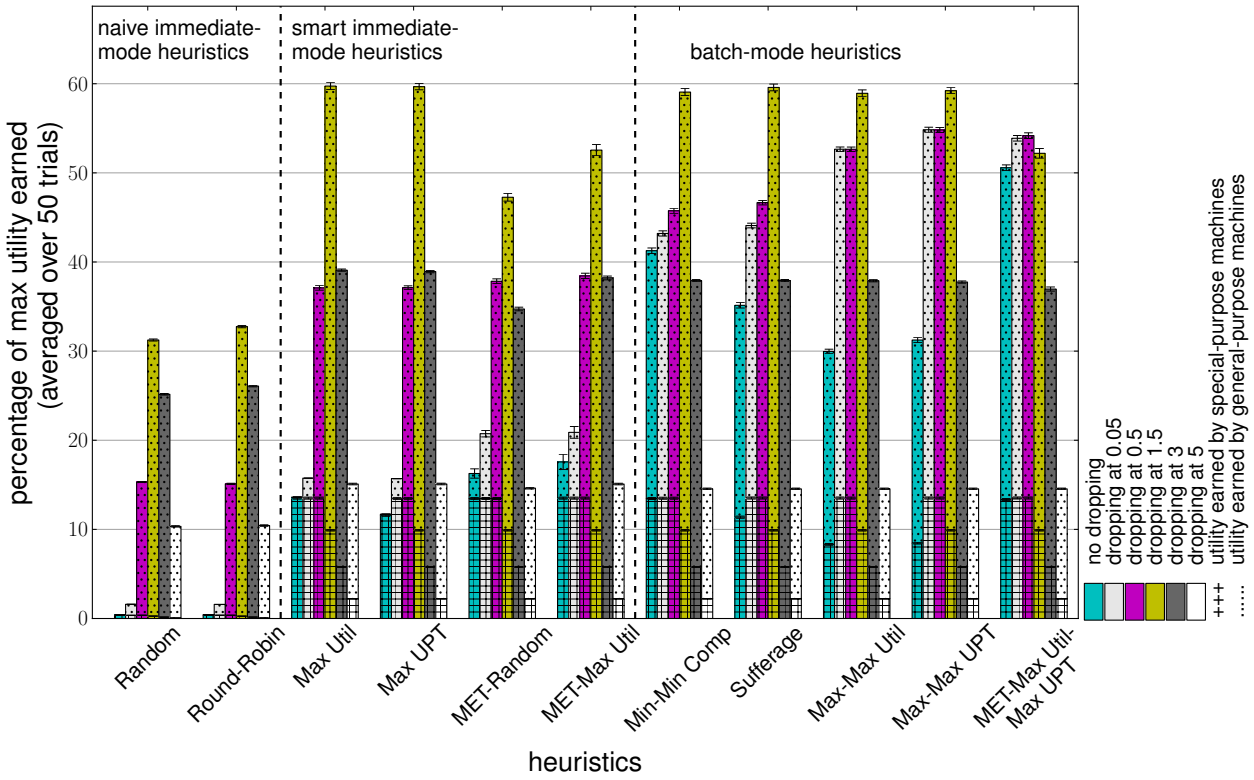

FIGURE 2.6. Percentage of maximum utility earned earned by all the heuristics for the different dropping thresholds with the oversubscription level of 50,000 tasks arriving during the day. The average maximum utility bound for this oversubscription level is 98,708.

sooner and earn higher utility. This helps the immediate-mode heuristics to earn utility from the general-purpose machines. The special-purpose machines were not oversubscribed and therefore there is no significant increase in performance from these machines because of the dropping operation. At the best dropping threshold, i.e., 1.5, Max Util and Max UPT have an approximately 450% performance improvement compared to the no dropping case. The performance of these two heuristics comparable to that of the batch-mode heuristics. As we increase the dropping threshold beyond 1.5, we drop too many tasks from our system and as a result earn less utility overall.

There are two main reasons why the batch-mode heuristics benefit from the dropping operation. The first is that the dropping operation helps them reduce the size of their batch

during each mapping event by dropping tasks that would only be able to earn low utility. This makes the mapping events execute faster and results in more mapping events. For the batch-mode heuristics, in all cases where some level of dropping was implemented, all of the 1440 mapping events were triggered. With the increase in the number of mapping events, the batch-mode heuristics are able to service high utility-earning tasks faster. This causes the improvement in performance in the dropping at 0.05 case compared to the no dropping case. The second reason the batch-mode heuristics benefit from the dropping operation is the prevention of low utility-earning tasks from blocking the pending and the executing slots of the machines. When tasks are arriving, there may be periods when most of the arriving tasks are neither *critical* nor *high* priority tasks. During this time period, other lower priority tasks get the opportunity to fill into the pending slots of the machines. If there is a burst of *critical* or *high* priority tasks after this period, these higher-priority tasks will have to wait in queue behind the lower priority task in the pending slot, because the pending slot tasks cannot be re-mapped. By dropping the lower priority tasks, we do not block the pending (and hence the executing) slots and when the high utility-earning tasks arrive they get to quickly start execution and provide higher utility to the system. This causes the performance improvement for batch-mode heuristics with further dropping beyond 0.05. Similar to the immediate-mode heuristics, dropping thresholds greater than 1.5 drop too many tasks.

Max-Max Util, Max-Max UPT, and MET-Max Util-Max UPT maximize the utility earned and push low utility-earning tasks to the back of the queue. Thus, for these heuristics, the biggest advantage of the dropping operation is to reduce the size of the batch, allowing for more mapping events.

The dropping operation also helps to make the Min-Min Comp and Sufferage heuristics more utility-aware, and we get the biggest performance improvement by increasing the

dropping threshold to 1.5 (even though the dropping threshold at 0.05 triggered all 1,440 mapping events).

In all cases where some level of dropping is implemented, almost all of the heuristics earn similar values of utility from the special-purpose machines because these machines are not oversubscribed. Utility earned from special-purpose machines decreases with dropping thresholds of 1.5 and higher because proportionally the number of special-purpose tasks become fewer.

Although the smart immediate-mode heuristics can earn utility comparable to the batch-mode heuristics, their performance is very sensitive to the value of the dropping threshold. For the immediate-mode heuristics, the dropping threshold parameter needs to be tuned based on the starting utility values for the different priority levels, arrival pattern of the tasks, degree of oversubscription of the environment, etc., because the immediate-mode heuristics rely on the dropping threshold to empty the machine queues. In contrast, the mechanism by which the dropping operation helps batch-mode heuristics such as Max-Max Util, Max-Max UPT, and MET-Max Util-Max UPT is different, i.e., it increases the number of mapping events. The performance of these batch-mode heuristics is less sensitive to the value of the dropping threshold.

The MET-based heuristics, i.e., MET-Random, MET-Max Util, and MET-Max Util-Max UPT, earn less utility compared to the other heuristics at a dropping threshold of 1.5. At this dropping threshold, all the *low* priority tasks are dropped from the system, and they account for approximately 53% of tasks (see App. D). Therefore, with a 1.5 dropping threshold the degree of oversubscription reduces significantly. The MET-based heuristics assign tasks to the machines that belong to the best execution time machine type. As a result, these heuristics hurt their case at this dropping threshold by oversubscribing certain

machines. This causes them to drop more tasks (because tasks wait longer) compared to the other heuristics and earn less utility overall. The effect of increased oversubscription by the MET-based heuristics is not apparent at the 0.5 and 3 dropping thresholds because at these dropping thresholds the system is much more oversubscribed and undersubscribed, respectively.

For dropping thresholds 1.5 and above, almost all the heuristics earn similar amounts of total utility (except naive heuristics and the MET-based heuristics). At these dropping thresholds, only tasks of higher priority levels are executing on the machines (as tasks with lower priority levels have starting utility values less than the dropping threshold) and as a result the degree of oversubscription is reduced. The non-dropped tasks start execution as soon as they because machines are idle most of the time, and therefore, all heuristics earn similar levels of utility.

The average mapping event execution times for the heuristics in both levels of oversubscription at a 0.5 dropping threshold are in App. G. Results of experiments with the maximum utility values for the priority levels set at 1000, 100, 10, and 1 are discussed in App. H.

2.7.4. Triggering Batch-mode Mapping Events. The ability of the batch-mode heuristics to update the machine queues with a high utility-earning task that may have arrived recently provides a distinct advantage. We now study the effect of varying the size of the batch by exploring other possibilities for triggering the next mapping event. We examine a technique to trigger batch-mode mapping events based on a combination of time interval and number of tasks that have arrived since the last mapping event. A mapping event will be triggered when either of the above (time interval or number of tasks) occur, or after the previous mapping execution if it takes longer. These studies are performed using the

0.5 dropping threshold and 50,000 tasks per day case. We experiment with the following five triggering cases: (1) number of tasks: 1; (2) number of tasks: 2, or time interval: 0.0576 minutes; (3) number of tasks: 35, or time interval: 1 minute; (4) number of tasks: 70, or time interval: 2 minutes; (5) number of tasks: 347, or time interval: 10 minutes. For each case, the time intervals are chosen to approximate the corresponding estimated number of task arrivals. These experiment parameters are set based on our simulation environment. One could perform such tests with different values for the parameters based on other environments.

Fig. 2.8 shows the performance of the Max-Max UPT heuristic with the different cases of triggering. The other batch-mode heuristics show similar trends as the Max-Max UPT heuristic. In all five triggering cases mentioned above and for all of the batch-mode heuristics, the average execution time of a mapping event with a dropping threshold of 0.5 is under 350 milliseconds.

The best performance is obtained when mapping events keep triggering every time a new task arrives. The batch-mode heuristics were able to execute 50,000 mapping events because we are using a dropping threshold of 0.5 and this makes the heuristics execute quickly. The performance benefit is due to the heuristics being able to use new information to quickly re-map tasks. However, the increase in performance is small because very few tasks among the newly arrived tasks would be *critical* or *high* priority tasks. It is usually the high utility-earning tasks that change the mapping of the previously mapped tasks. As mentioned in App. D, on average approximately 4% and 11% of tasks are *critical* and *high* priority tasks, respectively. Therefore, after a minute or after 35 task arrivals, there would probably be approximately one *critical* and four *high* priority tasks among the newly arrived

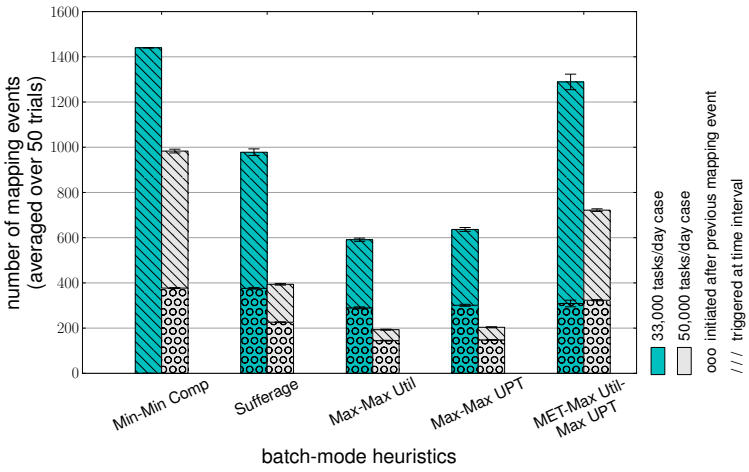

FIGURE 2.7. The number of mapping events initiated either because the one minute time interval has passed since the last mapping event or because the previous mapping event finished execution after one minute are shown for five batch-mode heuristics with the two levels of oversubscription: 33,000 tasks arriving within a day, and 50,000 tasks arriving within a day. No tasks were dropped in these cases.

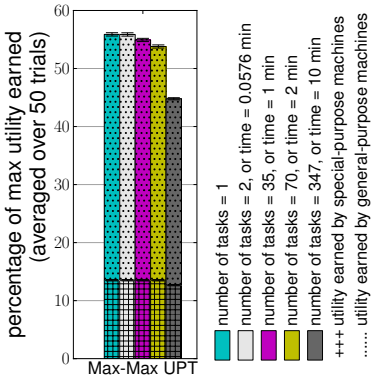

FIGURE 2.8. Percentage of maximum utility earned by the Max-Max UPT heuristic for the different cases of triggering batch-mode mapping events. The other batch-mode heuristics show similar trends.

tasks. Scheduling these as soon as they arrive instead of waiting for less than a minute provides only a marginal increase in the total performance.

2.8. Conclusions and Future Work

In this study, we develop a flexible metric that uses utility functions to compare the performance of resource allocation heuristics in an oversubscribed heterogeneous computing environment where tasks arrive dynamically throughout a 24 hour period. We model this type of environment based on the needs of the ESSC at ORNL. We design and analyze the

performance of seven immediate-mode heuristics and five batch-mode heuristics in our simulated environment based on the total utility they could earn during a one day time period. We observe that without the ability to drop tasks, the naive immediate-mode heuristics perform poorly compared to the smart immediate-mode heuristics, which in turn perform poorly compared to the batch-mode heuristics. Among the batch-mode heuristics, Max-Max UPT and MET-Max Util-Max UPT perform the best. This is because these batch-mode heuristics consider the minimization of the execution time of the task in addition to maximizing utility. This is helpful in an oversubscribed highly heterogeneous environment. Dropping low utility-earning tasks significantly helps improve performance of the immediate-mode heuristics because it allows other relatively high-utility earning tasks to execute sooner and thus earn more utility. Dropping tasks also improves the batch-mode heuristics in two ways, (a) by preventing large batch sizes which results in more mapping events being triggered due to faster heuristic execution times, and (b) by preventing lower-priority tasks from entering into the pending slot so that higher priority tasks that arrive subsequently can execute sooner. Immediate-mode heuristics are much more sensitive to the value of the dropping threshold and rely on its tuning to avoid low utility earning tasks from entering machine queues. Permuting the initial tasks at the head of the virtual queues does not affect the performance significantly in our environment. We also experiment with different triggers for the batch-mode mapping events. We observe that (in our environment) triggering every time a new task arrives is not providing significant benefit in the total utility earned compared to mapping after every minute. Possible future directions for this research are mentioned in Chapter 6.

CHAPTER 3

Trade-offs Between System Performance and Energy Consumption[2]

3.1. Introduction

During the past decade, large datacenters (comprised of supercomputers, servers, clusters, farms, storage, etc.) have become increasingly powerful. As a result of this increased performance the amount of energy needed to operate these systems has also grown. It was estimated that between the years 2000 and 2006 the amount of energy consumed by high performance computing systems more than doubled [38]. In 2006 an estimated 61 billon kWh was consumed by servers and datacenters, approximately equal to 1.5% of the total United States energy consumption for that year. This amounted to $4.5 billion in electricity costs [38]. Since 2005, the total amount of electricity used by HPC systems increased by another 56% worldwide and 36% in the U.S. Additionally, during 2010, global HPC systems accounted for 1.5% of total electricity use, while in the U.S., HPC systems accounted for 2.2% [2].

With the cost of energy and the need for greater performance rising, it is becoming increasingly important for HPC systems to operate in an energy-efficient manner. One way to reduce the cost of energy is to minimize the amount of energy consumed by a specific system. In this work, we show that we can reduce the amount of energy consumed by a system by making intelligent scheduling decisions. Unfortunately, consuming less energy

[2]This work was done jointly with Ph.D. student Ryan Friese. The full list of co-authors is at [37]. This research used resources of the National Center for Computational Sciences at Oak Ridge National Laboratory, supported by the Extreme Scale Systems Center at ORNL, which is supported by the Department of Defense under subcontract numbers 4000094858 and 4000108022. This research also used the CSU ISTeC Cray System supported by NSF Grant CNS-0923386.

often leads to a decrease in the performance of the system [39]. Thus, it can be useful to examine the trade-offs between minimizing energy consumption and maximizing computing performance for different resource allocations. Current resource managers, such as MOAB, cannot reasonably determine the trade-offs between performance and energy.

In this research, we model a computing environment and corresponding workload that is being investigated by the Extreme Scale Systems Center (ESSC) at Oak Ridge National Laboratory (ORNL). The ESSC is a joint venture between the United States Department of Defense (DoD) and Department of Energy (DOE) to provide research, tools, software, and technologies that can be utilitized in both DoD and DOE environments. Our goal is to design an analysis framework that a system administrator can use to analyze the energy and performance trade-offs of a system by using different resource allocations (i.e. mapping of tasks to machines). System performance is measured in terms of total utility earned, where each task in the workload is assigned a time utility function that monotonically decreases in value the longer a task remains in the system [4]. The computing environment is a heterogeneous mix of machines and tasks that represents an environment with system characteristics and workload parameters that are based on the expectations of future DoD and DOE environments.

In a heterogeneous environment, tasks may have different execution and power consumption characteristics when executed on different machines. One can change the performance and energy consumption of the system by using different resource allocations. A resource allocation is defined to be a complete mapping of tasks to machines, where we assume the number of tasks is much greater than the number of machines. To create these resource allocations, we model this scheduling problem as a bi-objective optimization problem that

maximizes utility earned and minimizes energy consumed. We adapt the Nondominated Sorting Genetic Algorithm II (NSGA-II) [40] to create the resource allocations.

To analyze the effect of different resource allocations, we implement our method in a static and offline environment. To create the offline environment we simulate a trace over a specified time period of the modeled environment. This allows us to gather information about the number of tasks that arrived during this time period, as well as the arrival times and types of tasks that were present in the system. The availability of this information makes this a static resource allocation problem. The knowledge gained from studies such as this can be used to set the parameters needed for designing dynamic or online allocation heuristics.

We utilize execution and power consumption characteristics from real machines and applications. We further use this real characteristic data to create a larger data set in order to simulate larger systems. In all cases, our results show that by using different resource allocations a system administrator can greatly change the amount of utility earned and power consumed based on the needs of their system.

In this chapter we make the following contributions:

(1) Modeling a bi-objective resource allocation problem between total utility earned and total energy consumed to address concerns about energy-efficient computing, specifically for environments of DoD and DOE interest.

(2) Creating and evaluating many intelligent resource allocations to show that the utility earned and energy consumed by the system can change greatly.

(3) Demonstrating our method by using real machine and task data.

(4) Providing a method to create synthetic data sets that preserve the heterogeneity measures found from real data sets.

(5) Analyzing the effect of using different seeding heuristics on the evolution of solutions found by the genetic algorithm.

The remainder of this chapter is organized as follows. Related work is discussed in Section 3.2. We construct the system model, and our real data set, in Section 3.3. In Section 3.4, we describe our bi-objective optimization problem and the NSGA-II. Our simulation setup is detailed in Section 3.5. Section 3.6 analyzes our simulation results. Finally, our conclusion and future work will be given in Section 3.7.

3.2. Related Work

The authors of [39] formulate a bi-objective resource allocation problem to analyze the trade-offs between makespan and energy consumption. Their approach is concerned with minimizing makespan as their measure of system performance, opposed to maximizing utility in our approach. Additionally, they model an environment where the workload is a bag of tasks, not a trace from a dynamic system. This is important because they do not consider arrival times or the specific ordering of tasks on machine. Finally, the authors do not demonstrate their approach using real historical data.

A bi-objective optimization problem between makespan and reliability is used to solve heterogeneous task scheduling problems in [41] and [42]. We perform the bi-objective optimization between utility earned and energy consumed.

The study in [43] implements a weighted sum simulated annealing heuristic to solve a bi-objective optimization problem between makespan and robustness. One run of this heuristic produces a single solution, and different weights can be used to produce different solutions. This differs from our approach in that we independently evaluate our two objective

functions that allows us to create a Pareto front containing multiple solutions with one run of our algorithm.

In [44], the authors minimize makespan and total tardiness to solve the bi-objective flowshop scheduling problem. The authors utilize a Pareto-ant colony optimization approach to create their solutions. This work differs from ours by not using a genetic algorithm nor is it concerned with utility nor energy consumption.

In [45], a job-shop scheduling problem is modeled as a bi-objective optimization problem between makespan and energy consumption. The authors model a homogeneous set of machines whereas our work models a heterogeneous set of machines. The work in [45] also differs from ours by using an algorithm that only produces a single solution.

Heterogeneous task scheduling in an energy-constrained computing environment is examined in [10]. The authors model an environment where devices in an ad-hoc wireless network are limited by battery capacity. The heuristics in [10] create a single solution while ours creates multiple solutions. In our study, we are not concerned with an energy-constrained system, but instead we try to minimize the total energy consumed.

Minimizing energy while meeting a makespan robustness constraint in a static resource allocation environment is studied in [46]. This work is not an explicit bi-objective optimization. Our work differs by using utility maximization as an objective instead of minimizing makespan.

A dynamic resource allocation problem in an energy-constrained environment is studied in [47]. Solutions to this problem must complete as many tasks as they can while staying within the energy budget of the system. In our work, we model a trace of a dynamic system allowing us to create a static allocation. We also do not constrain the amount of energy our system can consume.

Mapping tasks to computing resources is also an issue in hardware/software co-design [48]. This problem domain differs from ours, however, because it typically considers the hardware design of a single chip. Our work assumes a given collection of heterogeneous machines.

3.3. System Model

3.3.1. Overview. Our system environment is modeled based on the needs of the ESSC at ORNL. The system is intended to provide a model of both the machines and workload used in such an environment. This system model has been designed with detailed collaboration between members of Colorado State University, ORNL, and the United States DoD to ensure it accurately captures the needs and characteristics of the ESSC.

3.3.2. Machines. This model consists of a suite of M heterogeneous machines, where each machine in this set belongs to a specific machine type μ. Machine types exhibit heterogeneous performance, that is machine type A may be faster than machine type B for some task types but slower for others [36]. Machines types also exhibit heterogeneous energy consumption and belong to one of two categories. The first category is general-purpose machines. General-purpose machines are machines that are able to execute any of the task types in the system, and they make up the majority of the machines in the environment. The other category of machines is special-purpose machines. Machines within this category can only execute a small subset of task types and are incapable of executing the remaining task types. Special-purpose machines generally exhibit a 10x decrease in the execution times of the task types they can execute compared to the general-purpose machines. The heterogeneity between the machine types can be attributed to differences in micro-architectures, memory modules, hard disks, and/or other system components.

3.3.3. Workload. In the ESSC environment, tasks arrive dynamically throughout the day. Once a task arrives, the utility earned by a task may start to decay, see Subsection 3.4.2.1. Utility dictates how much useful work a given task can accomplish. Utility is represented by a monotonically-decreasing function with respect to time. Therefore the sooner a task completes execution the higher utility it might earn [4]. Because we are performing a bi-objective analysis of the system, we consider a trace of tasks that arrive into the system within a specified amount of time (e.g., one hour). The arrival times of each task in the trace must be recorded to accurately calculate how much utility a given task earns.

Every task in the trace is a member of a given task type. Each task type has unique performance and energy consumption characteristics for executing on the machine types. Similar to the machine types, task types belong to one of two categories; general-purpose tasks types and special-purpose tasks types. General-purpose tasks types are task types that can only execute on the general-purpose machine types. A special-purpose task type can execute on a specific special-purpose machine type at an increased rate of execution (compared to the general-purpose machine type), and it is also able to execute on the general-purpose machine types.

3.3.4. Execution and Energy Consumption Characteristics. It is common in resource allocation research to assume the availability of information about the performance characteristics of the tasks types and machine types present in a system (e.g., [14, 17, 15, 16]). This information is contained within an Estimated Time to Compute (ETC) matrix. An entry in this matrix, ETC(τ,μ), represents the estimated time a task of type τ will take to execute on a machine of type μ. The values contained within this matrix can be synthetically created to model various heterogeneous systems [36], or the values can be obtained from

historical data (e.g., [15, 17]). The assumption that ETC values can be obtained from historical data is valid for the intended ESSC environments.

In this study, we also require information about the power consumption characteristics of the task types and machine types. We call this set of data the Estimated Power Consumption (EPC) matrix. An entry in this matrix, EPC(τ,μ), represents the average amount of power a task of type τ consumes when executing on a machine of type μ. Different EPC values can represent different task type energy characteristics, e.g., computationally intensive tasks, memory intensive tasks, or I/O intensive tasks. The values within the EPC matrix can also be created synthetically or gathered from historical data. In this study we utilize ETC and EPC matrices that contain both real historical data (described in Section 3.3.4.1), and synthetic data derived from the historical data (described in Section 3.3.4.2).

3.3.4.1. *Gathering of Historical Data.* To accurately model the relationships between machine performance and energy consumption in a heterogeneous suite of machines, we first create ETC and EPC matrices filled with historical data. For this data, we use a set of online benchmarks [49] that tested a suite of nine machines (Table 3.1) over a set of five tasks (Table 3.2). The machines differ by the CPU and motherboard/chipset used, but all the machines use the same amount of memory (16GB) and the same type of hard drive and GPU. For each task, the benchmark produced the average execution time for that task on each of the machines as well as the average power consumed by that task on each of the machines. We were able to place these values into our ETC and EPC matrices. Each of the nine machines from the benchmark represents a specific machine type, and each of the five tasks from the benchmark represents a specific task type. This data provides us with initial ETC and EPC matrices of size 5×9.

TABLE 3.1. Machines (designated by CPU) used in benchmark

AMD A8-3870k
AMD FX-8159
Intel Core i3 2120
Intel Core i5 2400S
Intel Core i5 2500K
Intel Core i7 3960X
Intel Core i7 3960X @ 4.2 GHz
Intel Core i7 3770K
Intel Core i7 3770K @ 4.3 GHz

TABLE 3.2. Programs used in benchmark

C-Ray
7-Zip Compression
Warsow
Unigine Heaven
Timed Linux Kernel Compilation

3.3.4.2. *Creation of Synthetic Data.* From the historical data, we are able to derive a larger data set to study how our algorithm performs for a more complex problem. To create a larger data set, we need to increase the number of task types as well as introduce special-purpose machines. The real historical data will be included in this larger data set. For the new synthetic data set to resemble the real historical data as closely as possible, we need to preserve the heterogeneity characteristics of the historical data set. Heterogeneity characteristics of a data set can be measured using various standard statistical measures, such as the coefficient of variation, skewness, and kurtosis [50]. Two data sets that have similar heterogeneity characteristics would have similar values for these three measures.

To create a larger data set (we describe the process using the ETC matrix, but the process is identical for the EPC matrix), our first task is to create more task types. To do this, we first calculate the average execution time of each of the real task types across all the machines, this is also known as the row average of a task type. We then use these row average task execution times as the basis for creating new task types. We calculate the following

heterogeneity measures: mean, variation, skewness, and kurtosis (mksv) for the collection of row average task execution times. With the mvsk values we use the Gram-Charlier expansion [51] to create a probability density function (PDF) that produces samples of row average task execution times. By sampling this PDF we can create the row average task execution times for any number of new task types.

Once a desired number of task types are created, the next step is to populate the ETC entries for these new task types. While doing this, we want to preserve the relative performance from one machine to another. We calculate the task type execution time ratio. This ratio is the execution time of a specific task type on a specific machine, divided by the average task execution time (across all machines) for that task type. For example, let us assume task type 1 takes eight minutes to execute on machine type A, but it takes twelve minutes to execute on machine type B. Also assume task type 1 has an average execution time of ten minutes across all machines. On machine type A the task type has a task type execution time ratio of .8 while on machine type B, the task type has a task type execution time ratio 1.2. We calculate this ratio for all of the real task types on all of the real machines. Typically, faster machines will have values less than one for this ratio while slower machines have values greater than one.

Having found the relative performance of the machines to one another, the next step is to capture the task heterogeneities across the individual machines to create the new ETC matrix values. The following procedure is performed individually for each machine. On a given machine, we calculate the heterogeneity values of the task type execution time ratios for the real task types. By using the mvsk values produced, we then create a PDF that produces samples of task type execution time ratios for that specific machine. We sample this PDF to create task type execution time ratios for the new task types on that specific

machine. We can then take the task type execution time ratios for the new task types and multiply them by their respective average task type execution time values to produce the actual ETC values for the new task types.

The final step is to now create the special-purpose machines types. Based on the expectations of future DoD and DOE environments, special-purpose machine types are modeled to perform around 10x faster than the general-purpose machine types for a small number of task types (two to three for each special purpose machine type). To create these machines we first select the number of task types that can be executed on the special-purpose machines types. Then the average execution time (across all the machines) for each of these selected task types is found. The average execution time for each task type is divided by ten and is then used as the ETC value for the special-purpose machine type. When calculating EPC values, the average power consumption across the machines is *not* divided by ten.

This method allows us to create larger data sets that exhibit similar heterogeneity characteristics when compared to the real data. This method can be used to create both ETC and EPC matrices, with the exception of special-purpose EPC values as stated above.

3.4. Bi-Objective Optimization

3.4.1. Overview. In many real world problems, it is important to consider more than one goal or objective. It is often the case that these multiple objectives can directly or indirectly compete with each other. Optimizing for one objective may cause the other objective to be negatively impacted. In this work we try to maximize utility earned while minimizing energy consumed. We will show in our results that these two objectives do compete with each other. In general, a well-structured resource allocation that uses more energy will earn more utility and one that uses less energy will earn less utility. This relationship occurs

because we model utility as a monotonically-decreasing performance measure, that is, the longer a task takes to execute, the less utility it may earn. In [39], it is shown that spending more energy may allow a system to complete all the tasks within a batch sooner.

In Section 3.4.2, we define the two objective functions we are optimizing. Section 3.4.3 describes which solutions should be considered when solving a bi-objective optimization. The genetic algorithm used for this study is briefly explained in Section 3.4.4.

3.4.2. Objective Functions.

3.4.2.1. *Maximizing Utility.* One objective is maximizing total system utility earned. Total Utility Earned is a metric used to measure the performance of a computing system. Utility can be thought of as the amount of useful work a system accomplishes [4]. The amount of utility a task earns is determined by the completion time of the task, as well as by three sets of parameters; priority, urgency, and utility characteristic class. These parameters form what is called a time-utility function. This function is a monotonically-decreasing function [4].

Priority represents the total amount of utility a task could possibly earn, i.e., how important a task is. Urgency represents the rate of decay of utility a task may earn as a function of completion time. Utility characteristic class allows the utility function to be separated into discrete intervals. Each interval can have a beginning and ending percentage of maximum priority, as well as an urgency modifier to control the rate of decay of utility. The definition of these parameters are based on the needs of the ESSC. The value of these parameters in an actual system are determined by system administrators (not individual users) and are policy decisions that can be adjusted as needed.

Figure 3.1 illustrates a sample task time-utility function. We see that the function is monotonically decreasing. Additionally, we see the different intervals existing in the function.

By evaluating the function at different completion times, we can determine the amount of utility earned. For example, if a task finished at time 20, it would earn twelve units of utility, whereas if the task finished at time 47, it would only earn seven units of utility.

Every task t in the system is assigned its own utility function $\Upsilon(t)$. This function returns the utility earned by that task when it completes execution. Tasks that have hard deadlines can be modeled as having their utility decay to zero by a specific time. To optimize for total utility, the goal is to maximize the sum of utilities earned over all tasks in the system. Given that there are T tasks in the system, total utility earned, denoted U, can be defined as

$$U = \sum_{\forall t \in T} \Upsilon(t). \tag{3}$$

3.4.2.2. *Minimizing Energy Consumed.* The other objective we optimize for is minimizing total energy consumed. For a given resource allocation, the total energy consumed is the sum of the energy consumed by each task to finish executing. We first calculate the Expected Energy Consumption (EEC) for a given task on a given machine. This is found by multiplying the ETC and EPC values for that task on that machine. Assume the function $\Phi(t)$ returns the task type of a given task t and the function $\Omega(m)$ returns the machine type of a given machine. The expected energy consumption of task t on machine m can then be given as

$$EEC[\Phi(t), \Omega(m)] = ETC[\Phi(t), \Omega(m)] \times EPC[\Phi(t), \Omega(m)]. \tag{4}$$

Let T_m be the tasks that execute on machine m, where task $t_m \in T_m$. The total energy consumed by the system, denoted E, is found by

$$E = \sum_{\forall m \in M} \sum_{\forall t_m \in T_m} EEC[\Phi(t_m), \Omega(m)]. \tag{5}$$

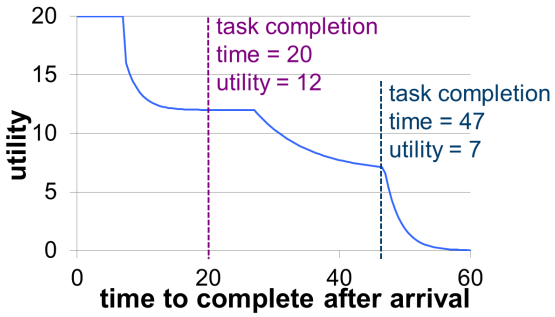

FIGURE 3.1. Task time-utility function showing values earned at different completion times.

3.4.3. GENERATING SOLUTIONS FOR A BI-OBJECTIVE OPTIMIZATION PROBLEM. When a problem contains multiple objectives, it is challenging to determine a single global optimal solution. Often, there is instead a *set* of optimal solutions. This set of optimal solutions may not be known, thus it is important to find a set of solutions that are as close as possible to the optimal set. The set of solutions that we find that best approximates the optimal set is called the set of Pareto optimal solutions [52]. The Pareto optimal set can be used to construct a Pareto front that can illustrate the trade-offs between the two objectives.

Not all solutions we find can exist within the Pareto optimal set. We select the eligible solutions by examining solution dominance. Dominance is used to compare two solutions to one another. For one solution to dominate another, it must be better than the other solution in at least one objective, and better than or equal in the other objective. Figure 3.2 illustrates the notion of solution dominance. In this figure we show three potential solutions: A, B, and C. The objectives we are optimizing for are minimizing total energy consumption along the x-axis and maximizing total utility earned along the y axis. A "good" solution would be one that consumes small amounts of energy and earns large amounts of utility (upper left corner).

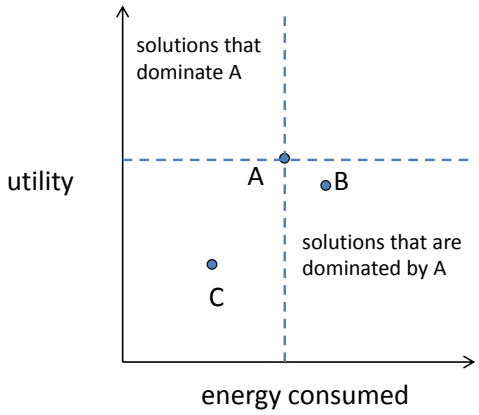

FIGURE 3.2. Illustration of solution dominance for three solutions: A, B, and C. Solution A dominates solution B because A has lower energy consumption as well as it earns more utility. Neither solution A nor C dominate each other because C uses less energy, while A earns more utility.

If we consider solutions A and B, we can say that B is dominated by A. This is because A uses less energy as well as earns more utility than B. The same is true for any solution located within the lower right region. Now, when we examine solutions A and C we cannot make any claims on the dominance of one solution over the other. This is because C uses less energy than A, but C does not earn as much utility, thus the two solutions can not be directly compared to each other, which means they are both located on the Pareto front. Finally, solution A will only be dominated by solutions that exist in the upper left region.

3.4.4. NONDOMINATED SORTING GENETIC ALGORITHM II. The Nondominated Sorting Genetic Algorithm II (NSGA-II) was designed for solving bi-objective optimization problems [40]. We adapt a version of the NSGA-II that we used in [39] for a different, simpler resource allocation problem. We will briefly describe the basic NSGA-II algorithm and how we have modified it for our specific problem.

The NSGA-II is a popular multi-objective genetic algorithm that utilizes solution dominance to allow the populations of chromosomes to evolve into better solutions over time.

For our problem domain, a single population represents a set of possible resource allocations (solutions). To use the NSGA-II for our problem we needed improve upon [39] and encode the algorithm so that it could solve bi-objective resource allocation problems where the two objectives are maximizing utility earned and minimizing energy consumed. To do this, the algorithm must be able to accurately track and calculate the individual utility earned by each task. This meant we needed to create our own genes, chromosomes, crossover operator, and mutation operator.

Genes represent the basic data structure of the genetic algorithm. For our problem, a gene represents a task. Each gene contains: the machine the gene will operate on, the arrival time of the task, and the global scheduling order of the task. The global scheduling order is a number from 1 to the number of tasks in the chromosome and it controls the order that tasks execute on the individual machines. The lower the number, the sooner the task will execute. The global scheduling order is independent of the task arrival times.

A chromosome represents a complete solution, i.e., resource allocation. Each chromosome is comprised of T genes, where T is the number of tasks that are present in the trace being studied. The i^{th} gene in every chromosome corresponds to the same task, in particular, the i^{th} task ordered based on task arrival times. To examine dominance relationships amongst the chromosomes in the population, each chromosome is individually evaluated with respect to utility earned and energy consumed. Because the global scheduling order is independent of task arrival times, we must ensure that any task's start time is greater than or equal to its arrival time. If this is not the case, the machine sits idle until this condition is met.

For populations and chromosomes to evolve from one generation to the next, the following crossover and mutation operations were implemented. For crossover, we first select two chromosomes uniformly at random from the population. Next, the indices of two genes

are selected uniformly at random from within the chromosomes. Finally, we swap all the genes between these two indices, from one chromosome to the other. In this operation, the machines the tasks execute on, and the global scheduling orders of the tasks are all swapped. The goal of this operation is to allow chromosomes making good scheduling decisions to pass on favorable traits to other chromosomes.

For the mutation operation, we randomly select a chromosome from the population. We then select a random gene from within that chromosome. We then mutate the gene by selecting a random machine that that task can execute on. Additionally, we select another random gene within the chromosomes and then swap the global scheduling order between the two genes.

Within a given population, a solution is ranked based on how many other solutions dominate it. If no other solutions dominate a solution, it is said to be nondominated and is given a rank of 1. A solution's rank can be found by taking *1 + the number of solutions that dominate it.* All solutions of rank 1 within a given population represent the current Pareto optimal set. The process of sorting the solutions is performed using the nondominating sorting algorithm, and is one step of the NSGA-II algorithm. A basic outline of the NSGA-II is taken from [39] and shown in Algorithm 1.

An important step to understand in the algorithm is the creation of offspring populations (step 3). We start with a parent population of size N. We then perform $N/2$ crossover operations (each crossover operation produces two offspring) to produce an initial offspring population also of size N. Next, the mutation operation is then performed with a probability (selected by experimentation) on each offspring within the population. If a mutation occurs, only the mutated offspring remains in the population.

Algorithm 1 NSGA-II algorithm from [39]

1: create initial population of N chromosomes
2: **while** termination criterion is not met **do**
3: create offspring population of size N
4: perform crossover operation
5: perform mutation operation
6: combine offspring and parent populations into a single meta-population of size $2N$
7: sort solutions in meta-population using nondominated sorting algorithm
8: take all of the rank 1, rank 2, etc. solutions until we have at least N solutions to be used in the parent population for the next generation
9: **if** more than N solutions **then**
10: for solutions from the highest rank number used, take a subset based on crowding distance [40]
11: **end if**
12: **end while**
13: the final population is the Pareto front used to show the trade-offs between the two objectives

We can now combine the parent and offspring population into a single meta-population of size $2N$ (step 6). This combining of populations allows elitism to be present within the algorithm, that is the algorithm keeps the best chromosomes from the previous generation and allows them to be evaluated in the current generation. From this new meta-population, we then select the next generation's parent population (steps 7, 8, 9, and 10). To create the new parent population, we need to select the best N chromosomes from the meta-population.

To illustrate this procedure, we provide the following example. Assume we currently have a parent population and offspring population, each with 100 chromosomes, which combines to make a meta-population with 200 chromosomes. We then perform the nondominated sorting algorithm from step 7. We find that we have 60 chromosomes of rank 1, 30 chromosomes of rank 2, 20 chromosomes of rank 3, and 90 chromosomes that have a rank higher than 3. We need to create a new parent population with only 100 chromosomes in it. First we take the 60 chromosomes that are rank 1 and place them into the new population. This leaves room for 40 more chromosomes. We then place the rank 2 chromosomes in the new population.

There is space in the population for 10 additional chromosomes. To select only 10 out of the 20 rank 3 chromosomes we use the method of crowding distance [40] to arrive at our full 100 chromosome population. Crowding distance is a metric that penalizes chromosomes that are densely packed together, and rewards chromosomes that are in remote sections of the solutions space. This operation creates a more equally spaced Pareto front.

3.5. Simulation Setup

3.5.1. Datasets and Experiments. To illustrate how our analysis framework allows system administrators to analyze the trade-offs between utility earned and energy consumed of a given system, we have conducted numerous simulations using three different sets of data.

The first set consists of the real historical ETC and EPC data gathered from the online benchmarks (nine machine types and five task types) [49]. This set only allotted one machine to each machine type and simulated 250 tasks comprised of the five task types arriving over a period of 15 minutes. We are performing a post-mortem static resource allocation as we are using a trace of a (simulated) system, thus the arrival times of all tasks are known *a priori*. This real data set is used as the basis for the second and third data sets, as described is Subsection 3.3.4.2.

The second and third sets consist of the ETC and EPC data manufactured from the real data (Subsection 3.3.4.2). For these sets, we created four special-purpose machine types for a total of 13 machine types and 25 additional task types for a total of 30 task types. Additionally, for both sets there were 30 machines across the 13 machine types. The break up of those machines can be seen in Table 3.3. Data sets 2 and 3 differ from one another by the number of tasks each set simulates. Set 2 simulates 1000 tasks arriving within the span of 15 minutes, while set 3 simulates 4000 tasks arriving within the span of an hour.

TABLE 3.3. Breakup of machines to machine types

machine type	number of machines
Special-purpose machine A	1
Special-purpose machine B	1
Special-purpose machine C	1
Special-purpose machine D	1
AMD A8-3870k	2
AMD FX-8159	3
Intel Core i3 2120	3
Intel Core i5 2400S	3
Intel Core i5 2500K	2
Intel Core i7 3960X	4
Intel Core i7 3960X @ 4.2 GHz	2
Intel Core i7 3770K	5
Intel Core i7 3770K @ 4.3 GHz	2

We conducted experiments on each data set. For the first group of experiments, we let the genetic algorithm execute for a given number of generations and then we analyze the trade-offs between utility earned and energy consumed. The second group of experiments compare the effect of using different seeds within the initial population on the evolution of the Pareto fronts. The seeding heuristics used for these experiments are described in the section below.

3.5.2. SEEDING HEURISTICS. Seeding heuristics provide the genetic algorithm with initial solutions that try to intelligently optimize one or both of the objectives. The seeds may help guide the genetic algorithm into better portions of the search space faster than an all random initial population. We implement the following four heuristics: Min Energy, Max Utility, Max Utility-per-Energy, and Min-Min Completion Time. The execution times of the greedy heuristics are negligible compared to the NSGA-II, making solutions found by these heuristics plausible to use. To use a seed within a population, we generate a new chromosome from one of the following heuristics. We place this chromosome into the population and create the rest of the chromosomes for that population randomly.

3.5.2.1. *Min Energy.* Min Energy is a single stage greedy heuristic that maps tasks to machines that minimize energy consumption. This heuristic maps tasks according to their arrival time. For each task the heuristic maps it to the machine that consumes the least amount of energy to execute the task. This heuristic will create a solution with the minimum possible energy consumption. Solutions may exist that consume the same amount of energy while earning more utility.

3.5.2.2. *Max Utility.* Max Utility is also a single stage greedy heuristic similar to the min energy heuristic except that it maps tasks to the machines that maximizes utility earned [4]. This heuristic must consider the completion time of the machine queues when making mapping decisions. There is no guarantee this heuristic will create a solution with the maximum obtainable utility.

3.5.2.3. *Max Utility-per-Energy.* Max Utility-per-Energy tries to combine aspects of the previous two heuristics. Instead of making mapping decisions based on either energy consumption or utility earned independently, this heuristic maps a given task to the machine that will provide the most utility earned per unit of energy consumed.

3.5.2.4. *Min-Min Completion Time.* Min-min completion time is a two-stage greedy heuristic that maps tasks to the machines that provide the minimum completion time [20, 53, 11]. During the first stage, the heuristic finds for every task the machine that minimizes that task's completion time. In the second stage, the heuristic selects from among all the task-machine pairs (from the first stage) the pair that provides the overall minimum completion time. That task is then mapped to that machine, and the heuristic repeats this operation until there are no more tasks to map.

3.6. Results

In Figures 3.3, 3.4, and 3.6 we show the location of numerous Pareto fronts. In each figure we show different fronts corresponding to different initial populations, for each of our three data sets respectively. Each of the four subplots show the Pareto fronts through a specific number of NSGA-II iterations. The x-axis is the number of megajoules consumed by the system, and the y-axis is the amount of utility earned by the system. Each marker within the subplots represents a complete resource allocation. Each marker style represents a different population. The diamond marker represents the population that contained the "Min Energy" seed, the square marker represents the population with the "Min-Min completion time" seed, the circle marker represents the population with the "Max Utility" seed, the triangle maker represents the population with the "Max Utility-per-Energy" seed, and finally the star marker represents the population with a completely random initial population. We also considered an initial population that contained all four of the seeding heuristics, but we found that this population performed similarly to the min-energy seeded population, and thus did not include it in our results.

Figure 3.3 shows the Pareto fronts for the real historical data set. For this data set we evaluated the evolution of the Pareto fronts through four different number of iterations; 100, 1000, 10,000, and 100,000 iterations. First, in the top left subplot we see that after 100 iterations the populations have formed distinct Pareto fronts covering various parts of the solution space. This occurs because of the use of the different seeds within each population. The presence of the seed within a population allows that population to initially explore the solution space close to where the seed originated. As the number of iterations increase though, the presence of the seed starts to become irrelevant because all the populations, even the all random initial population, start converging to very similar Pareto fronts.

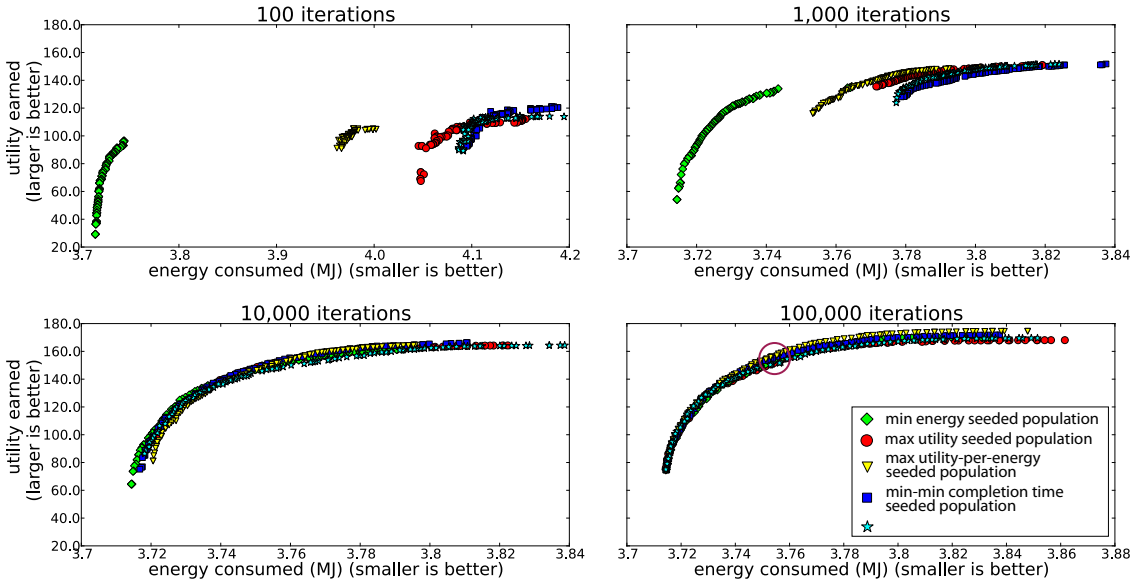

FIGURE 3.3. Pareto fronts of total energy consumed vs. total utility earned for the real historical data set (data set 1) for different initial seeded populations through various number of iterations. The circled region represents the solutions that earn the most utility per energy spent. The y-axis values are shared across subplots and while the x-axis values are specific to each subplot.

In the 100,000 iteration subplot, the region highlighted by the circle represents the solutions that earn the most utility per energy consumed. This circle does not represent the best solution in the front, because all solutions along the front are best solutions, each representing a different trade-off between utility and energy. The system administrator may not have energy to reach the circled solution, or may be willing to invest more energy for more utility. To the left of this region, the system can earn relatively larger amounts of utility for relatively small increases in energy. To the right of this region, the system could consume a relatively larger amount of energy but would only see a relatively small increase in utility.

A system administrator can use this bi-objective optimization approach to analyze the utility-energy trade-offs for any system of interest, and then set parameters, such as energy constraints, according to the needs of that system. These energy constraints could then be used in conjunction with a separate online dynamic utility maximization heuristics.

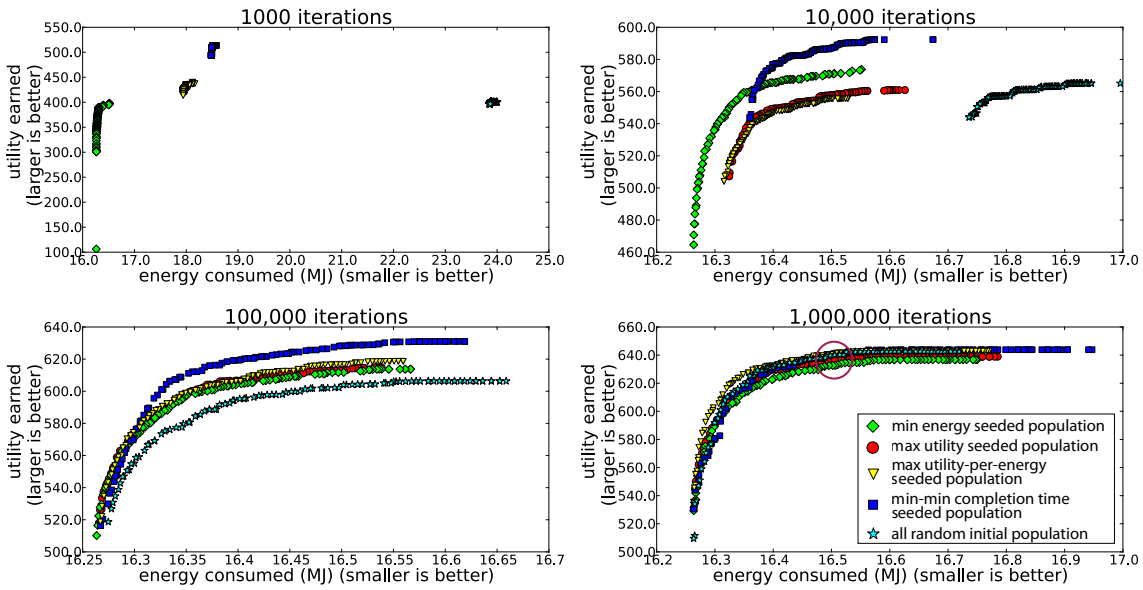

FIGURE 3.4. Pareto fronts of total energy consumed vs. total utility earned for the data set containing 1000 tasks (data set 2) for different initial seeded populations through various number of iterations. The circled region represents the solutions that earn the most utility per energy spent. Both the y-axis and x-axis values are specific to each subplot.

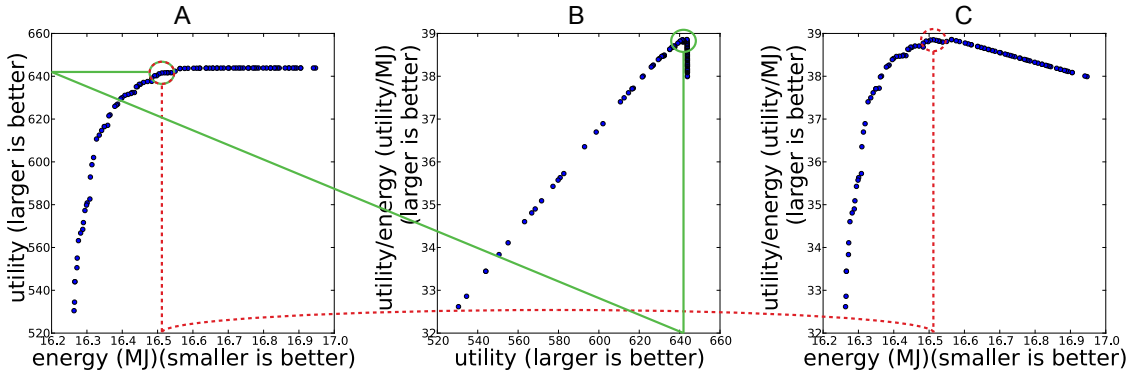

FIGURE 3.5. Subplot A shows the Pareto front through 1,000,000 iterations for the "max utility-per-energy" seeded population. The circled region represents the solutions that earn the most utility per energy spent. Subplot B provides the utility value that gives the highest utility earned per energy spent, shown by the solid line. Subplot C provides the energy value that gives the highest utility earned per energy spent, shown by the dashed line.

The Pareto fronts in Figure 3.4 illustrate the trade-offs between total energy consumed and total utility earned for the data set that contains 1000 tasks. These fronts were evaluated at 1000, 10,000, 100,000, and 1,000,000 iterations. We increased the number of iterations

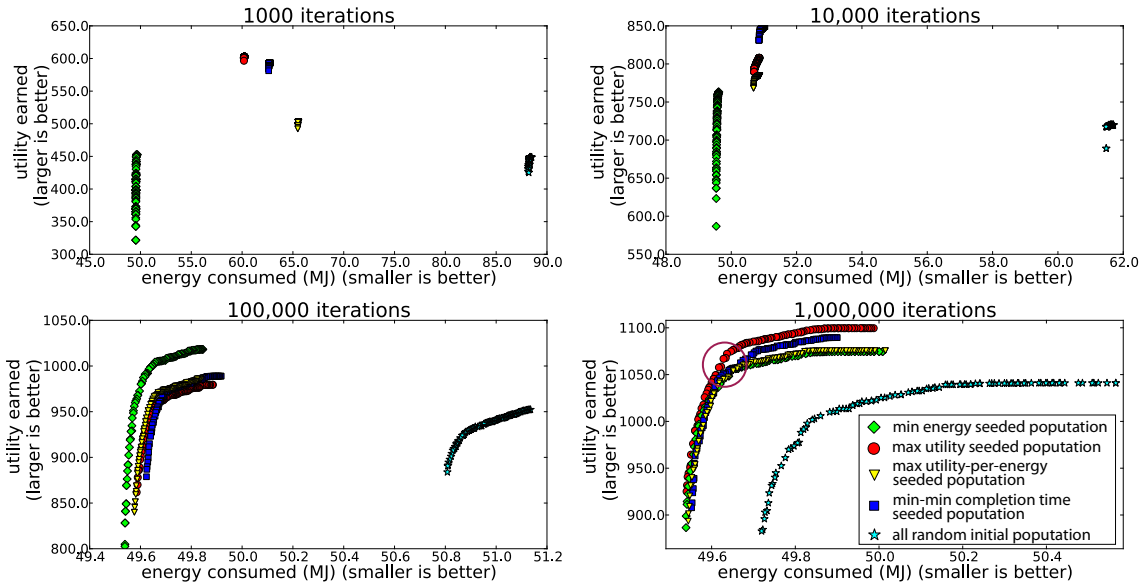

FIGURE 3.6. Pareto fronts of total energy consumed vs. total utility earned for the data set containing 4000 tasks (data set 3) for different initial seeded populations through various number of iterations. The circled region represents the solutions that earn the most utility per energy spent. Both the y-axis and x-axis values are specific to each subplot.

executed for this data set compared to the real historical data set because we are simulating a larger and more difficult problem.

Examining the top two subplots, we see the effect the initial seeds have on each of the populations. This provides the chance for system administrators to make some interesting observations about their systems. For example, the "min energy" population typically finds solutions that perform better with respect to energy consumption, while the "min-min completion time" population typically finds solutions that perform better with respect to utility earned. This analysis could provide insight into what type of dynamic heuristics could be used to either maximize utility or minimize energy depending on the needs of a given system. These subplots also show that using smart resource allocation seeds can produce better solutions in a limited number of iterations

In the lower two subplots, we see that all the populations have started to converge towards the same Pareto front. This allows us to find the region containing the solutions that earn the most utility per energy and can provide system administrators with valuable information about the trade-offs between the total energy consumed and the total utility earned of their specific systems. Figure 3.5 illustrates how the maximum utility per energy region is found. Subplot 3.5.A shows the final Pareto front for the "max utility-per-energy" seeded population. Subplot 3.5.B shows a plot of utility earned per energy spent vs. utility while Subplot 3.5.C shows a plot of utility earned per energy spent vs. energy. By locating the "peaks" in both these plots we can find the utility and energy values, respectively, for which utility earned per energy spent is maximized. We can then translate these values onto the Pareto front to find where this region is located. This is shown using the solid lines for utility and the dashed lines for energy.

Finally, Figure 3.6 contains the Pareto fronts for the largest of our three data sets (4000 tasks). This data set is also evaluated at 1000, 10,000, 100,000, and 1,000,000 iterations. Due to the larger size of this problem, it takes more iterations for the Pareto fronts to start converging. This allows us to see the benefit of using the seeds in the initial populations over the all random initial population. In all cases, our seeded populations are finding solutions that dominate those found by the random population. This occurs because the random initial population has to rely on only crossover and mutation to find better solutions, whereas the seeded populations have the advantage of a solution that is already trying to make smart resource allocation decisions.

Similar to the first two data sets, we see that Pareto fronts for this data set also exhibit a region where the amount of utility earned per energy spent is maximized. This is the

location where the system is operating as efficiently as possible, and can help guide system administrators in making decisions to try and reach that level of efficiency for their systems.

3.7. Conclusions

Rising costs of energy consumption and the push for greater performance make the need for energy-efficient computing very important as HPC continues to grow. To begin computing in an energy-efficient manner, system administrators must first understand the energy and performance characteristics of their systems. In this work, we have provided an analysis framework for investigating the trade-offs between total utility earned and total energy consumed. We have developed a method for creating a synthetic data set that preserves the heterogeneity characteristics of a data set constructed from real historical data.

We showed that by using the NSGA-II we can create well defined Pareto fronts and analyzed how using different seeding heuristics within the initial populations affected the evolution of the Pareto fronts. Finally, we tested our method using three data sets. The first data set contained only real data gathered from online benchmarks. The other two data sets contained synthetic data created from the real data to simulate a larger computing system. These two data sets differed in the number of tasks that were required to execute. Our method successfully illustrates the trade-offs between energy consumption and utility earned for all three data sets. Possible future work are mentioned in Chapter 6.

In summary we have designed an analysis framework that: 1) provides the ability to create synthetic data sets that preserve the heterogeneity measures found from real data sets, 2) provides the ability to take traces from any given system and then use our resource allocation heuristic and simulation infrastructure to plot and analyze the trade-offs between

total utility earned and total energy consumed, 3) find the region of the Pareto front where a given system is operating as efficiently as possible, and 4) show the effect different genetic algorithm seeds have for various systems, and how using seeds can create populations that dominate completely random populations.

CHAPTER 4

Energy Constrained Utility Maximization[3]

4.1. Introduction

During the past decade, large-scale computing systems have become increasingly powerful. As a result, there is a growing concern with the amount of energy needed to operate these systems [56, 57]. An August 2013 report by Digital Power Group estimates the global Information-Communications-Technologies ecosystem's use of electricity was approaching 10% of the world electricity generation [58]. As another energy comparison, it was using about 50% more energy than global aviation [58]. In 2007, global data center power requirements were 12 GW and in the four years to 2011, it doubled to 24 GW. Then, in 2012 alone it grew by 63% to 38 GW according to the 2012 DatacenterDynamics census [59]. Some data centers are now unable to increase their computing performance due to physical limitations on the availability of energy. For example, in 2010, Morgan Stanley, a global financial services firm based in New York, was physically unable to draw the energy needed to run a data center in Manhattan [60]. Many high performance computing (HPC) systems are now being forced to execute workloads with severe constraints on the amount of energy available to be consumed.

The need for ever increasing levels of performance among HPC systems combined with higher energy consumption and costs are making it increasingly important for system administrators to adopt energy-efficient workload execution policies. In an energy-constrained

[3]This work was done jointly with the Ph.D. student Ryan Friese. The full list of co-authors is at [54]. A preliminary version of portions of the work mentioned in this chapter appeared in [55]. This research used resources of the National Center for Computational Sciences at Oak Ridge National Laboratory, supported by the Extreme Scale Systems Center at ORNL, which is supported by the Department of Defense under subcontract numbers 4000094858 and 4000108022. This research also used the CSU ISTeC Cray System supported by NSF Grant CNS-0923386.

environment, it is desirable for such policies to maximize the performance of the system. This research investigates the design of energy-aware scheduling techniques with the goal of maximizing the performance of a workload executing on an energy-constrained HPC system.

Specifically, we model a compute facility and workload of interest to the Extreme Scale Systems Center (ESSC) at Oak Ridge National Laboratory (ORNL). The ESSC is a joint venture between the United States Department of Defense (DoD) and Department of Energy (DOE) to perform research and deliver tools, software, and technologies that can be integrated, deployed, and used in both DoD and DOE environments. Our goal is to design resource management techniques that maximize the performance of their computing systems while obeying a specified energy constraint. Each task has a monotonically-decreasing utility function associated with it that represents the task's utility (or value) based on the task's completion time. The system performance is measured in terms of cumulative utility earned, which is the sum of utility earned by all completed tasks [4]. The example computing environment we model, based on the expectations of future DoD and DOE environments, incorporates heterogeneous resources that utilize a mix of different machines to execute workloads with diverse computational requirements. We also create and study heterogeneous environments that are very similar to this example environment but have different heterogeneity characteristics, as quantified by a Task-Machine Affinity (TMA) measure [61]. TMA captures the degree to which some tasks are better suited on some unique machines. An environment where all tasks have the same ranking of machines in terms of execution time has zero TMA. In an environment with high TMA, different tasks will most likely have a unique ranking of machines in terms of execution time. It is important to analyze the impact on performance if the TMA of the environment is changed. We model and analyze the performance of low and high TMA environments compared to the example environment

based on interests of the ESSC. This analysis also can help guide the selection of machines to use in a computing system (based on the expected workload of tasks) to maximize the performance obtainable from the system.

In a heterogeneous environment, tasks typically have different execution time and energy consumption characteristics when executed on different machines. We model our machines to have three different performance states (P-states) in which tasks can execute. By employing different resource allocation strategies, it is possible to manipulate the performance and energy consumption of the system to align with the goals set by the system administrator. We develop four novel energy-aware resource allocation policies that have the goal of maximizing the utility earned while obeying an energy constraint over the span of a day. We compare these policies with three techniques from the literature designed to maximize utility [4, 3] and show that for energy-constrained environments, heuristics that manage their energy usage throughout the day outperform heuristics that only try to maximize utility. We enhance the resource allocation policies by designing an energy filter (based on the idea presented in [47]) for our environment. The goal of the filtering technique is to remove high energy consuming allocation choices that use more energy than an estimated fair-share. This step improves the distribution of the allotted energy across the whole day. We perform an in-depth analysis to demonstrate the benefits of our energy filter. We also study the performance of all the heuristics in the low and high TMA environments and perform extensive parameter tuning tests.

In summary, we make the following contributions: (a) the design of four new resource management techniques that maximize the utility earned, given an energy constraint for an oversubscribed heterogeneous computing system, (b) the design of a custom energy filtering mechanism that is adaptive to the remaining energy, enforces "fairness" in energy consumed

by tasks, and distributes the energy budgeted for the day throughout the day, (c) a method to generate new heterogeneous environments that have low and high TMA compared to the environment based on interests of the ESSC without changing any of its other heterogeneity characteristics, (d) show how heuristics that only maximize utility can become energy-aware by adapting three previous techniques to use an energy filter, (e) a sensitivity analysis for all the heuristics to the parameter that controls the level of energy-awareness and/or level of energy filtering, (f) an analysis of the performance of all the heuristics in the low and high TMA environments, and (g) a recommendation on how to select the best level of filtering or the best balance of energy-awareness versus utility maximization for heuristics based on a detailed analysis of the performance of our heuristics.

The remainder of this chapter is organized as follows. The next section formally describes the problem we address and the system model. Section 3 describes our resource management techniques. We then provide an overview of related work in Section 4. Our simulation and experimental setup are detailed in Section 5. In Section 6, we discuss and analyze the results of our experiments. We finish with our conclusion and plans for future work in Section 7.

4.2. Problem Description

4.2.1. System Model. In this study, we assume a workload where tasks arrive dynamically throughout the day and the scheduler maps the tasks to machines for execution. We model our workload and computing system based on the interests of the ESSC. Each task in the system has an associated utility function (as described in [4]). Utility functions are monotonically-decreasing functions that represent the task's utility (or value) of completing the task at different times. We assume the utility functions are given and can be customized by users or system administrators for any task.

Tasks are assumed to be independent (they do not require inter-task communication) and can execute concurrently (each on a single machine, possibly with parallel threads). This is typical of many environments such as [62]. We do not allow the preemption of tasks, i.e, once a task starts execution, it must execute until completion

Our computing system environment consists of a suite of heterogeneous machines, where each machine belongs to a specific machine type (rather than a single large monolithic system, such as Titan). Machines belonging to different machine types may differ in their microarchitectures, memory modules, and/or other system components. We model the machines to contain CPUs with dynamic voltage and frequency scaling (DVFS) enabled to utilize three different performance states (P-states) that offer a trade-off between execution time and power consumption. We group tasks with similar execution characteristics into task types. Tasks belonging to different task types may differ in characteristics such as computational intensity, memory intensity, I/O intensity, and memory access pattern. The type of a task is not related to the utility function of the task. Because the system is heterogeneous, machine type A may be faster (or more energy-efficient) than machine type B for certain task types but slower (or less energy-efficient) for others.

We assume that for a task of type i on a machine of type j running in P-state k, we are given the Estimated Time to Compute ($ETC(i,j,k)$) and the Average Power Consumption ($APC(i,j,k)$). It is common in the resource management literature to assume the availability of this information based on historical data or experiments [13–17, 63, 18]. The APC incorporates both the static power (not affected by the P-state of the task) and the dynamic power (different for different P-states). We can compute the Estimated Energy Consumption ($EEC(i,j,k)$) by taking the product of execution time and average power consumption, i.e., $EEC(i,j,k) = ETC(i,j,k) \times APC(i,j,k)$. We model general-purpose

machine types and special-purpose machine types [37]. The special-purpose machine types execute certain special-purpose task types much faster than the general-purpose machine types, although they may be incapable of executing the other task types. Due to the sensitive nature of DoD operations, for the ESSC environment, historical data is not publicly available. Therefore, for the simulation study conducted in this chapter, we synthetically create our ETC and APC matrices based on the recommendations provided by ESSC.

We model three degrees of heterogeneity by varying the level of Task-Machine Affinity (TMA) of the system [61]. TMA uses singular value decomposition (SVD) for its computation and captures the degree to which certain tasks execute faster on certain unique machines. Section 4.5.3.2 describes how TMA is computed. Task Difficulty Homogeneity (TDH) and Machine Performance Homogeneity (MPH) are given as orthogonal metrics for quantifying the heterogeneity of the system [61]. TDH and MPH capture the homogeneity in the aggregate performance of tasks and machines, respectively. We study the performance of all the heuristics in an example environment (based on the interests of the ESSC), a modified environment with low TMA, and a modified environment with high TMA. The low and high TMA environments differ only in their TMA compared to the example environment. All three environments have similar values of TDH and MPH.

In an environment with extremely low TMA, all tasks will have the same sorted ordering of machines in terms of execution time. The actual execution time values of different tasks on the machines can be different, but all the tasks will rank the machines in the same order. In contrast, in an extremely high TMA environment, each task will have a unique ordering of machines if the machines were to be sorted in terms of execution time for that task. Environments that have different TMA but similar MPH and TDH do not have more powerful or less powerful machines or more difficult or less difficult tasks in general,

but instead they differ in the level of uniqueness of the affinity of different tasks to the machines. An environment with higher TMA does not have more powerful machines, but instead has machines that are suited to perform well for different tasks. On the contrary, in an environment with lower TMA, it is easy to rank machines in terms of performance (irrespective of the tasks). It is desirable to analyze the performance of these different types of systems. Given the expected workload for an environment, such analyses can help guide the selection of resource management heuristics and associated tuning parameters in use. In Section 4.5.3.2, we describe our technique to create the relatively low and high TMA environments with negligible difference in the values of MPH and TDH of the system.

4.2.2. Problem Statement. Recall that we consider a workload model where tasks arrive dynamically. The scheduler does not know which task will arrive next, the utility functions of the task, nor its task type. The goal of the scheduler is to maximize the total utility that can be earned from completing tasks while satisfying an annual energy constraint. To simplify the problem, we divide the annual energy constraint into daily energy constraints and ensure that a given day's energy constraint is met. We can calculate an appropriately scaled value for a given day's energy constraint ($\underline{energy\ constraint_{day}}$) by taking the ratio of the total energy remaining for the year and the number of days remaining in the year. This reduces the problem to that of maximizing the total utility earned per day while obeying $energy\ constraint_{day}$. We use the duration of a day to keep the simulation time tractable. Instead of one day we could base our constraint on any interval of time (e.g., two hours, six months, a year). If a task starts execution on one day and completes execution on the next, the utility earned and the energy consumed for each day is prorated based on the proportion of the task's execution time in each day. This is done so that each day gets the utility for

the executions that consumed its energy to permit a fair comparison of different heuristic approaches. For ESSC, constraints on power (energy per second) are not a concern.

4.3. Resource Management

4.3.1. Overview. It is common to use heuristics for solving the task to machine resource allocation problem as it has been shown, in general, to be NP-complete [1]. A mapping event occurs any time a scheduling decision has to be made. We use batch-mode heuristics that trigger mapping events after fixed time intervals as they performed best in our previous work [4]. To account for oversubscription (i.e., more tasks arrive than can possibly be executed while they are still valuable), we use a technique that drops tasks with low potential utility at the current time. We also design an energy filter that helps guarantee the energy constraint by avoiding allocating tasks that use more than their "fair-share" of energy. Our simulation results show the benefit of this technique.

Mapping events for our batch-mode heuristics are triggered every minute. If the execution of the previous mapping event takes longer than a minute, then the next mapping event is triggered after the previous one completes execution. The task that is next-in-line for execution on a machine is referred to as the pending task. All other tasks that are queued for the machines are said to be in the virtual queues of the scheduler. Figure 4.1 shows a small example system with four machines, the executing tasks, the tasks in the pending slots, and the virtual queues of the scheduler. At a mapping event, the batch-mode heuristics make scheduling decisions for a set of tasks comprising the tasks that have arrived since the last mapping event and the tasks that are currently in the virtual queues. This set of tasks is called the mappable tasks set. The batch-mode heuristics are not allowed to remap the pending tasks so that the machines do not idle if the currently executing tasks complete

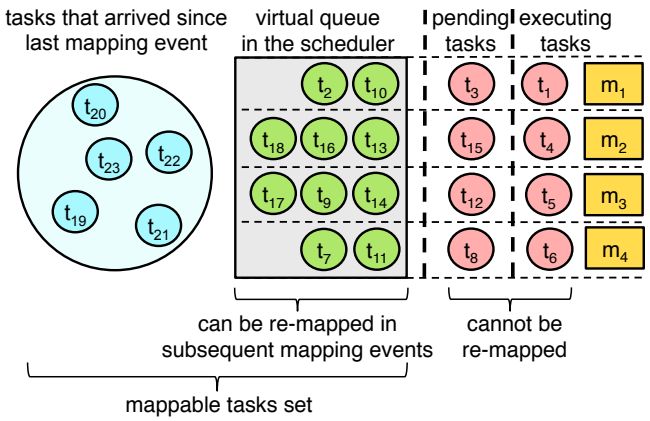

FIGURE 4.1. An example system of four machines showing tasks that are currently executing, waiting in pending slots, waiting in the virtual queue, and have arrived since the last mapping event (and are currently unmapped).

while the heuristic is executing. In this study, we adapt three batch-mode heuristics (from our previous work [4, 3]) to the new environment, design four new energy-aware batch-mode heuristics, and analyze and compare their performances.

The scheduling decisions made for a task may depend on the energy that currently remains in the system for the day (among other factors). The value of the per day energy constraint can change each day based on the energy that has been consumed thus far in the year. Therefore, we want to avoid making scheduling decisions for a task that starts its execution on the next day. Therefore, the batch-mode heuristics are not allowed to map a task to a machine where it will start execution on the next day. In addition, the batch-mode heuristics are not allowed to schedule a task that will violate the day's energy constraint.

If no machine can start the execution of the task within the current day or if the task will violate the current day's energy constraint, then the task's consideration is postponed to the next day. At the start of the next day, all postponed tasks are added to the mappable tasks set and the heuristics make mapping decisions for these tasks as well.

4.3.2. Batch-mode Heuristics. We present four new heuristics that try to maximize the utility earned while being energy-aware. The Max-Max Utility-Per-Energy consumption (**Max-Max UPE**) heuristic is a two-stage heuristic based on the concept of the two-stage Min-Min heuristic that has been widely used in the task scheduling literature [20, 21, 27, 25, 26, 64, 28, 10, 11, 30]. In the first stage, the heuristic finds for each task independently in the mappable tasks set the machine and P-state that maximizes "utility earned / energy consumption." If none of the machine-P-state choices for this task satisfy the day's energy constraint nor start the execution of the task within the current day, then, the task is postponed to the next day and removed from the mappable tasks set. In the second stage, the heuristic picks the task-machine-P-state choice from the first stage that provides the overall highest "utility earned / energy consumption." The heuristic assigns the task to that machine, removes that task from the set of mappable tasks, updates the machine's ready time, and repeats this process iteratively until all tasks are either mapped or postponed.

The Weighted Utility (**Weighted Util**) heuristic is designed to explicitly control the extent to which allocation decisions should be biased towards maximization of utility versus minimization of energy consumption. It does this by using a utility-energy weighting factor (*U-E weighting factor* or *U-E wf*) that controls the relative significance of normalized utility and normalized energy in the heuristic's objective function. To normalize the utility value across different allocation choices, we divide by the maximum utility any task in the system could have (*max util*). For normalizing energy consumption, we determine the highest EEC value from all possible task, machine, and P-state combinations (*max energy consumption*). The Weighted Util heuristic is also a two-stage heuristic. In the first stage, for each mappable

task, it finds the machine-P-state pair that has the highest value for the weighted expression:

$$(1 - \textit{U-E } wf) \times \frac{\textit{utility earned}}{\textit{max util}} - \textit{U-E } wf \times \frac{\textit{energy consumed}}{\textit{max energy consumption}}. \tag{6}$$

As done in Max-Max UPE, if no allocation choices for this task satisfy the day's energy constraint or start the execution of the task within the current day, then, the task is removed from the mappable tasks set and is postponed to be considered the next day. In the second stage, it picks from the pairs of the first stage the one that has the highest value for the above expression, makes that assignment, removes that task from the set of mappable tasks, updates that machine's ready time, and repeats the two stages iteratively until all tasks have either been mapped or postponed.

By normalizing the utility and the energy terms in the weighted expression, we ensure that each of those terms has a value between 0 and 1. This makes it convenient to compare utility and energy in a single expression as we do. The value of *U-E wf* can be varied between 0 and 1 to bias the effect of the normalized energy term to the value of the weighted expression.

The Weighted Utility-Per-Time (**Weighted UPT**) heuristic is similar to the Weighted Util heuristic but the normalized utility term in expression 6 is replaced by "normalized utility earned / normalized execution time." To normalize the execution time, we determine the minimum execution time in the ETC matrix from all task, machine, P-state choices (*min execution time*). The weighted expression for this heuristic is:

$$(1 - \textit{U-E } wf) \times \frac{\textit{utility earned/execution time}}{\textit{max util/min execution time}} - \textit{U-E } wf \times \frac{\textit{energy consumed}}{\textit{max energy consumption}}. \tag{7}$$

The Weighted Utility-Per-Energy consumption (**Weighted UPE**) heuristic is similar to the Weighted Util heuristic but the normalized utility term in expression 6 is replaced by "normalized utility earned / normalized energy consumption." To normalize energy, we determine the minimum energy consumption value in the EEC matrix from all task, machine, P-state choices (*min energy consumption*). The weighted expression for this heuristic is:

$$(1 - \textit{U-E } wf) \times \frac{\textit{utility earned/energy consumed}}{\textit{max util/min energy consumption}} - \textit{U-E } wf \times \frac{\textit{energy consumed}}{\textit{max energy consumption}}. \tag{8}$$

For comparison, we analyze the following three utility maximization heuristics to examine how heuristics that do not consider energy perform in an energy-constrained environment. These heuristics assign tasks while there still remains energy in the day.

The Min-Min Completion time (**Min-Min Comp**) heuristic is a fast heuristic adapted from [4] and is a two-stage heuristic like the Max-Max Utility-Per-Energy heuristic. In the first stage, this heuristic finds for each task the machine and P-state choice that completes execution of the task the soonest. This also will be the machine-P-state choice that earns the highest utility for this task (because we use monotonically-decreasing utility functions). In the second stage, the heuristic picks the task-machine-P-state choice from the first stage that provides the earliest completion time. This batch-mode heuristic is computationally efficient because it does not explicitly perform any utility calculations

The Max-Max Utility (**Max-Max Util**) heuristic introduced in [4] is also a two-stage heuristic like the Min-Min Comp heuristic. The difference is that in each stage Max-Max Util maximizes utility, as opposed to minimizing completion time. In the first stage, this heuristic finds task-machine-P-state choices that are identical to those found in the first stage of the Min-Min Comp heuristic. In the second stage, the decisions made by Max-Max

Util may differ from those of Min-Min Comp. This is because picking the maximum utility choice among the different task-machine-P-state pairs depends both on the completion time and the task's specific utility function.

The Max-Max Utility-Per-Time (**Max-Max UPT**) heuristic introduced in [3] is similar to the Max-Max Util heuristic, but in each stage it maximizes "utility earned / execution time," as opposed to maximizing utility. This heuristic selects assignments that earn the most utility per unit time, which can be beneficial in an oversubscribed system.

We collectively refer to the Weighted Util, Weighted UPT, and Weighted UPE heuristics as the weighted heuristics. We also collectively refer to the Min-Min Comp, Max-Max Util, Max-Max UPT, and Max-Max UPE heuristics as the non-weighted heuristics.

The weighted heuristics can be viewed as more generalized versions of their non-weighted counterparts. For example, the Weighted Util heuristic can be viewed as a more generalized version of the Max-Max Util heuristic. If *U-E* $wf = 0$, then Weighted Util reduces to Max-Max Util. For higher values of *U-E* wf, the Weighted Util heuristic is more energy-aware and has the goal of simultaneously maximizing utility while minimizing energy.

4.3.3. Dropping Low Utility Earning Tasks. We use a technique to drop tasks with low potential utility at the current time (introduced in our previous work [3]). Dropping a task means that it will never be mapped to a machine. This operation allows the batch-mode heuristics to tolerate high oversubscription. Due to the oversubscribed environment, if a resource allocation heuristic tried to have all tasks execute, most of the task completion times would be so long that the utility of most tasks would be very small. This would negatively impact users as well as the overall system performance. Given the performance measure is the total utility achieved by summing the utilities of the completed tasks, dropping tasks leads to higher system performance, as well as more users that are satisfied.

The dropping operation reduces the number of scheduling choices to consider and therefore at a mapping event the dropping operation is performed before the heuristic makes its scheduling decisions. When a mapping event is triggered, we determine the maximum possible utility that each mappable task could earn on any machine assuming it can start executing immediately after the pending task is finished. If this utility is less than a dropping threshold (determined empirically), we drop this task from the set of mappable tasks. If the utility earned is not less than the threshold, the task remains in the mappable tasks set and is included in the batch-mode heuristic allocation decisions.

Because of oversubscription in our environment, the number of tasks in the mappable tasks set increases quickly. This can cause the heuristic execution time to be long enough to delay the trigger of subsequent mapping events. This results in poor performance because it now takes longer for the heuristics to service any high utility earning task that may have arrived. By the time the next mapping event triggers, the utility from this task may decay substantially. By dropping tasks with low potential utility at the current time, we reduce the size of the mappable tasks set and enable the heuristics to complete their execution within the mapping interval time (a minute). This allows the heuristics to move any new high utility-earning task to the front of the virtual queue to complete its execution sooner.

If a batch-mode heuristic postpones a task to the next day, a check is performed to make sure that the maximum possible utility that the task could earn (at the start of the next day) is greater than the dropping threshold. If it is not, the task is dropped instead of being postponed.

4.3.4. Energy Filtering. The goal of our new energy filter technique is to remove potential allocation choices (task-machine-P-state combinations) from a heuristic's consideration if the allocation choice consumes more energy than an estimated fair-share energy

budget. We call this budget the *task budget*. The value of the *task budget* needs to adapt based on the energy remaining in the day and the time remaining in the day. Therefore, the value of the *task budget* is recomputed at the start of every mapping event. We do not recompute the value of the *task budget* within a mapping event (based on the allocations made by the heuristic in that mapping event) because we want the *task budget* to only account for execution information that is guaranteed to occur (i.e., executing and pending tasks).

We denote *energy consumed* as the total energy that has been consumed by the system in the current day, and *energy scheduled* as the energy that will be consumed by tasks queued for execution. At the start of a mapping event, the virtual queued tasks are removed from the machine queues and inserted into the mappable tasks set. Therefore, *energy scheduled* will account for the energy that will be consumed by all tasks that are currently executing and the tasks that are in the pending slot. The total energy that can be scheduled by heuristics (without violating the day's energy constraint) is denoted by *energy remaining*. It is computed using Equation 9.

$$\begin{aligned} \textit{energy remaining} = \textit{energy constraint}_{day} \\ - \textit{energy consumed} \\ - \textit{energy scheduled} \end{aligned} \tag{9}$$

To estimate the *task budget*, the filter also needs to compute the time remaining in the day within which the above energy can be consumed. The availability time of a machine is set to either the completion time of the last task to be queued for the machine or the current time, whichever is greater. At the start of the mapping event, the last task to be queued for

a machine will be the pending task. The total time remaining for computations (summed across machines) in the day is denoted as the *aggregate time remaining*. We compute it by summing across machines the difference between the end time of the day and the availability time of the machine. Figure 4.2 shows its computation for an example small-scale system with three machines. As shown, even though machine m3 is not executing a task after time 16, the available compute time from that machine is obtained by taking the difference between end of the day and the current time.

The average of the execution time values of all task types, machine types, and P-states is represented as *average execution time*. The energy filtering technique needs to estimate the total number of tasks that can be executed in the remaining part of the day. It does this by taking the ratio of *aggregate time remaining* and *average execution time*. The energy filter has to use *average execution time* because the scheduler is unaware of the type of tasks that may arrive or which machine or P-state they will be assigned to for the rest of the day.

To adjust the value of the *task budget* around its estimate, we use a multiplier called *energy leniency*. Higher values of the *energy leniency* imply more leeway for high energy allocation choices to pass through the filter, whereas a low value for the *energy leniency* would filter out many more choices. This value is determined empirically. The *task budget* is computed using Equation 10.

$$task\ budget = energy\ leniency \times \frac{energy\ remaining}{\left(\frac{aggregate\ time\ remaining}{average\ execution\ time}\right)} \tag{10}$$

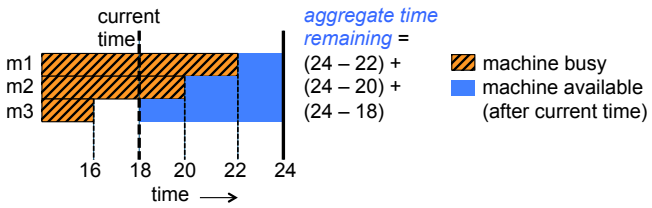

FIGURE 4.2. An example system of three machines showing the computation of *aggregate time remaining*. It represents the total computation time available from the current time till the end of the day.

This *task budget* is recomputed at the start of each mapping event and is an estimate of the amount of fair-share energy that we want an execution of a task to consume. At each mapping event, the heuristics consider only those task-machine-P-state allocation choices that consume less energy than the *task budget*.

4.4. Related Work

Heterogeneous task scheduling in an energy-constrained computing environment is examined in [10]. The authors model an environment where devices in an ad-hoc wireless network are limited by battery capacity and each task has a fixed priority. This differs significantly for our environment where we model a larger and more complex heterogeneous system with a utility performance metric based on the exact completion time of each task rather than a metric that aims to finish more higher priority tasks, as in their work. Additionally, in our study, the energy available for use under the constraint is shared across all resources, while in [10] each resource has its own energy constraint (a battery).

In [4] and [3], the concept of utility functions to describe a task's time-varying importance is introduced. The authors deal with the problem of maximizing the total utility that can be earned from task completions. Energy is not considered at all in those papers. In this work, we are concerned with maximizing utility while obeying an energy constraint. For accomplishing this, we design four new energy-aware heuristics and an energy filtering

technique that adapts to the remaining energy. We perform extensive analysis of all the heuristics along with parameter tuning tests. We also create low and high TMA environments and examine the performance of the heuristics in these environments.

An energy-constrained task scheduling problem in a wireless sensor network environment is studied in [65]. The authors analyze how the presence of an energy constraint affects the schedule length (i.e., makespan) when executing a set of dependent tasks. A wireless sensor network is significantly different from the environment we are modeling. In our model, each task contributes a certain amount of utility to the system. We are not concerned with minimizing a schedule length, as tasks continuously arrive through out the day.

In [66], a set of dynamically arriving tasks with individual deadlines are allocated to machines within a cluster environment with the goal of conserving energy. Specifically, the authors try to optimize the energy consumption while meeting the constraint of completing all tasks by their deadlines. Our environment tries to maximize the total utility earned while operating under an energy constraint. Additionally, [66] uses constant arrival patterns in an undersubcribed system, while our work focuses on highly oversubscribed environments where tasks arrive in varying sinusoidal or bursty patterns.

A dynamic resource allocation problem in a heterogeneous energy-constrained environment is studied in [47]. Tasks within this system contain individual deadlines, and the goal is to complete as many tasks by their individual deadlines as possible within an energy constraint. This is a different problem from our work as we are trying to maximize the utility earned (based on each task's completion time) and not the number of tasks that meet their hard deadlines. The authors of [47] use heuristics that map each task to a machine as soon as the task arrives and do not allow remapping, whereas in our environment we map groups of tasks at a time, allowing us to use more information when making allocation decisions

and can also remap tasks in the virtual queue. The concept of an energy filter is used in [47], and we build on that for a more complex filter.

In [67], the authors formulate a bi-objective resource allocation problem to analyze the trade-offs between makespan and energy consumption. Their approaches use total makespan as a measure of system performance as opposed to individual task utility values as we do in our work. Additionally, they model static environments where the entire workload is a single bag-of-tasks, unlike our work that considers a system where tasks arrive dynamically. In our work, we consider maximizing the utility earned while meeting an energy constraint whereas [67] does not consider an energy constraint in its resource allocation decisions.

4.5. Simulation Setup

4.5.1. Overview. We simulate the arrival and mapping of tasks over a two day span with the first day used to bring the system up to steady-state operation. We collect our results (e.g., total utility earned, energy consumed) only for the second day to avoid the scenario where the machines start with empty queues. We average the results of our experiments across 48 simulation trials. Each of the trials represents a new workload of tasks (with different utility functions, task types, and arrival times), and a different computing environment by using new values for the entries in the ETC and APC matrices (but without changing the number of machines). All of the parameters used in our simulations are set to closely match the expectations for future environments of interest to the ESSC.

4.5.2. Workload Generation. A utility function for each task in a workload is given and each task has a maximum utility value that starts at one of 8, 4, 2, or 1. These values are based on the plans of the ESSC, but for other environments, different values of maximum utility may be used. Furthermore, for our environment we have four choices of

maximum utility but in other environments greater or fewer choices may be used. A method for generating utility functions can be found in [4, 3].

For our simulation study, we generate the arrival patterns to closely match patterns of interest to ESSC [3]. In this environment, general-purpose tasks arrive in a sinusoidal pattern and special-purpose tasks follow a bursty arrival pattern.

4.5.3. Execution Time and Power Modeling.

4.5.3.1. *Example Environment.* This example environment is based on the expectation of some future DoD/DOE environments. In our simulation environment, approximately 50,000 tasks arrive during the duration of a day and each of them belongs to one of 100 task types. Furthermore, each task's utility function is generated using the method in [3]. The compute system that we model has 13 machine types consisting of a total of 100 machines. Among these 13 machine types, four are special-purpose machine types while the remaining are general-purpose machine types. Each of the four special-purpose machine types has 2, 2, 3, and 3 machines on them, respectively, for a total of ten special-purpose machines. The remaining 90 machines are general-purpose and are split into the remaining nine machine types as follows: 5, 5, 5, 10, 10, 10, 10, 15, and 20. The machines of a special-purpose machine type run a subset of special-purpose task types approximately ten times faster on average than the general-purpose machines can run them (as discussed below). The special-purpose machines do not have the ability to run tasks of other task types. In our environment, three to five special-purpose task types are special for each special-purpose machine type.

We assume that all machines have three P-states in which they can operate. We use techniques from the Coefficient of Variation (COV) method [36] to generate the entries of the ETC and APC matrices in the highest power P-state. The mean value of execution time on the general-purpose and the special-purpose machine types is set to ten minutes and one

minute, respectively. The mean value of the static power for the machines was set to 66 watts and the mean dynamic power was set to 133 watts. To generate the dynamic power values for the intermediate P-state and the lowest power P-state, we scale the dynamic power to 75% and 50%, respectively, of the highest power P-state. The execution time for these P-states are also generated by scaling the execution time of the highest power P-state. To determine the factor by which we will scale the execution time of the highest power P-state for the intermediate and lowest power P-states, we sample a gamma distribution with a mean value that is approximately $1/\sqrt{(\%\ scaled\ in\ power)}$. For example, the lowest power P-state's execution time will be scaled by a value sampled from a gamma distribution that has a mean approximately equal to $1/\sqrt{0.5}$. The execution time of any task is guaranteed to be the shortest in the highest power P-state, but the most energy-efficient P-state can vary across tasks. These are done to model reality where the impact on execution time and energy consumption by switching P-states depends on the CPU-intensity/memory-intensity of the task, overhead power of the system, etc. We refer to this set of matrices as the example environment.

4.5.3.2. *Low and High TMA Environments.* We modify the ETC matrices at the highest power P-state of the example environment to create low and high TMA environments with minimal difference in the MPH and TDH of the environments. All three of these measures are functions of the Estimated Computation Speed (ECS) matrices. An ECS matrix is created by taking the reciprocal of each entry in the ETC matrix. Figure 4.3 shows two 3×3 ECS matrices that significantly differ in TMA but would have the same value for TDH. In the high TMA ECS matrix, each task has a unique ranking of the machines in terms of speed of execution.

To make the TMA measure orthogonal to the MPH and TDH measures, alternate row and column normalizations are performed on the ECS matrix so that the matrix has equal row sums and equal column sums (called a standard matrix) before the TMA is computed for the ECS matrix [61]. As mentioned in [61], this iterative procedure is not guaranteed to converge to a standard matrix if the ECS matrix can be organized into a block matrix (after reordering rows and columns) with one block containing only 0s. Such a matrix is said to be decomposable [61]. In our environment, the entries in the ECS matrix for the special-purpose machines and the tasks that are not special on them contain 0s (because the special-purpose machines are unable to execute them), and therefore, our ECS matrices are decomposable. To overcome this problem, we remove the columns of the special-purpose machines from the matrices and compute the TMA of only the general-purpose-machines matrix that has the general-purpose machines. We then modify this part of the ECS matrix to have low and high TMA. For each of the low and high TMA matrices, we then obtain the values for the special-purpose tasks (on the one machine on which they are special) by taking the average of the entries of this task from the general-purpose-machines matrix and multiplying that average speed by 10. By doing this, we retain the characteristics of the special-purpose machines and tasks as desired by the ESSC at ORNL, but we are able to study the performance of the heuristics in environments with different TMA. The TMA of the general-purpose-machines ECS matrices do not capture the actual TMA of the whole environment. However, as we are only concerned with creating relatively low and high TMA matrices compared to the example environment, our computation of the TMA measure is valid for our purposes.

As mentioned in [61], after a standard matrix is obtained (by performing alternate row and column normalizations), the first step for computing the TMA of the matrix is to determine the SVD. An ECS matrix with T task types and M machine types has dimension

very low TMA	machine1	machine 2	machine 3
task 1	25	10	5
task 2	25	10	5
task 3	25	10	5

high TMA	machine1	machine 2	machine 3
task 1	25	10	5
task 2	5	25	10
task 3	10	5	25

FIGURE 4.3. Two sample 3×3 ECS matrices that have equal Task Difficulty Homogeneity but very different values of Task Machine Affinity. In the matrix with the high TMA, each task has a unique ranking of machines in terms of execution speed, i.e., for task 1 the best to worst machines are: 1, 2, and 3, whereas for task 2 the ranking of machines would be: 2, 3, and 1. In contrast, in the very low TMA matrix, all tasks would have the same ranking of machines.

$T \times M$. The SVD results in the factorization $U\Sigma V^T$. The U and V^T are orthogonal matrices representing the column and the row space, respectively. The matrix Σ is a diagonal matrix consisting of $min(T, M)$ singular values ($\underline{\sigma_i}$) along the diagonal in a monotonically decreasing order, i.e., $\sigma_1 \geq \sigma_2 \geq ... \geq \sigma_{min(T,M)} \geq 0$. The singular values represent the degree of correlation (linear dependence) between the columns of the ECS matrix. The higher the first singular value (σ_1), the more correlated the columns of the matrix are. The higher the other singular values ($\sigma_2, \sigma_3, ..., \sigma_{min(T,M)}$), the less correlated all the columns are. When the correlation in the columns of the ECS matrix is low (i.e., high TMA), most tasks will have unique ranking of the machines in terms of execution speed. Alternatively, when the correlation in the columns of the ECS matrix is high (i.e., low TMA), most tasks will have the same ranking of machines in terms of execution speed performance. The TMA of the matrix is defined as the average of all the non-maximum singular values (i.e., not including σ_1) of the standard matrix:

$$TMA = \sum_{i=2}^{min(T,M)} \sigma_i/(min(T,M)-1). \tag{11}$$

For creating the low TMA matrices, we want to have an environment where the columns of the ECS matrix are completely correlated. We do this by removing the effect of all non-maximum singular values and only retain the characteristics of the first singular value. This is equivalent to taking the rank-1 approximation of the ECS matrix (i.e., make all the non-maximum singular values to be equal to 0).

For creating the high TMA matrices, simply increasing the non-maximum singular values or decreasing the maximum singular value will typically result in matrices with negative values or result in very little increase in the TMA. Negative values in an ECS matrix are meaningless representations of execution speed of a task on a machine and are therefore undesirable. We design an iterative method to increase the components of the ECS matrix in the directions that result in higher TMA while making sure that negative values are never introduced into the matrix. To do this, we first take the SVD of the ECS matrix A. Let u_1, u_2, u_3, etc., represent the columns of the U matrix and let v_1^T, v_2^T, v_3^T, etc., represent the rows of the V^T matrix resulting from the SVD of A. Our goal is to increase the non-maximum singular values (without introducing negative values) to get a new ECS matrix with a higher TMA. We examine how much of the matrix resulting from the product of u_2 and v_2^T we can add to A, without making any of the elements in the matrix negative. We then do this with u_3 and v_3^T, and continue to do this iteratively for all the non-maximum singular values. This allows one to increase the TMA of the environment without having any negative values in the matrix.

These procedures to create low and high TMA environments ensure that only the TMA of the environment is affected while maintaining the other characteristics of the matrix. The MPH and the TDH of the low and high TMA environments have negligible difference compared to that of the example environment. Table 4.1 shows the range of TMA values for the matrices of the example environment and also of the low and high TMA environments (that we created using our technique described above). Recall that the construction of these TMA environments are for simulation experiments to evaluate the heuristics. They are not part of the heuristics or system model.

TABLE 4.1. Range of Task-Machine Affinity (TMA) Values for the 48 Simulation Trials of the Different Environments

type of ETC	**TMA range**
example environment	0.082 to 0.091
low TMA	$< 10^{-15}$
high TMA	0.14 to 0.18

4.5.4. OBTAINING AN ENERGY CONSTRAINT. In many real-world scenarios, an annual energy budget is typically given for an HPC system. As mentioned in Section 4.2.2, we can estimate the energy constraint of the current day using a given annual energy constraint to help ensure each day uses an equal portion of the remaining energy from the annual budget.

For simulation purposes, we need to create an energy constraint that we can use to analyze our resource management techniques. We first run Max-Max UPT (the heuristic that provides the best utility earned from our previous work [3]) for a full 24-hour time period, disregarding the energy constraint. Based on the resource allocations generated by this heuristic, we average the total energy consumption throughout the day across 48 simulation trials and use 70% of this average value as our energy constraint. We obtain the simulated annual energy constraint by multiplying this value by the number of days in a

year. For our simulations, we used a value of 405.84 GJ for the year, which averages out to 1.11 GJ per day.

4.6. Results

4.6.1. Overview. All results shown in this section display the average over 48 simulation trials with 95% confidence interval error bars (the simulator uses two 24 core nodes on the Colorado State University ISTeC Cray HPC cluster [62]). We first discuss the performance of the heuristics in the energy-constrained environment when not using the energy filtering technique. All the heuristics used a dropping threshold of 0.5 units of utility to tolerate the oversubscription, i.e., a task is dropped if the best possible utility it can earn is lower than 0.5. We use a dropping threshold of 0.5 units of utility as it gave the best performance in our previous work [3]. When selecting a dropping threshold, we must consider the level of oversubscription of the environment in addition to the utility values of tasks. We then examine the effect of the filtering mechanism on the heuristics with a sensitivity study and an analysis of the performance. We then analyze the performance of the heuristics in the relatively low and the high TMA environments and finally compare the best performing case for all the heuristics in the different types of environments.

4.6.2. Example Environment Results in No-Filtering Case. Figure 4.4 shows the total utility earned by the heuristics in the filtering and no-filtering cases. We first discuss the performance of the heuristics in the no-filtering case. Our four new heuristics outperform the heuristics from the literature (i.e., Min-Min Comp, Max-Max Util, and Max-Max UPT). Among the non-weighted heuristics, Max-Max UPE earns the highest utility even though it consumes the same amount of energy as the others. This is because the heuristic accounts for energy consumption while trying to maximize utility, and thus is able to avoid high

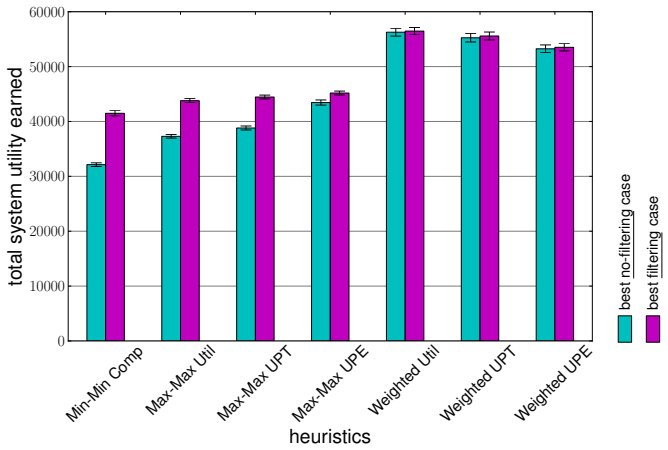

FIGURE 4.4. Total utility earned by the heuristics in the no-filtering case and their best filtering case (case with the best performing value of *energy leniency*). For the weighted heuristics, in both the cases, the best performing *U-E weighting factor* was chosen. The simulated system has 100 machines and approximately 50,000 tasks arriving in the day. These results are for the example environment. The results are averaged over 48 trials with 95% confidence intervals.

energy-consuming allocation choices without significantly affecting the utility earned. Once the allotted energy for the day ($energy\ constraint_{day}$) is consumed, the heuristics were not allowed to map any more tasks until the following day.

The weighted heuristics perform much better than the other heuristics because of their ability to balance the extent to which they want to bias their allocations towards utility maximization versus energy minimization. For each of the weighted heuristics, tests were performed with different values of the *U-E weighting factor* from 0.02 to 0.8. A higher *U-E weighting factor* biases the allocation decisions more towards energy minimization. Figures 4.5a and 4.5b show the total utility earned by the Weighted Util and Weighted UPT heuristics for different values of the *U-E weighting factor*. Similarly, Figures 4.6a and 4.6b show the total energy consumption by the Weighted Util and Weighted UPT heuristics for different values of the *U-E weighting factor*. Weighted UPE showed similar trends as the Weighted UPT heuristic.

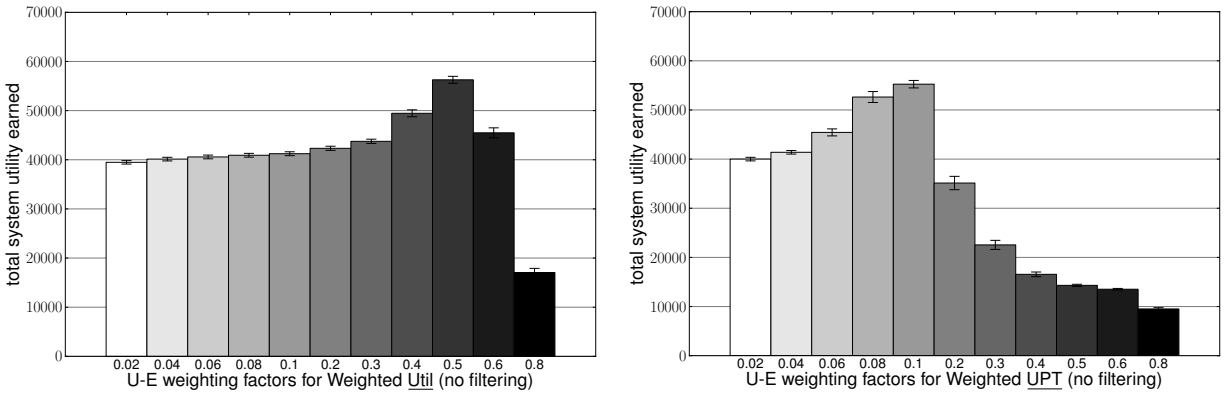

(A) (B)

FIGURE 4.5. Tests showing the total utility earned in the no-filtering case as the *U-E weighting factor* is varied for (a) Weighted Util and (b) Weighted UPT. The simulated system has 100 machines and approximately 50,000 tasks arriving in the day. These results are for the example environment. The results are averaged over 48 trials with 95% confidence intervals.

As we vary the *U-E weighting factor* from 0.02 to 0.8, the utility earned by the weighted heuristics increases and then decreases. At very low values of the *U-E weighting factor*, the energy term in the weighted expression has very little impact and the Weighted Util and Weighted UPT heuristics approaches the Max-Max Util and Max-Max UPT heuristics, respectively. With very high values of the *U-E weighting factor*, the heuristics are too conservative in their energy expenditure and only execute tasks that consume the least energy with little regard to the utility being earned. As can be seen in Figures 4.5a and 4.5b, the best performance is obtained between these extremes. For the Weighted Util heuristic, the best performance is obtained at a *U-E weighting factor* that is larger than the best performing *U-E weighting factor* for the Weighted UPT and Weighted UPE heuristics. This is because the Weighted Util heuristic completely depends on the energy term in the weighted expression to be energy-aware. The Weighted UPE and the Weighted UPT heuristics already are able to account for energy minimization (directly or indirectly) using the first part of their weighted expression, and therefore need a smaller portion of the

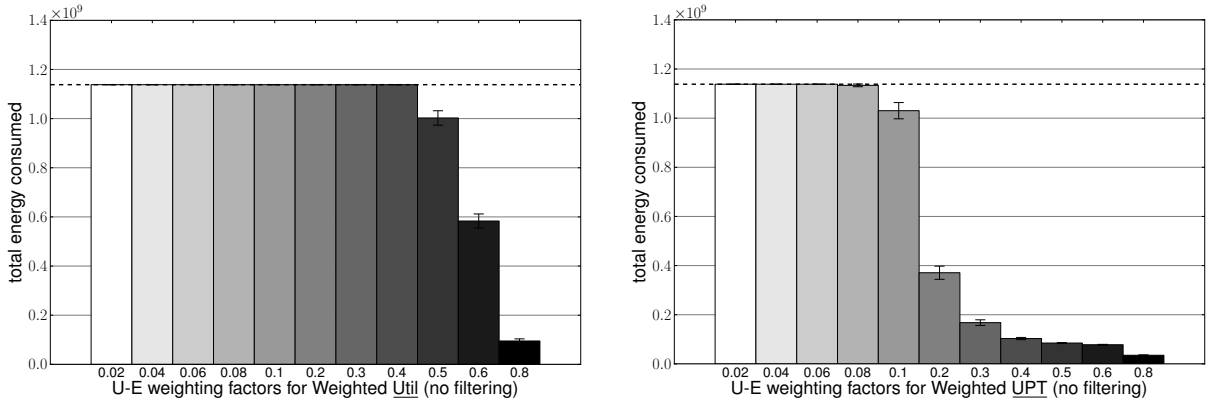

(A) (B)

FIGURE 4.6. Tests showing the total energy consumption in the no-filtering case as the *U-E weighting factor* is varied for (a) Weighted Util and (b) Weighted UPT. The dashed horizontal line shows the energy constraint of the system. The simulated system has 100 machines and approximately 50,000 tasks arriving in the day. These results are for the example environment. The results are averaged over 48 trials with 95% confidence intervals.

energy term to help make good low energy consuming choices. The energy consumption by these heuristics always hits the energy constraint for the weighting factors lower than the best performing weighting factor. Higher values of the *U-E weighting factor* further minimize energy consumption (so it unnecessarily goes below the constraint) leading to reduced performance.

To illustrate why *U-E weighting factor* of 0.5 is the best for the Weighted Util heuristic, Figures 4.7a and 4.7b show the trace of the total utility being earned and the trace of the total energy consumption for the Weighted Util heuristic in the no-filtering case for different values of the *U-E weighting factor*. For *U-E weighting factors* 0.4 and lower, the energy constraint is hit before the end of the day and therefore high utility-earning tasks that arrive after that point in time are unable to execute. This causes a drop in performance because no utility is earned from such tasks after this point. Values of *U-E weighting factor* higher

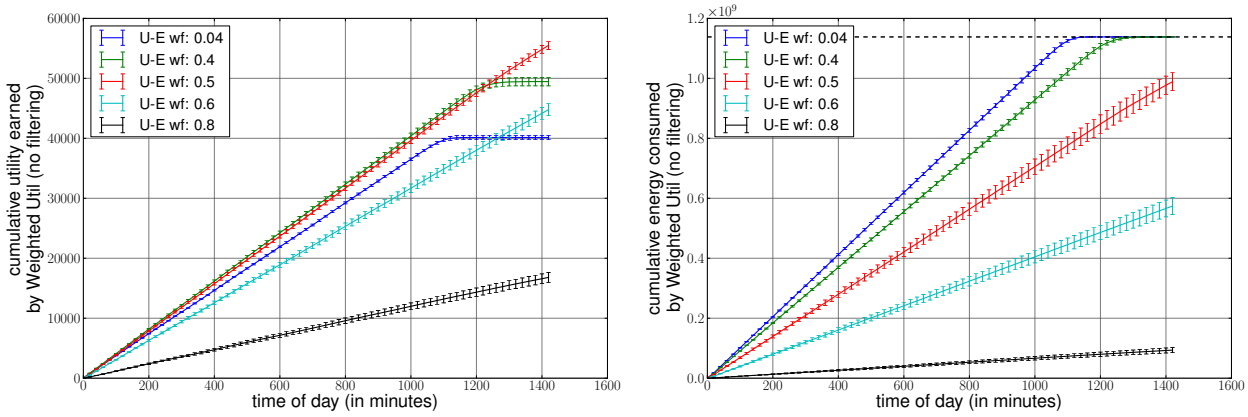

(A) (B)

FIGURE 4.7. Traces of (a) the cumulative utility earned and (b) the cumulative energy consumption for the Weighted Util heuristic in the no-filtering case throughout the day at 20 minute intervals at different *U-E weighting factors*. The dashed horizontal line in (b) shows the energy constraint of the system. The simulated system has 100 machines and approximately 50,000 tasks arriving in the day. These results are for the example environment. The results are averaged over 48 trials with 95% confidence intervals.

than 0.5 are too conservative in energy consumption and have too much energy left over at the end of the day.

These results indicate that for energy-constrained environments it is best to use heuristics that consider energy, rather than heuristics that try to solely optimize for maximizing utility. In the no-filtering case, Weighted Util is approximately 28% better than Max-Max UPE, and Max-Max UPE is approximately 11% better than Max-Max UPT (the best-performing utility maximization heuristic from the literature [3]).

4.6.3. EXAMPLE ENVIRONMENT RESULTS WITH ENERGY FILTERING. We now examine the effect of the energy filtering mechanism on the batch-mode heuristics. The extent to which energy filtering is performed is controlled by the *energy leniency* term (see Equation 10). A higher value for the *energy leniency* would result in a higher value of the *task budget* and would therefore let more allocation choices pass through the filter. Alternatively, a lower value of *energy leniency* would let fewer allocations pass through the filter. Not using

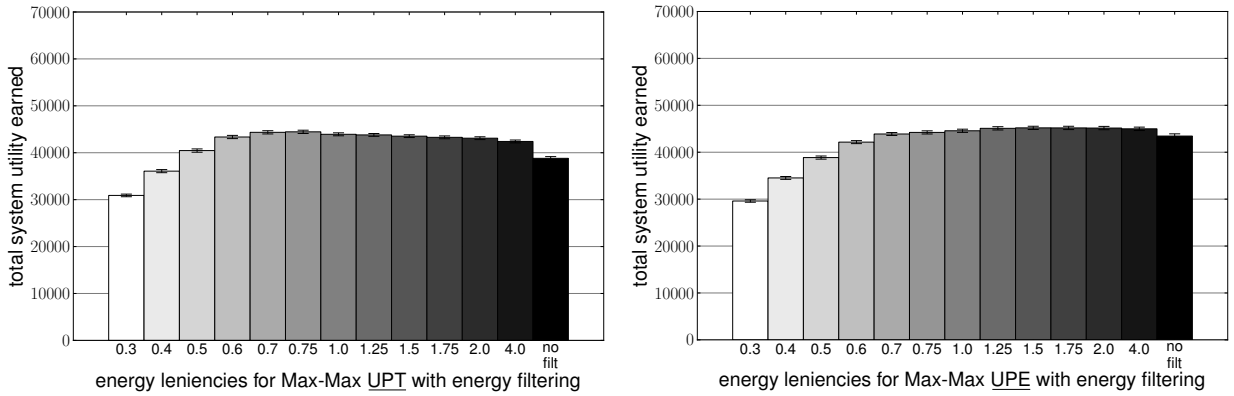

(A) (B)

FIGURE 4.8. Sensitivity tests showing the total utility earned as the *energy leniency* is varied for (a) Max-Max UPT and (b) Max-Max UPE. The simulated system has 100 machines and approximately 50,000 tasks arriving in the day. These results are for the example environment. The results are averaged over 48 trials with 95% confidence intervals.

filtering implies an *energy leniency* value of infinity. We performed a sensitivity test for all the heuristics by varying the value of *energy leniency* from 0.3 to 4.0, and compared the performance with the no-filtering case. We first analyze the performance of the non-weighted heuristics in Section 4.6.3.1, and then examine the weighted heuristics in Section 4.6.3.2.

4.6.3.1. *Non-weighted Heuristics.* Figures 4.8a and 4.8b show the effect of varying the value of *energy leniency* on the total utility earned by the Max-Max UPT and the Max-Max UPE heuristics, respectively. Figure 4.9 shows the energy consumption of the Max-Max UPE heuristic as the *energy leniency* value is varied. Sensitivity tests of the utility earned for the Min-Min Comp and Max-Max Util heuristics show trends similar to that of the Max-Max UPT heuristic, while the sensitivity tests of the energy consumed for Min-Min Comp, Max-Max Util, and Max-Max UPT showed trends similar to Max-Max UPE.

In general, for the non-weighted heuristics, as we increase the value of *energy leniency* from 0.3, the utility earned increases and then decreases as we approach the no-filtering case. All of these heuristics benefit from the filtering operation. The best-performing case

for Min-Min Comp, Max-Max Util, and Max-Max UPT occurs at an *energy leniency* of 0.75, whereas the Max-Max UPE heuristic performance peaks at an *energy leniency* of 1.5. We observe that the performance benefit for the Max-Max UPE heuristic is less sensitive to the value of *energy leniency*, especially in the range 1.0 to 4.0. The drop in performance for this heuristic in the no-filtering case (compared to its best performance case) is less substantial than the similar difference for the other heuristics. This is because the Max-Max UPE heuristic already accounts for energy consumption, reducing the benefits associated with the energy filter. Therefore, the best-performing case of *energy leniency* for this heuristic is at a higher value of *energy leniency* than the best-performing case for the other heuristics. The other heuristics require a stricter filtering technique to incorporate energy consumption in allocation choices, therefore they require lower values of *energy leniency* to obtain the best results, because energy is not considered otherwise.

For the non-weighted heuristics, when we use *energy leniency* values from 0.3 to 0.6, the filtering is so strict that it prevents the heuristic from using all of the available energy that was budgeted for the day. Not being able to use all of the budgeted energy results in fewer tasks being executed and therefore a drop in the total utility earned throughout the day. Alternatively, when using high values of *energy leniency* (and the no-filtering case), all heuristics use all of the day's budgeted energy early in the day and thus are unable to execute tasks that arrive in the later part of the day. We are able to observe this using trace charts that show the gain in total utility and increase in total energy consumption.

Figures 4.10a and 4.10b show the utility trace for the Max-Max UPT and the Max-Max UPE heuristics, respectively. Figures 4.11a and 4.11b show the energy trace for the Max-Max UPT and the Max-Max UPE heuristics, respectively. For the no-filtering case, we see that the system uses all of the available energy for the day in the early part of the day,

and then all future tasks are unable to execute and are dropped from the system earning no utility. The no-filtering case for the Max-Max UPE heuristic uses all available energy that was budgeted for the day slightly later (approximately three hours) than the Max-Max UPT heuristic because the heuristic considers energy at each mapping event throughout the day. The slope of its no-filtering energy consumption trace is less steep than the slope of the similar trace for the Max-Max UPT heuristic. As a result, Max-Max UPE is able to execute more tasks and earn higher utility.

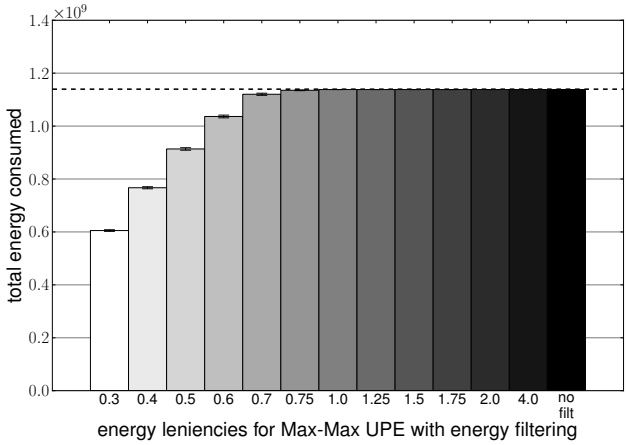

FIGURE 4.9. Sensitivity tests showing the total energy consumed as the *energy leniency* is varied for the Max-Max UPE heuristic. The dashed horizontal line shows the energy constraint of the system. The simulated system has 100 machines and approximately 50,000 tasks arriving in the day. These results are for the example environment. The results are averaged over 48 trials with 95% confidence intervals.

The energy trace charts show the adaptive ability of the filtering technique. Recall the task budget is dependent on the *aggregate time remaining* and the *energy remaining*. When comparing low values of *energy leniency* to high values of *energy leniency*, the *energy remaining* will be similar at the beginning of the day, but later in the day, there will be more energy remaining for low values compared to the lower energy remaining for higher values. Therefore, because the *task budget* will change with the energy remaining, it will

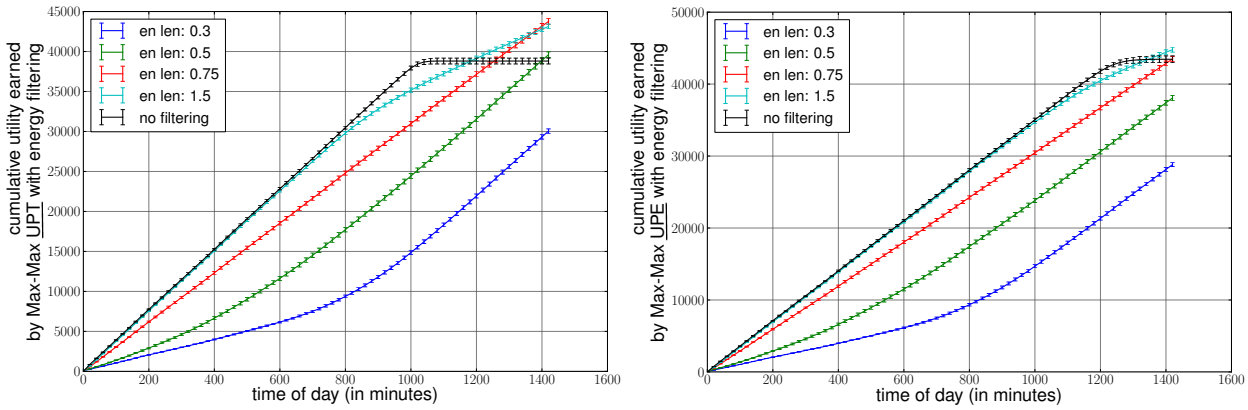

(A) (B)

FIGURE 4.10. Traces of the cumulative utility earned throughout the day at 20 minute intervals as the *energy leniency* (en len) is varied for the (a) Max-Max UPT and (b) Max-Max UPE heuristics. The simulated system has 100 machines and approximately 50,000 tasks arriving in the day. These results are for the example environment. The results are averaged over 48 trials with 95% confidence intervals.

become larger when there is more energy remaining in the day and smaller when there is less energy remaining in the day. For example, the slope increases for the *energy leniency* line of 0.3 during the day in Figures 4.11a and 4.11b. Similarly, with high values of *energy leniency*, the filter eventually adapts to lower its value of *task budget*. This is shown by the decrease in slope for the 1.5 *energy leniency* line in Figures 4.11a and 4.11b.

The best performance for each of the non-weighted heuristics comes at an appropriate *energy leniency* that allows the total energy consumption of the heuristic to hit the energy constraint of the day right at the end of the day, saving enough energy for any high-utility earning tasks that may arrive at later parts in the day. Higher values of *energy leniency* (above 1.5) result in the energy constraint being hit in the earlier part of the day, while lower values of *energy leniency* can result in a strict environment that prevents the consumption of all of the energy budgeted for the day. Therefore, in energy-constrained environments, the best performance is obtained by permitting allocation choices with a fair-share of energy so

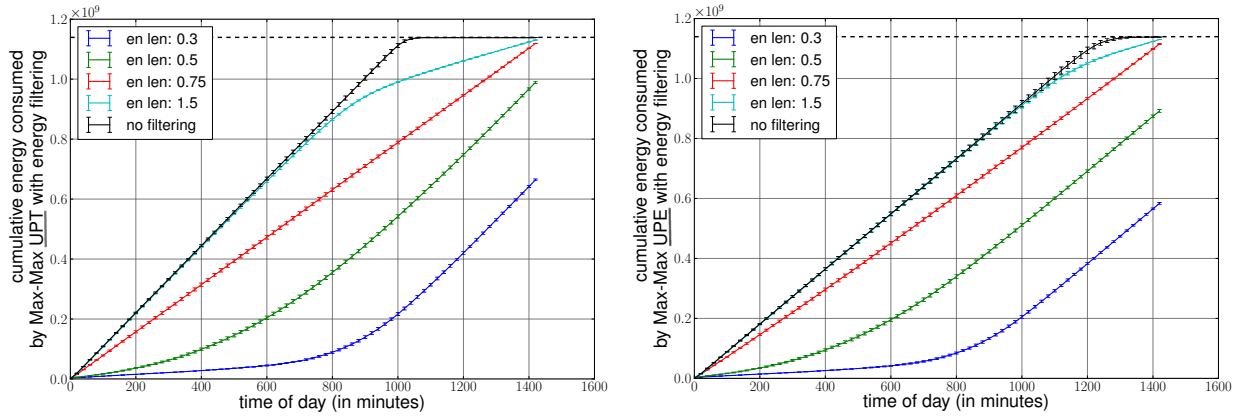

FIGURE 4.11. Traces of the cumulative energy consumed throughout the day at 20 minute intervals as the *energy leniency* (en len) is varied for the (a) Max-Max UPT and (b) Max-Max UPE heuristics. The dashed horizontal line shows the energy constraint of the system. The simulated system has 100 machines and approximately 50,000 tasks arriving in the day. These results are for the example environment. The results are averaged over 48 trials with 95% confidence intervals.

that the total energy consumption for the day hits the energy constraint right at the end of the day. By doing so relatively low utility-earning tasks that arrive early in the day do not consume energy that could be used by relatively higher utility-earning tasks arriving later in the day. If the energy consumption is not regulated, then the allocations in the earlier part of the day can consume too much energy preventing task executions later in the day. Our energy filtering technique gives this ability to these heuristics.

Among the non-weighted heuristics, Max-Max UPE performs the best and its performance is the least sensitive to the value of *energy leniency*. These are because this heuristic accounts for the energy consumed to earn each unit of utility. The performance of all the non-weighted heuristics improves because of the energy filtering technique. When designing an energy filter for a heuristic in an oversubscribed environment, the best performance is likely to be obtained when the level of filtering is adjusted to distribute the consumption of the energy throughout the day and meet the constraint right at the end of the day. This can

be used to design filters for such heuristics in energy-constrained environments to maximize performance.

4.6.3.2. *Weighted Heuristics.* The weighted heuristics already have the ability to tune their energy consumption throughout the day and therefore they do not benefit from the energy filtering technique, as shown in Figure 4.4. Figure 4.12 shows the utility earned by the Weighted Util heuristic for different combinations of *U-E weighting factor* and *energy leniency*. As seen in Figure 4.6a, even in the no-filtering case, the Weighted Util heuristic did not consume the total energy budgeted for the day with *U-E weighting factors* 0.5 and above. Therefore, adding energy filtering (that may further limit the energy consumption) to these cases does not help to improve the performance of the heuristic in comparison to the no-filtering case. Using moderate values of *energy leniency* helps in cases where we use lower *U-E weighting factors*, because in these cases, the weighting factor alone is unable to accomplish the desired level of energy minimization. At the best performing *U-E weighting factor* (i.e., 0.5 for Weighted Util), the no-filtering case performs just as well as the best performing *energy leniency* cases.

Both, the filtering technique and the weighting technique, have the ability to regulate the energy consumption throughout the day and allow the energy constraint to be hit only at the end of the day, but the weighting technique performs better than the filtering technique. We now analyze why the best performing *U-E weighting factor* (without any energy filtering, i.e., *energy leniency* of infinity) performs better than the best performing energy filtering case (without using any weighting, i.e., *U-E weighting factor* $= 0$). To study this difference, we plot the utility and energy trace charts of the Weighted Util heuristic for the following three scenarios:

(1) no filtering (*energy leniency* = infinity) and no weighting (*U-E weighting factor* = 0),

(2) best filtering case (*energy leniency* = 0.75) and no weighting, and

(3) no filtering and best weighting case (*U-E weighting factor* = 0.5).

These trace charts are shown in Figures 4.13a and 4.13b. Recall that without the weighting i.e., a *U-E weighting factor* of 0, the weighted heuristics reduce to their non-weighted counterparts (e.g. Weighted Util becomes Max-Max Util).

The weighting case outperforms the filtering case because of two reasons. Each of these reasons can be explained by examining the trace up to the point where the no filtering-no weighting case hits the energy constraint at approximately 1000 minutes. Recall that the no filtering-no weighting case is only attempting to maximize utility with no regard to energy. The first reason why the weighting performs better than the filtering is because the filtering removes allocation choices that consume more energy than the fair-share *task budget* (of a mapping event) without considering the utility that that allocation choice may earn. This causes the filtering case to avoid certain high energy consuming (but high utility earning) allocation choices to execute. This can be seen by the lower values of utility being earned by the heuristic in the filtering case compared to the no filtering-no weighting case up to 1000 minutes. The weighting case does not have this problem as it is able to rank choices in terms of both the utility they earn and the energy they consume. So, if an allocation choice consumes high energy but proportionally earns high utility then this allocation choice may be a viable option in the weighting case. Weighting, if tuned correctly, allows the heuristic to balance the required amount of energy minimization versus utility maximization. The second reason why the weighting case performs better is because the weighting case biases decisions to pick low energy consuming allocation choices, and in our environment this also

leads to minimization of execution time. Therefore, Weighted Util gets the ability to make allocations that behave as utility-per-time. Because of the minimization of execution time, we observed that the weighting case was able to complete many more tasks compared to the no filtering-no weighting case. This causes the heuristic's weighting case to earn higher utility than the unconstrained no filtering-no weighting case even in the region up to 1000 minutes.

The weighting and filtering techniques both allow a heuristic to regulate its energy consumption throughout the day and permit task executions in the later part of the day that help them to earn more utility than a case that does not use either weighting or filtering. Filtering does not attempt to minimize energy consumption, it only tries to prune high energy consuming choices. It makes its filtering mechanism stricter or more lenient if the energy consumption rate is higher or lower than what it should ideally be, respectively. As opposed to this, weighting works by attempting to minimize energy consumption right from the start of the allocation process. It picks allocation choices that have a good balance of earning utility versus consuming energy.

Figure 4.4 shows the total utility earned by the heuristics in the no-filtering case and their best *energy leniency* case. The non-weighted heuristics have a significant performance increase with the energy filtering because it allows them to control their energy expenditure throughout the day. The weighted heuristics already have the ability to control their energy consumption and therefore do not have any increase in performance when using energy filtering.

4.6.4. Low and High TMA Environment Results with Filtering. We ran similar experiments as mentioned thus far for all the heuristics with the low and high TMA

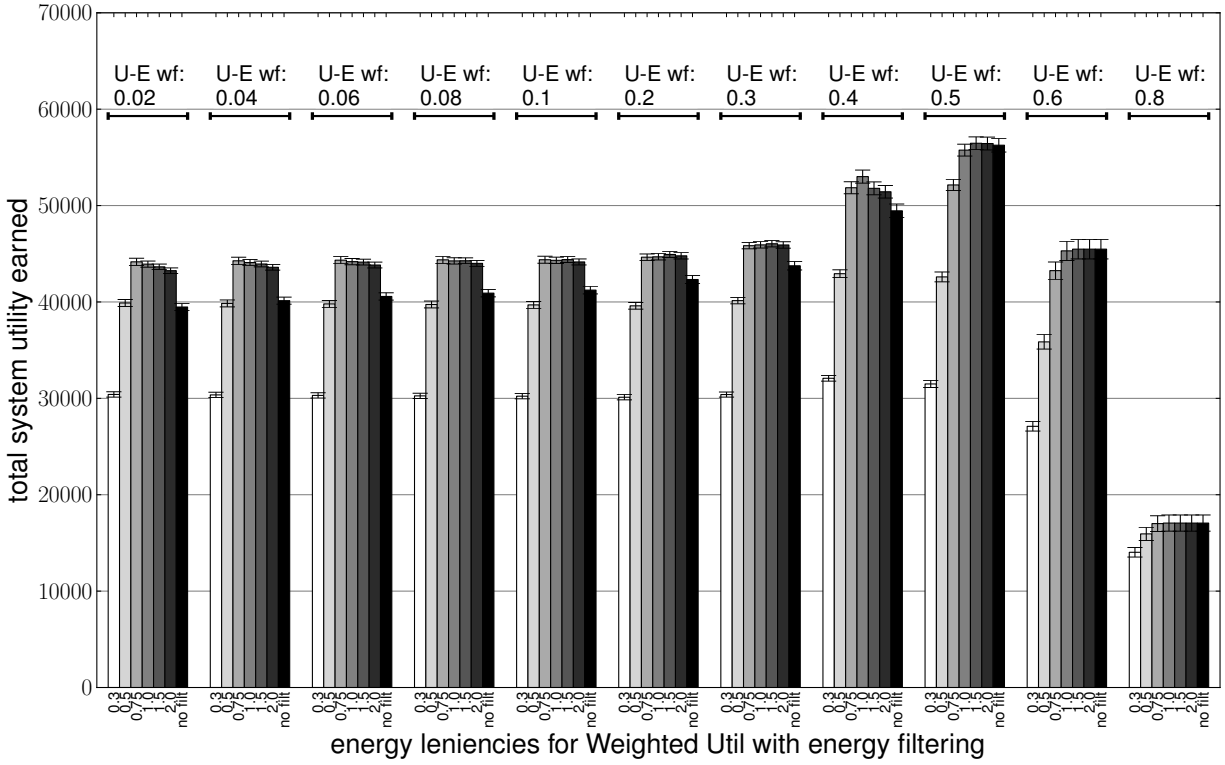

FIGURE 4.12. Sensitivity tests showing the total utility earned for different combinations of *U-E weighting factor* (U-E wf) and *energy leniency* for the Weighted Util heuristic. The simulated system has 100 machines and approximately 50,000 tasks arriving in the day. These results are for the example environment. The results are averaged over 48 trials with 95% confidence intervals.

environments. These environments have the same set of task utility functions, task arrival times, oversubscription levels, dropping threshold, overall aggregate performance of the machines and tasks with similar values of MPH and TDH compared to the example environment. The only difference is the TMA of the environment, and that affects the uniqueness by which certain task types execute faster on certain machine types. In the low TMA environment, all tasks have the same ranking of machines in terms of execution time, whereas in the high TMA environment, most tasks have unique ranking of the machines in terms of execution time performance. We ran parameter tuning tests to find the best performing *energy leniency* case for the non-weighted heuristics and the best performing

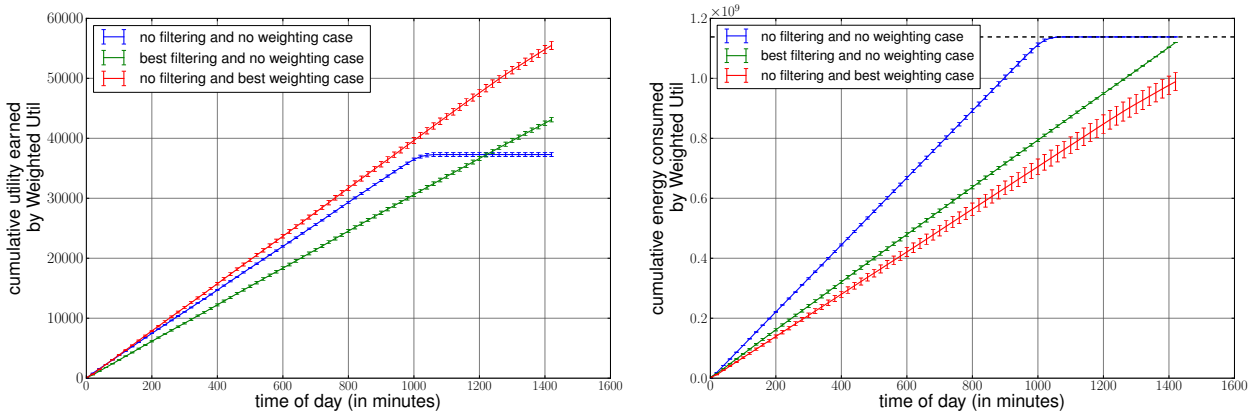

(A) (B)

FIGURE 4.13. Traces of (a) the cumulative utility earned and (b) the cumulative energy consumption throughout the day at 20 minute intervals of different cases of using the best/not using energy filtering and/or weighting for the Weighted Util heuristic. The dashed horizontal line in (b) shows the energy constraint of the system. The simulated system has 100 machines and approximately 50,000 tasks arriving in the day. These results are for the example environment. The results are averaged over 48 trials with 95% confidence intervals.

energy leniency and *U-E weighting factor* case for the weighted heuristics. Here, we summarize the conclusions obtained from these tests. The actual results of the tests are omitted from the draft for brevity.

For the non-weighted heuristics in the low TMA environment, the best performance was obtained at a higher value of *energy leniency*. This was because in the low TMA environments, as all tasks have the same ranking of the machine types in terms of execution time, fewer tasks get to execute on the machines where they have better execution times. On average, this results in longer task execution times than that in the example environment. Therefore, the *average execution time* estimate is not as accurate as it was in the example environment. To compensate for this, the best performance is obtained at higher values of *energy leniency*. See Equation 10 for understanding how an increase in *energy leniency* helps to make up for the lower value of the *average execution time* estimate.

For the weighted heuristics in the low TMA environment, the best performance was obtained at lower values of the *U-E weighting factor* (i.e., more weighting towards utility term) compared to the *U-E weighting factors* for the best case in the example environment. The energy term of the weighted expression does not account for how oversubscribed the machine is. In a low TMA environment, all tasks would have the same ranking of machine-P-state choices in terms of energy consumption. Assigning all tasks to these energy efficient machines would oversubscribe them resulting in low utility being earned from the tasks. By having a lower value for the *U-E weighting factor*, the preferred allocation choice would be less biased towards the minimization of energy consumption, therefore allowing for a better load balance in a low TMA environment.

In contrast, in high TMA environments, the non-weighted heuristics performed their best at lower values of *energy leniency*. In such environments, different tasks have different ranking of the machine types in terms of execution time and this makes it easier for tasks to be assigned to their best execution time machine type. As a result, the estimate of the *average execution time* (calculated based on ETC values) is not as accurate as it was in the example environment. The best performance is obtained at lower values of *energy leniency* as that helps to compensate for the higher value of the *average execution time* estimate.

For the weighted heuristics, in high TMA environments, the best performance is obtained at higher values of *U-E weighting factor* (i.e., more weighting towards energy term). This is because in the high TMA environment, different tasks would generally have different machine-P-state choices that execute fast and consume less energy. Therefore, biasing the scheduling decisions more towards the minimum energy consumption choices provides automatic load balancing across the machine types and assigns tasks to the machine types that execute them the best (i.e., quickest and least energy consuming).

Figure 4.14a shows the utility earned by the best performing case of each of the heuristics in the low and high TMA environments in comparison to the best performance obtained in the example environment. The overall trend is that heuristics earn less utility in the low TMA environment and more utility in the high TMA environment compared to the example environment. This is because in the low TMA environment, all tasks have the same machine type as their best execution time machine type and as a result fewer tasks get to execute on the machines of this type. This leads to longer execution times on average for the tasks and results in fewer tasks being pushed through the system during the day. Alternatively, in the high TMA environment, different task types execute fastest on different machine types, and therefore, assigning tasks to their best execution time machine type is feasible as it implicitly provides load balancing. In such an environment, the average execution time of the tasks is lower and more tasks complete execution during the day earning higher utility overall. In high TMA environments, resource allocation decisions are easier to make (as minimizing execution time provides some load balancing) and therefore the performance of all the heuristics is quite similar. Although, the weighted heuristics still perform slightly better than their non-weighted counterparts. Figure 4.14b shows that compared to the example environment, the number of tasks completed for the low TMA environment is significantly fewer while the number of tasks completed for the high TMA environment is significantly greater. The average execution time of a task across the machines (taken from the ETC) is similar for the low and example environment and slightly higher for the high TMA environment. We still get better performance in the high TMA environment from all the heuristics because of the diversity in the tasks' execution time performance across machine types.

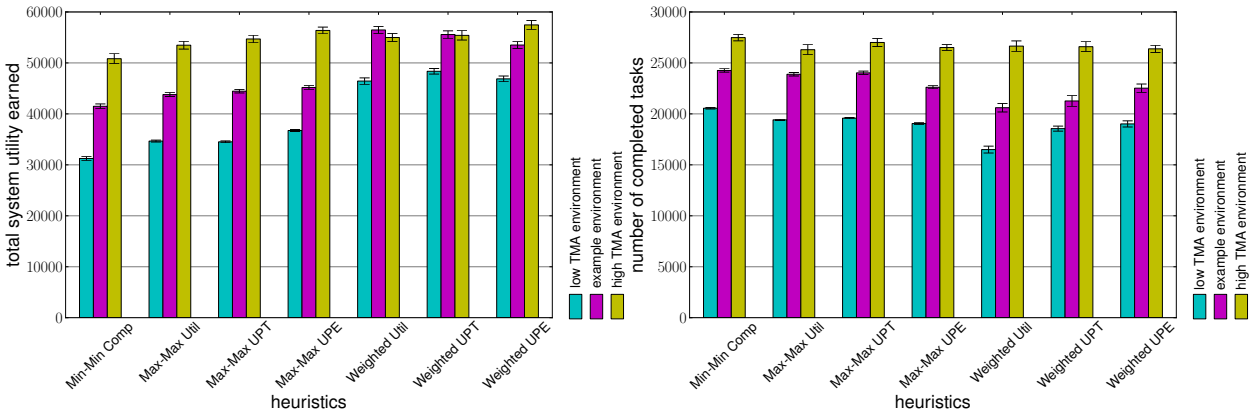

(A) (B)

FIGURE 4.14. (a) Total utility earned and (b) Total number of completed tasks by the best performing cases for all the heuristics with energy filtering in the three types of environments: low TMA, example, and high TMA. The simulated system has 100 machines and approximately 50,000 tasks arriving in the day. The results are averaged over 48 trials with 95% confidence intervals.

4.7. Conclusions and Future Work

In this study, we address the problem of energy-constrained utility maximization. We model an oversubscribed heterogeneous computing system where tasks arrive dynamically and are mapped to machines for execution. The system model is designed based on types of systems of interest to DoD/DOE. A heuristic's performance in our system is measured in terms of the total utility that it could earn from task completions. We design four heuristics for this problem and compare their performance with other heuristics adapted from our previous work, and integrate an energy filtering technique into our environment.

We show that in an energy-constrained environment our energy-aware heuristics earns more utility than heuristics that only optimize for utility. Our new energy filter helps to improve the performance of all the non-weighted heuristics by distributing the consumption of the budgeted energy throughout the day. The energy filtering technique adapts to the energy remaining in the system and accordingly budgets the permitted energy for a task's execution. For the non-weighted heuristics, the best performance from the filtering is obtained

for all heuristics at a level of filtering that distributes energy consumption approximately equally throughout the day and meets the energy constraint right at the end of the day. This can be used to guide the design of heuristics and filtering techniques in oversubscribed heterogeneous computing environments.

The weighted heuristics have the ability to minimize energy consumption throughout the day and can be tuned so that their energy consumption meets the energy constraint right at the end of the day. These heuristics outperform their non-weighted counterparts (even when they use energy filtering). This is because, filtering considers energy regardless of utility while weighting considers them together. The filtering removes certain high energy-consuming allocation choices, but among the remaining choices it simply picks the one that maximizes the objective of the heuristic. Alternatively, the weighted heuristics rank all allocation choices by accounting for both utility and energy and have the ability to balance the degree to which they are energy-aware. As a result, these heuristics perform much better than the non-weighted heuristics (even when they use filtering).

In the low and high TMA environments, all the heuristics earn lower and higher utility overall, respectively. This is because the higher the TMA of the environment, the higher the number of tasks that can be completed because more tasks can be assigned to the machine on which they have the fastest execution time. This is because assigning tasks to their best execution time machine implicitly balances the load. Also, in high TMA environments, we observe that mapping decisions are easier to make and most heuristics perform similarly.

One of the main goals of this study was to perform an in-depth analysis of the performance of the energy-constrained heuristics. As part of future work, we plan to use our knowledge of the performance of the heuristics, filtering, and weighting techniques to design adaptive techniques that can auto-tune the value of *energy leniency* and/or *U-E weighting factor*

dynamically. Other possible directions for future research include: (1) designing energy-aware robust resource allocation techniques that account for various sources of uncertainty, such as stochastic task execution times, (2) creating different patterns for the arrival of utility into the system (e.g., high utility tasks arriving for certain fixed times of the day) and designing techniques that can account for and adapt to these changes, (3) designing heuristics that use the information about the slope of the utility-functions to make allocation decisions, and (4) considering workloads of dependent and parallel tasks to broaden the scope of this work.

CHAPTER 5

Resource Allocation Policies in Environments with Random Failures[4]

5.1. Introduction

High performance and distributed computing systems are currently used to solve a host of scientific problems. Many of the applications running on these systems are time-critical. Examples of such applications include meteorological workflows, influenza modeling, economic forecasting, storm surge modeling, and monitoring or modeling the hazardous effects of oil spills or airborne contaminants. These kinds of applications typically have hard deadlines, and their results are not useful if unavailable by the deadline. The large-scale computing systems needed to run such applications currently have high failure rates and these are estimated to become more pronounced as the size of high performance computing systems approach exa-scale levels. Further, these computing systems are often oversubscribed, that is, the workload of tasks submitted exceeds the capacity of the system. In such an environment, it is important to make resource allocation decisions that both tolerate uncertain availabilities of compute resources and complete tasks successfully by their deadlines.

We model a computing environment where the compute resources are high performance computing (HPC) machines, and tasks submitted to this system are large-parallel jobs. An example of HPC resources being integrated together is the Extreme Science and Engineering Discovery Environment (XSEDE) program [69]. The environment may be heterogeneous, which means that each of the tasks may have different execution times on the different HPC

[4]A preliminary version of portions of the work mentioned in this chapter appeared in [68]. This work was supported by the National Science Foundation under grant number CNS-0905399, and by the Colorado State University George T. Abell Endowment.

machines. We assume that each submitted task has a reward, and that reward is earned if the task successfully completes before its deadline. In this chapter, we study the problem of assigning dynamically arriving tasks to machines to maximize the total reward earned in an environment where the machines may randomly fail. We design new heuristic techniques to solve this problem, and improve the performance of heuristics from the literature [70]. We study and analyze the performance of the different heuristics in a variety of environments that differ in their heterogeneity.

One method to achieve a certain level of fault-tolerance is to checkpoint tasks and restart them from their last checkpoint in case they encounter a failure. This is a common method used to alleviate the damage caused by the failure of resources [71–74] and we model our applications to have checkpointing.

In this simulation study, we use the analysis of failure data from real systems [75, 76] to model our machine time to failures and repair/recovery times. The work in [75] analyzes the failure data from the United States Los Alamos National Laboratory (LANL) comprising 22 HPC systems over the span of nine years (from 1996 to 2005) [77]. Similarly, the work in [76] analysis failure data from the Google cluster tracelog comprising 12,532 servers spanning a duration of 29 days starting May 2011 [78].

The contributions of this chapter are: (a) an enhancement in the prediction mechanism used in some of the heuristics from the literature [70], (b) multiple enhancements to the heuristics from the literature that are designed based on the concepts of the Derman-Lieberman-Ross theorem [79], (c) design of new heuristics for the problem of maximizing reward in heterogeneous environments, (d) an improved model of the system using the analyses from real-world machine failure and recovery data, and (e) a study of the performance of different heuristics on environments that differ in their types of heterogeneities.

The remainder of this chapter is organized as follows. Section 4.2 explains the model of our machines and workload. We formally state our resource allocation problem in Section 4.3. Section 4.4 explains the different heuristic techniques that we use to solve our problem, including our improvements to the heuristics from the literature and our new heuristics. Section 4.5 mentions our setup for the simulations. We analyze our experimental results in Section 4.6. Section 4.7 gives a sample of related work and we conclude this chapter in Section 4.8.

5.2. System Model

5.2.1. Modeling the Machines. We define a machine as a high performance computer. A task in this study is a large parallel application that can consume the resources on an entire HPC machine. Once a machine is assigned a task, it is considered unavailable and no other task can be assigned to it until it completes execution of that task or encounters a failure.

These large-scale machines are prone to failures. It has been shown that hardware is the biggest cause of failures in HPC environments compared to other causes e.g., software, network, environment [75]. Therefore, we focus on modeling and analyzing the impacts of hardware failures. It has been shown in the literature that exponential distributions can be used to approximate hardware failures [80–83]. In our environment, each machine has an exponential distribution associated with it to model the probability of failure. There are a total of M machines in the system. The failure rate for each machine j is λ_j.

Once a machine encounters a failure, it first needs to be repaired before any task can be assigned to it. Lognormal distributions have been found to be the best model for mean

time to repair values [75, 76]. For each machine j, we represent the mean and coefficient of variation of the lognormal repair time distribution by t_j^{repair} and COV_j^{repair}, respectively.

5.2.2. Modeling the Workload. In our oversubscribed environment, we assume that each task i has an associated reward r_i (representing the worth of the task) and a time to deadline Δd_i. Tasks in our environment dynamically arrive and the deadline of the task d_i is set based on the arrival time of the task a_i and Δd_i, i.e., $d_i = a_i + \Delta d_i$. The reward value of the task is earned if the task's computation is successfully completed by its deadline. We model our tasks to checkpoint their execution. If the machine on which the task is executing fails, the task is returned back to the pool of tasks (called the batch) that are waiting for a machine. If this task is remapped to a machine for execution, it resumes from its last checkpoint. The task can repeatedly cycle between execution and waiting in the batch as long as its deadline has not passed. Once its deadline expires, the task is discarded from the batch and cannot be assigned to a machine. This model of the life cycle of a task is very similar to the one described in [84].

In our environment, a mapping decision is made whenever a machine becomes available for executing a task. Machines become available in two cases: when they successfully complete a task that was assigned to them, or when they have encountered a failure and have returned after being repaired. Therefore, in our environment, machine availability triggers a mapping event and at the mapping event the resource manager has to decide which task from the batch should be assigned to that machine. The number of tasks in the batch is represented as T. T changes across the mapping events depending on the number of task arrivals and completions.

An Estimated Time to Compute (ETC) matrix is used to model the execution time characteristics of the various tasks in the heterogeneous system. We use task classes to group

together tasks that have the same execution time characteristics. Each entry t_{ij} in the ETC matrix gives the mean execution time of tasks of class i on machine j of our heterogeneous suite. The actual execution time of the tasks are modeled using exponential distributions with the means obtained from the entries of the ETC matrix. We use exponential distributions to model task completion times, based on the tests conducted at Ricoh InfoPrint [85]. For simulation purposes, we create and use synthetic workloads, but in real-world environments one could build such a matrix based on historical data or benchmarking experiments.

We test the performance of various resource allocation policies under different types of ETC matrices that represent some of the different types of heterogeneity of computing systems. We model five types of ETC matrices. Sample 3×3 ETC matrices for each of these types are shown in Figure 5.1. We model homogeneous workloads and homogeneous compute resources by having a fixed value for all the entries in the ETC matrix. We call this type of ETC matrix *constant*. We model another environment in which the workload can be considered homogeneous, but the compute resources have different computational capabilities. We model such an environment by having unique values for each of the columns of the ETC matrix, and refer to this matrix as *column-varying*. Similarly, an environment where the tasks are heterogeneous but the compute resources are completely homogeneous is represented by having unique values for each of the rows of the ETC matrix. We call such a matrix *row-varying*. A completely heterogeneous environment is modeled by having random values for each cell in the ETC matrix. In an environment, modeled by such a matrix, it is possible (and likely) for a machine to be better than another machine for a particular task class and worse for another. Such a matrix is referred to as *inconsistent*. If we independently sort the elements within each of the rows of such an *inconsistent* ETC, and then independently sort the entries in each of the columns, we obtain what we call a

constant	mach A	mach B	mach C
task class 1	4	4	4
task class 2	4	4	4
task class 3	4	4	4

column-varying	mach A	mach B	mach C
task class 1	5	2	4
task class 2	5	2	4
task class 3	5	2	4

row-varying	mach A	mach B	mach C
task class 1	4	4	4
task class 2	7	7	7
task class 3	2	2	2

inconsistent	mach A	mach B	mach C
task class 1	6	5	7
task class 2	9	3	4
task class 3	2	10	1

task-mach-consistent	mach A	mach B	mach C
task class 1	1	2	7
task class 2	3	4	9
task class 3	5	6	10

FIGURE 5.1. Sample ETC matrices modeling different types of heterogeneity in an environment with three task classes and three machines

task-mach-consistent matrix. In such an environment, if a machine executes a task faster than another machine, then it will do so for all tasks. Similarly, if a task executes faster than another task on a single machine, then it will do so on all machines.

We set the checkpoint time of a task based on the percentage of its execution that has completed. In this study, we set the tasks to checkpoint after every 5% of their execution. We checkpoint based on percent-complete (as opposed to checkpointing based on fixed time intervals) so that the periodicity of checkpointing is independent of the machine on which the task is running.

As mentioned previously, we assume that the task is large and parallelizable enough to use all the resources of a HPC machine. Once a task is assigned to a machine, the machine is not available for mapping. Also, we do not allow the pre-emption of tasks. The scheduling of

the dependencies of the different sub-parts of the large parallel task within a machine can be done separately using any Directed Acyclic Graph (DAG) scheduling technique. The entries in the ETC matrix represent the parallelized time of the tasks on the different machines including the time for checkpointing.

5.3. Problem Statement

We consider an oversubscribed environment where tasks are dynamically arriving. Once the task arrives, the scheduler knows the task's reward, deadline, and task class. Based on historical information, we assume we are given the ETC entries of the different task classes and machines, and the machines' mean times to failure and mean times to repair. The goal of our resource manager is to assign tasks to machines with the goal of maximizing the total reward earned by completing tasks before their respective deadlines.

5.4. Resource Allocation Policies

5.4.1. Overview. We use heuristics to solve the NP-complete resource management problem. We adapt some heuristics from the literature [70], modify and improve some of them, as well as design new ones.

Shestak et al. [70] have shown how a distribution of machine availability can be obtained using the average execution time of tasks on a machine j (referred to as $\underline{t_j^{av}}$), and the failure rate of the machine λ_j. This probability mass function consists of as many pulses as there are machines in the environment. In that work, the availability rate of each machine j, denoted by $\underline{w_j}$, is computed as

$$w_j = \lambda_j + \frac{e^{-\lambda_j t_j^{av}}}{t_j^{av}}. \tag{12}$$

We denote the probability of machine j being available for an assignment as p_j. We compute p_j by normalizing the w_j terms, i.e.,

$$p_j = \frac{w_j}{\sum_j w_j}. \tag{13}$$

The distribution created using these p_j values gives the normalized probability each machine j becomes available for a mapping event. In the environment in [70], machines become available for a mapping event under two scenarios: if they have encountered a failure (first term of the summation in Equation 12), or if they have successfully completed a task (second term of the summation in Equation 12). In that study, it was assumed that failed machines become operational immediately. The distribution sorts the machines in an ascending order of their "quality." A machine has better "quality" if it has a lower value for $\lambda_j t_j^{av}$. Therefore, a machine that has a lower failure rate and/or a lower value for mean execution time, is considered "better." The Cumulative Mass Function (CMF) of this probability distribution is used to guide resource allocation decisions by some heuristics.

As our environment has checkpointing for tasks and as we have machine recovery times, we modify the computation of the above terms to correctly represent our model. Let $perc_i^{remain}$ represent the remaining percentage of computation for task i. Therfore, a task i that has not been executed yet or that has no saved checkpoints would have a $perc_i^{remain}$ value equal 100%. To consider checkpointing when computing t_j^{av}, instead of simply taking the average of the ETC values for all the tasks in the batch on machine j, we take the average of $t_{ij} \times perc_i^{remain}$ over all tasks i in the batch. This considers the checkpointing of the tasks and accurately represents the average execution time of the tasks in the batch. To also include the recovery times, we modify the computation of the availability rate of a machine.

The first term used in computing w_j represents the rate at which the machine fails (λ_j). We want to replace that term with the rate at which the machine fails and subsequently recovers. Therefore, the modified equation for w_j is:

$$w_j = \frac{1}{\frac{1}{\lambda_j} + t_j^{repair}} + \frac{e^{-\lambda_j t_j^{av}}}{t_j^{av}}. \tag{14}$$

5.4.2. Heuristics from the Literature.

5.4.2.1. *Reward Heuristics.* The *Reward* and *Expected Reward* heuristics were introduced in [70]. In *Reward*, the task that has the highest value for reward is assigned to the machine that just became available.

For a task i at time t, $P_i(t)$ is the probability of successfully completing task i through multiple assignments before its deadline expires. The expected reward for a task i is given by the product $r_i P_i(t)$.

$V_i(t)$ is the estimated number of reassignments that task i may undergo starting at time t up to its deadline. The derivation of $V_i(t)$ is given in [70]. $P_i(t)$ is calculated using the equation shown below.

$$P_i(t) = 1 - \left(\sum_{j=1}^{M} p_j (1 - e^{-\lambda_j t_{ij}}) \right)^{V_i(t)} \tag{15}$$

The term $(1 - e^{-\lambda_j t_{ij}})$ gives the probability of task i failing on machine j. This factor is weighed by the probability of machine j being available for an assignment (p_j), and therefore the weighted sum, $\sum_{j=1}^{M} p_j (1 - e^{-\lambda_j t_{ij}})$, gives the probability of failure when task i is mapped to a machine. Therefore, Equation 15 represents the probability at time t that task i will successfully complete before its deadline, even through multiple assignments. In

the *Expected Reward* heuristic, the task with the highest value for expected reward is assigned to the machine that becomes available.

5.4.2.2. *Matching Heuristics.* There are two heuristics in [70] that use the concepts of the Derman-Lieberman-Ross (DLR) Theorem [79] to guide mapping decisions, the *Matching* heuristic and *Expected Matching* heuristic. A brief overview of the DLR theorem is given below, followed by the *Matching* heuristics that are implemented using the DLR concept.

The DLR theorem [79] provides an algorithm for optimally assigning a set of available workers to incoming jobs. Each incoming job is assumed to have a reward value associated with it. Each worker is assumed to have a probability (that represents the quality and skill of the worker), with which the reward earned for a job is scaled. We create a sorted list of workers in an ascending order of probability (i.e., skill). It is also assumed that one has the distribution from which the reward values for all the incoming jobs are sampled. This distribution lists the reward values of the jobs in an ascending order. Using the distribution of the reward values of the incoming jobs, and the notion of the skill of the workers (determined by their probabilities), the DLR method describes an algorithm that maps high reward jobs to more-skilled workers and low reward tasks to less-skilled workers. The distribution that represents the probabilities of different reward values for incoming jobs is vital to making these decisions. The algorithm partitions this distribution into bins of varying sizes. The number of bins created is equal to the number of workers left. The theorem creates the sizes of the bins depending on the shape of the distribution. When a job arrives, we find the bin number that has this job in the distribution. If it is the n^{th} bin, we choose the worker that is in the n^{th} position in our sorted list of workers. The chosen worker is then assigned to the arrived job. In this way, the DLR theorem matches the worth of arriving jobs to the quality of the workers.

The *Matching* heuristics [70] try to implement the DLR concept within the resource allocation problem. Jobs and workers in the DLR environment translate to machines and tasks in our environment, respectively. In our problem, machines become available, and tasks need to be chosen from a batch and assigned to them. This is analogous to jobs coming in and choosing a worker that can be assigned to them. The distribution described in Section 5.4.1 is used to describe the quality and the likelihood of the incoming machine, analogous to the distribution that governs the likelihood of various reward values for the incoming jobs. The only other factor that needs to be accounted for is the ranking of the tasks, analogous to the ranking of the workers (based on their probabilities). It is in this aspect that the *Matching* and the *Expected Matching* heuristics differ. In *Matching*, the tasks are sorted based on their reward values, whereas, in *Expected Matching*, the tasks are sorted based on their value of expected reward. As before, expected reward of a task i is given by the product $r_i P_i(t)$.

5.4.3. Modifications to Heuristics.

5.4.3.1. *Improved Computation for $P_i(t)$.* We modify Equation 15 to incorporate the knowledge of the machine that just became available for a mapping event. Let $\underline{J}$ be the machine that just became available. The probability that this machine will become available p_J will be 1, and by a similar logic $p_j = 0, \forall j \neq J$. Therefore, the summation term for this mapping event reduces to $(1 - e^{-\lambda_J t_{iJ}})$. We know that this counts as an assignment for task i, and therefore we extract the term $(1 - e^{-\lambda_J t_{iJ}})$ out, and reduce the count of the number of reassignments of task i (denoted by $V_i(t)$) by one. This gives us our new equation for $P_i(t)$:

$$P_i(t) = 1 - (1 - e^{-\lambda_J t_{iJ}}) \times \left(\sum_{j=1}^{M} p_j (1 - e^{-\lambda_j t_{ij}}) \right)^{V_i(t)-1}. \tag{16}$$

We use the updated computation of w_j mentioned in Equation 14 to consider checkpointing. Recall, w_j is used in the computation of p_j. To further consider the reduced computation needed by checkpointed tasks, we modify Equation 16 to the following:

$$P_i(t) = 1 - (1 - e^{-\lambda_J t_{iJ}}) \times \left(\sum_{j=1}^{M} p_j (1 - e^{-\lambda_j t_{ij} perc_i^{remain}}) \right)^{V_i(t)-1} \tag{17}$$

We use these updated versions of these heuristics when analyzing our results, i.e., they use Equation 17 for their expression of $P_i(t)$ instead of Equation 15. Considering the machine that just became available significantly improves the performance of the *Expected Reward* and *Expected Matching* heuristics.

5.4.3.2. *Oversubscription-awareness for Matching Heuristics.* There are multiple differences in our environment compared to that in the original DLR theorem that present difficult challenges. For one, in the DLR theorem, it is assumed that the number of arriving jobs equals the number of workers available. It is also assumed that once a worker is assigned to a job, the worker successfully completes the job and the job never returns. Therefore, the DLR environment is perfectly subscribed. When we examine the tasks that the Matching heuristics attempted to execute versus those that it did not get a chance to execute, we observe that tasks that were never mapped (because of the high oversubscription) were present across the whole range of reward values. As opposed to this, for the *Reward* heuristic, the tasks that were never mapped were present in the low-reward range. This happens because the *Matching* heuristics attempt to map good quality machines to high-ranked tasks and poor quality machines to low-ranked tasks. Recall that tasks can be ranked either in terms of reward or expected reward. Therefore, it is important to make the *Matching* heuristics aware of the level of oversubscription in the environment. This will allow the Matching heuristics to plan appropriately, and when the worst machine becomes available they can assign it a

task that is ranked reasonably as opposed to assigning the worst task. In other words, we do not want to partition the distribution into the number of tasks that are available in the system, but instead into the number of tasks that we can hope to finish (given that the system is oversubscribed). Let us call this the number of tasks that the heuristic should consider $\underline{T_{consider}}$. Then, from our sorted list of task rankings, we only include the $T_{consider}$ number of best tasks. Therefore, if the worst machine becomes available, the $T_{consider}$-worst task is assigned to it as opposed to the worst task.

We now explain our calculation of $T_{consider}$. Let $\widetilde{exec_i}$ denote the average execution time of task i across the M machines, calculated as:

$$\widetilde{exec_i} = \frac{\sum_{j=1}^{M} t_{ij} perc_i^{remain}}{M}. \tag{18}$$

Because we have checkpointing, even though the task may successfully complete its computation gradually through multiple assignments, $\widetilde{exec_i}$ is a good approximation of the total computation time it may need. Therefore, an estimate of the total computation time needed by the tasks in the batch, $\underline{compute\ time_{needed}}$, is computed by summing $\widetilde{exec_i}$ over all the tasks in the batch.

Let $\underline{\tilde{d}}$ be the average deadline of all tasks in the batch. Knowing the $\underline{current\ time}$, an estimate of the compute time available for successfully executing the tasks, $\underline{compute\ time_{available}}$, is computed as $compute\ time_{available} = (\tilde{d} - current\ time) \times M$.

An estimate of the percentage of tasks that the heuristic can hope to complete, $T_{consider}$, is obtained using the following computation:

$$T_{consider} = \frac{compute\ time_{available}}{compute\ time_{needed}} \times T. \tag{19}$$

If $T_{consider} > T$, then $T_{consider}$ is set to T. This ensures that we do not unreasonably create more bins than the number of tasks. If $T_{consider} < M$, then $T_{consider}$ is set to M. This is done so that there are at least as many bins as there are machines in the system. Without this step, the *Matching* heuristics might reduce to the *Reward* heuristics where only the best task (irrespective of the machine) is considered.

5.4.3.3. *Heterogeneity-awareness for Matching Heuristics.* The *Matching* heuristics rank machines in terms of their quality and the tasks based on either reward or expected reward. They then match good and bad quality machines to high and low ranked tasks, respectively. They do not consider individual performance of a task across different machines, i.e., they do not explicitly account for heterogeneity. We add heterogeneity-awareness to the *Matching* heuristics by allowing them to explore a neighborhood of bins as opposed to blindly picking the bin suggested by the DLR theorem. By examining the neighboring bins, the concept of the DLR is affected the least as the tasks in the neighboring bins will have very similar ranks compared to the chosen bin. We pick the bin among the neighbors that has the least execution time on the current machine. The execution times are calculated as the product of the ETC information and $perc_i^{remain}$.

It is important to control the number of bins that are designated as "neighbors." We consider two different techniques for selecting the designated number of neighbors: (1) using a fixed value, and (2) adaptively computing this value. The adaptive method estimates the number of neighboring bins by dividing the number of tasks being considered by the number of machines in the system. The motivation for such a computation is to define the size of

the neighborhood that changes based on the total number of tasks being considered and reduces the possibility of the neighborhood crossing over into the region that is designated for other machines. Another important aspect to control when defining the neighborhood is the direction in which to explore. We experiment with the following two cases: (1) neighbors are examined solely in the direction of improving ranks, and (2) neighbors are examined in both the directions of the chosen bin.

5.4.3.4. *Alternative Objectives.* The last modification we did to all the versions of the *Reward* and *Matching* heuristics is to experiment with using different objectives for which these heuristics greedily optimize by dividing the objective by the execution time or deadline of the task being considered for mapping. For example, the first modified version of the *Reward* heuristic would be called *Reward-per-time*, and if machine j is available for mapping, the heuristic selects the task i that has the highest value for the ratio: $r_i/(t_{ij}.perc_i^{remain})$. The other modified version of the *Reward* heuristic, called the *Reward-per-deadline* heuristic, would pick the task i that maximizes the ratio: $r_i/(d_i - current\ time)$. It is to be noted that the per-time versions account for the checkpointing and the per-deadline versions are technically per-time-to-deadline.

We similarly modify the objectives for the *Expected Reward* heuristic. For the *Matching*-based heuristics, doing a per-time version does not make sense as it would change the ranking of the tasks for each machine. Therefore, for the *Matching*-based heuristics, we only experiment with the per-deadline version.

5.4.4. New Heuristics.

5.4.4.1. *Min Exec Time-Max Reward Heuristic.* When a mapping event is triggered because of the availability of machine j, this heuristic picks the task i from the batch that has

the lowest value for $t_{ij}.perc_i^{remain}$. If there are ties, they are broken by picking the choice that earns the highest reward.

5.4.4.2. *Affinity Heuristic.* The *Affinity* heuristic tries to identify the "affinity" that may exist between certain task classes and heterogeneous machines in terms of execution time and gives preference for those allocations with high "affinity." It is motivated by the concept of the Task-Machine Affinity (TMA) [61] heterogeneity measure. TMA captures the degree to which certain tasks prefer certain unique machines (in terms of execution time). In highly heterogeneous environments such as the inconsistent environment, the TMA is typically high, whereas for a low heterogeneous environment (e.g., our column-varying environment), the TMA would be zero because the ranking of machines in terms of execution time would be identical for all the tasks (as opposed to being unique).

The *Affinity* heuristic examines the ETC matrix of an environment and computes the affinity information that is used when performing mapping decisions. The computation is best explained with an example ETC. Figure 5.2 shows a sample ETC matrix with five task classes and three machines. As shown in the figure, this information can be viewed in another way by graphing the machine entries for each task class on a time axis. For each task class c, we compute the mean value $\underline{\mu_c}$ and the standard deviation $\underline{\sigma_c}$ of its execution time entries across the machines in the ETC matrix. Then, for each machine, we compute the deviation of its execution time from the mean of each task class, i.e., for machine j executing task class c, the deviation $\underline{dev_{jc}}$ is computed as:

$$dev_{jc} = \frac{t_{cj} - \mu_c}{\sigma_c} \tag{20}$$

ETC	m1	m2	m3
t1	2	1	3
t2	7	3	4
t3	2	3	1
t4	1	6	4
t5	4	3	2

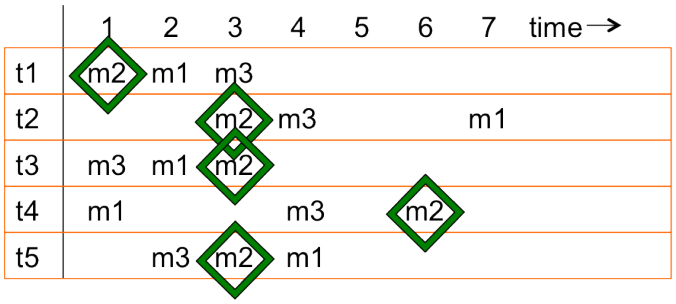

FIGURE 5.2. Representing the information from a sample ETC matrix in a way that highlights the computation of the affinity information for machine 2 (m2) for the *Affinity* heuristic

A low value for dev_{jc} shows that machine j and task class c have a high affinity. dev_{jc} can also be negative. Then, for each machine j the entries dev_{jc} are sorted across all the task classes. We then store this sorted list of task classes for machine j as its affinity information. A similar computation is performed for all the machines. As this computation only uses the ETC information, it can be precomputed offline.

For the example system showed in Figure 5.2, we highlight machine 2 across the different task classes. Intuitively, we want to say that machine 2 has the highest affinity to task class 2 because not only does it perform the best among all the machines for task class 2 (which it also does for task class 1), but it does so by a bigger margin, i.e., on task class 2 there is a bigger spread of execution times, and therefore there would be a bigger loss if task class 2 was assigned to some other machine (compared to the loss if task class 1 was assigned to some other machine). This is captured by our affinity computation. For machine 2, the affinity information computed would have the task classes in the following order: t2, t1, t5, t3, t4. It is important to note that even though machine 2 had the same execution time for task classes 2, 3, and 5, their affinity values are very different, and that it did not matter that task class 1 has the least execution time on it.

At a mapping event, the *Affinity* heuristic considers only a subset of the tasks in the batch. We experiment with 50% and 20%. The subset is created by considering task classes in the order mentioned in this machine's affinity information. For each task class (considered in order), all the tasks in the batch that belong to that task class are added to the subset. When the subset has more than the required percentage of the tasks from the batch, we stop adding tasks to it. After finding this subset of tasks that have the highest affinity to our current machine, we pick from them the task that maximizes a desired objective. The different objectives we experimented with are: reward, reward-per-time, reward-per-deadline, expected reward, expected reward-per-time, and expected reward-per-deadline.

The affinity information computed for each machine are compared with each other and if they are completely identical (which means there is no affinity in the system), then irrespective of the percentage set, the heuristic considers all the tasks in the batch. This happens when we have ETC types: constant, column-varying, or row-varying. In these cases, the *Affinity* heuristic reduces to a version of the *Reward* heuristic (because it considers all the tasks).

5.5. Simulation Setup

We model a system that has 25 HPC machines. In [75], one system was shown to have an average time between failure around 8.5 to 14 hours. As mentioned in [75], there is a very large variance in mean time between failure values across machines with some being as low as 7.5 hours to others going up to 516 hours. Therefore, we select the average fail time of machines from a uniform probability in the range [8, 80] hours. We use exponential distributions for modeling the hardware failure times of machines. Exponential distributions have been used to stochastically approximate failure times [80–83].

It has been shown that lognormal distributions provide the best model for recovery or repair times of machines [75, 76]. From [76], we calculate the weighted sum of the mean times to repair to obtain a mean value of 5.22 hours. We observe that this is consistent with the values of time to repair in [75] when considering the system on average for the years after the first year. Therefore, we pick the mean repair times of the machines in the range: [2, 5] hours. From [76], the weighted coefficient of variation is 3.6325. In [75], it is mentioned that within a system, the data of repair times tend to be well approximated by exponential distributions. Exponential distributions have a coefficient of variation of 1. As we have a different repair time distributions for each machine in our system, we wanted to capture this fact and have less variance. Therefore, for each machine the coefficient of variation is selected in the range: [1.1, 3.6325].

We modeled different ETC matrices, as described in Section 5.2.2. As [75] mentioned, these HPC systems are used for executing long running jobs. Therefore, we set the execution times of the jobs in the range: [6, 360] hours.

There are 30 task classes that any of the incoming tasks will belong to. The tasks arrive in a bursty arrival pattern. The reward values of the tasks are selected randomly (with uniform probability) in the range: [1, 100]. The Δd_i for a task i was set in the range [3, 7] times the average execution time of that task on any machine. As mentioned before, the tasks checkpoint after every 5% of their total computation. The number of tasks that arrive was set differently for the different types of ETC environments with the goal of keeping the system oversubscribed. The following are the number of tasks that arrived for each ETC type:

- constant ETC: 800 tasks
- column-varying ETC: 1,200 tasks

- row-varying ETC: 1,200 tasks
- inconsistent ETC: 2,500 tasks
- task-mach-consistent ETC: 1,200 tasks

5.6. Experimental Results and Analysis

As different ETC types model completely different environment types, it serves to only compare the relative performance of the heuristics with each other within the various ETCs, as opposed to comparing the absolute performance of a heuristic across the ETC types. For each result shown, we experiment with 48 scenarios and present the average and 95% confidence interval bars of these scenarios. For each scenario, different values were used for the following: entries of the ETC matrix, reward values of the tasks, arrival times of the tasks, deadline times of the tasks, task to task class mapping, fail rates and recovery times of the machines.

Among the many different versions of the *Matching* heuristics, Figures 5.3 and 5.4 show the best cases among these variations. The results from the other ETC types show similar trends. Shown in these figures are (in order): *Matching*, *Matching* while accounting oversubscription, *Matching* that examines a neighborhood of 15 bins in both directions (for a total of 30 bins), *Expected Matching*, *Expected Matching* while accounting oversubscription, *Expected Matching* that examines a neighborhood of 30 bins in the direction of increasing task ranks, and *Expected Matching* that examines a neighborhood of an adaptive number of bins in the direction of increasing task ranks while also accounting for oversubscription. Examining neighbors significantly helps in the inconsistent environment, but does not help that much in the column-varying environment. This is because in the column-varying environment, all the tasks have the same execution time and a neighbor is chosen only if its

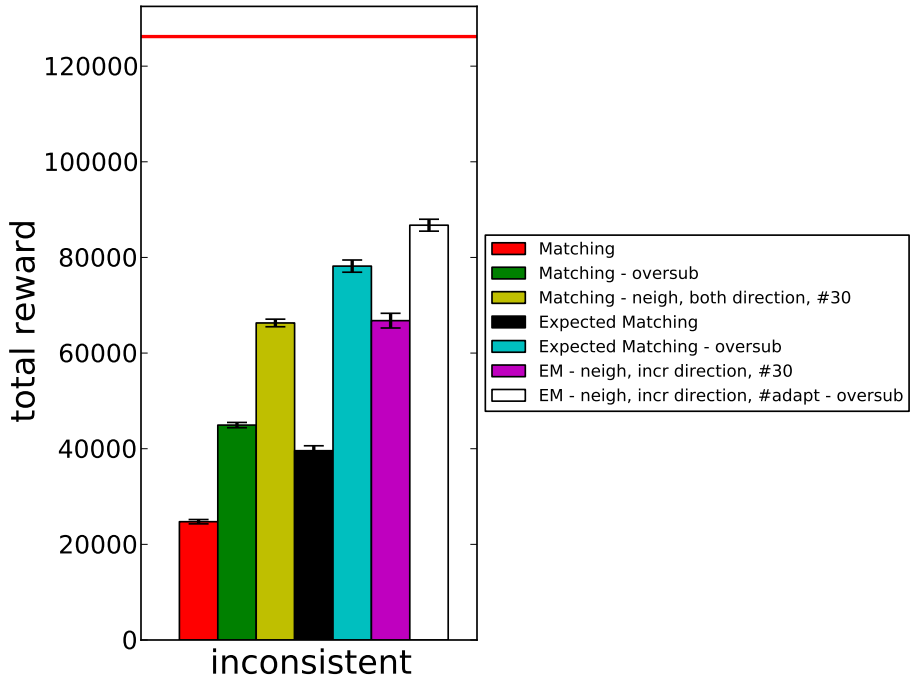

FIGURE 5.3. Total reward earned by the best versions of the *Matching* and *Expected Matching* heuristics with the inconsistent type of ETC. The red horizontal line shows the bound on the maximum reward that could possibly be earned.

$perc^{remain}$ is lower. Accounting for oversubscription significantly improves the performance of the *Matching* heuristics. In the inconsistent environment, the heuristic variation that performs both techniques (i.e., accounting oversubscription and examining neighbors) performs the best. This highlights the non-overlapping benefits of these two techniques to improve the performance of the *Matching* heuristics.

The best case of the *Affinity* heuristic was obtained when 50% of the tasks from the batch were considered, and the reward-per-time objective was used. We now plot the performance of all the best case heuristics together to contrast their performance.

Figures 5.5 and 5.6 show the performance of the best cases of the heuristics in the inconsistent and task-mach-consistent type of ETC matrices. The other ETC types show similar types of trends. We experimented with many heuristic versions. In this section,

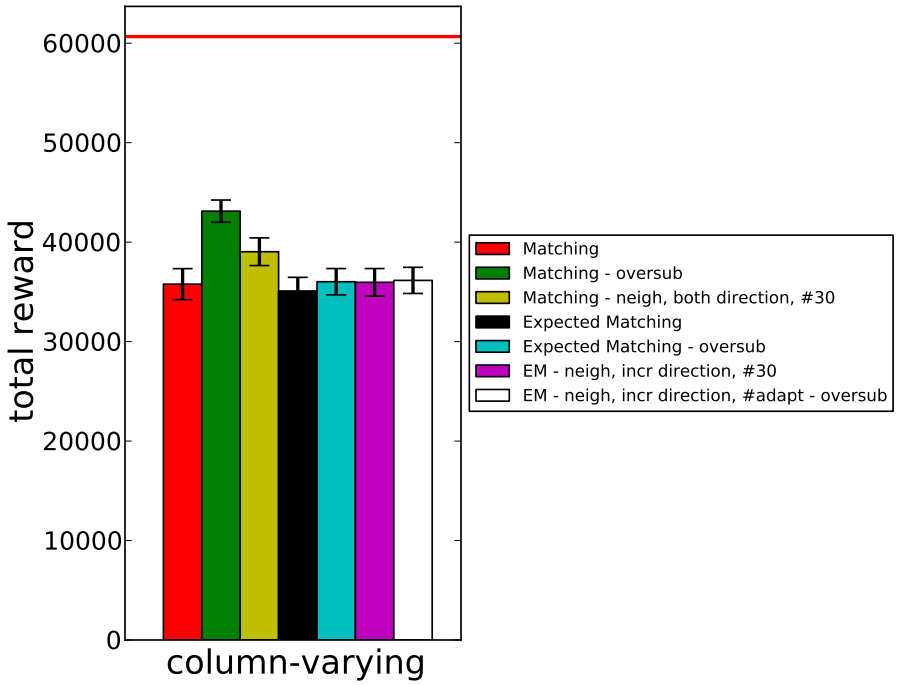

FIGURE 5.4. Total reward earned by the best versions of the *Matching* and *Expected Matching* heuristics with the column-varying type of ETC. The red horizontal line shows the bound on the maximum reward that could possibly be earned.

we show the results for the cases that performed the best across all ETC types. For the *Reward* heuristic, using *Reward-per-time* as its objective provided the best results as it considers a task's execution time in addition to the reward. For the *Expected Reward* heuristic variants, using *Expected-Reward-per-time* and *Expected-Reward-per-deadline* performed best depending on the environment. The *Reward-per-time* and the *Affinity* heuristics perform the best across the different ETC types, except in the task-machine-consistent type of ETC environment, where the *Reward-per-time* heuristic beats the *Affinity* heuristic.

The *Min Exec Time-Max Reward* heuristic performs well in the inconsistent environment but does not perform as well in the task-mach-consistent environment as it considers the tasks in their execution order first, i.e., first completes all the tasks that belong to the task class that has the least execution time and then considers the other task classes.

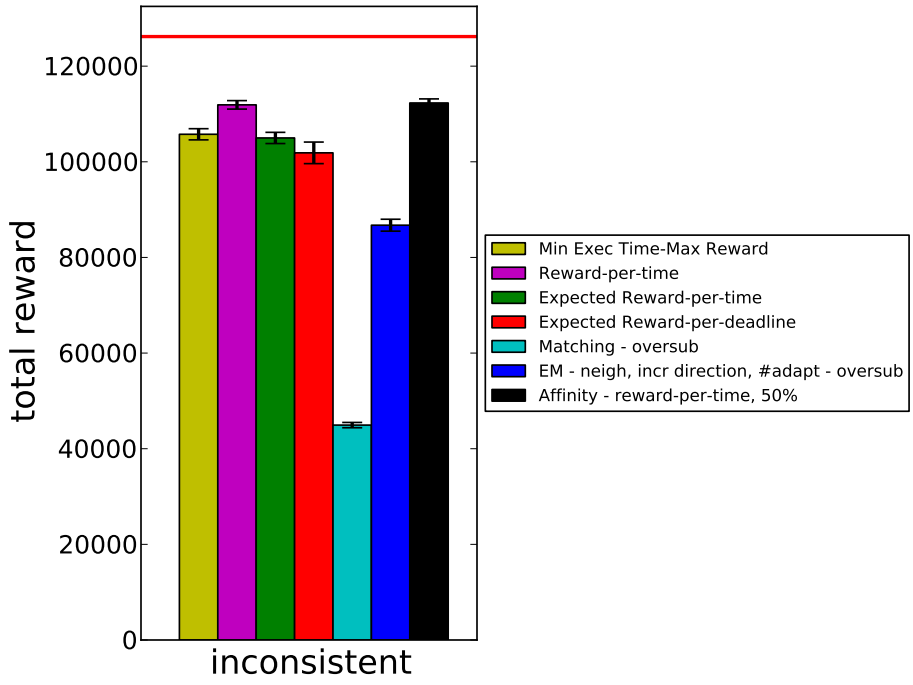

FIGURE 5.5. Total reward earned by the best versions of the different heuristics with the inconsistent type of ETC. The red horizontal line shows the bound on the maximum reward that could possibly be earned.

The *Matching* heuristics perform very poorly in the inconsistent environment. This is because in such an environment it is very hard for the *Matching* heuristics to accurately rank machines in terms of their performance.

5.7. Related Work

The scheduling problem has been widely studied in heterogeneous computing environments (eg., [11, 20, 22]). It is important to make the resource allocations be fault tolerant, especially in HPC and distributed computing environments. Various techniques have been used to cope with the ill-effects of failures of compute resources. Checkpointing and roll-back recovery are common techniques used to avoid having to restart failed tasks from the beginning (e.g., [71–74]). Another method used to improve the reliability of the system, in

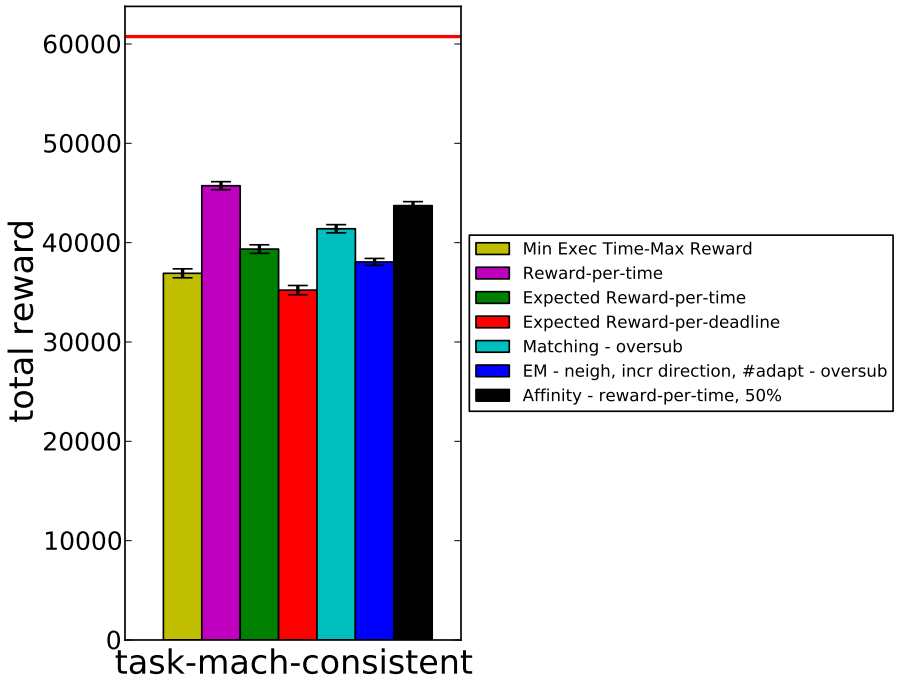

FIGURE 5.6. Total reward earned by the best versions of the different heuristics with the task-mach-consistent type of ETC. The red horizontal line shows the bound on the maximum reward that could possibly be earned.

terms of increasing the chances of completing tasks, is to run replicas of the tasks on multiple compute resources (e.g., [86, 87, 74, 88]).

Shestak et al. [70] addressed the problem of maximizing the reward earned by the tasks in an oversubscribed environment where the compute nodes may randomly fail. Their work used the concepts of a theorem introduced by Derman et al. [79]. Our study builds on the work done in [70] by significantly expanding the model, improving heuristics' performance, and designing new heuristics. There have been other works on scheduling that look at maximizing reward earned by the tasks [4], but they do not model environments where the machines tend to fail.

5.8. Conclusions

The goal of this study was to model an environment where large, parallel tasks are assigned for execution on HPC machines (with high failure rates) and to design resource management techniques that maximize the total reward that can be earned by completing tasks before their deadlines expire. We design two heuristics to solve this problem, and significantly improve the performance of heuristics from the literature. Particularly, we improve the performance of the *Matching* heuristics by enhancing them to include awareness of the oversubscription and awareness of the heterogeneity in the system. We also improve the prediction mechanism of the expected reward computation by using the latest information about the system. We model the machine failure and recovery characteristics based on the analyses of real-world data from [75, 76]. We simulated and tested all of our heuristic variations under a variety of ETC types. Our results show that the best performance is obtained by the *Reward-per-time* and the *Affinity* heuristics. Future directions for this research are mentioned in Chapter 6.

CHAPTER 6

Future Work

One direction for future work for extending the study mentioned in Chapter 2 is to use stochastic estimates of execution time to more closely model a real environment and to analyze the tolerance of the resource management policies to such uncertainties. It would also be interesting if a model of expected arrival time of tasks could be obtained from historical data to create a global scheduling problem, where the dropping threshold could be varied dynamically throughout the day based on the expected system load. To broaden the scope of this study, we could introduce utility functions that do not have to be monotonically-decreasing. It would help to develop heuristics that take the utility-functions' slopes into consideration to guide their resource allocation decisions. Introducing parallel jobs (that require multiple machines concurrently to execute) and permitting pre-emption of tasks would also broaden the scope of this work.

There are many possible directions for future work for the study mentioned in Chapter 3. We could implement the tecnique to drop tasks that will generate negligible utility when they complete. Incorporating dynamic voltage and frequency scaling capabilities of processors would make this research more applicable. Adapting the bi-objective genetic algorithm to be used as a heuristic in an online (dynamic) method could lead to an innovation in this field. It would also help to compare the NSGA-II to another bi-objective algorithm. We could also explore a multi-objective genetic algorithm by defining and maximizing robustness in addition to optimizing for performance and energy. We could explore the island model of the genetic algorithm in detail and see how that applies to our environment.

The work in Chapter 5 can be extended in many ways. It would also be interesting to modify the workload to have tasks whose reward values degrade with time, instead of having a fixed reward value until a hard deadline. We would also like to improve the failure model by using Weibull distributions instead of exponential distributions. It would be useful to run additional experiments with a variety of environments to study which heuristics perform the best in which environments.

Bibliography

[1] M. R. Gary and D. S. Johnson, *Computers and Intractability: A Guide to the Theory of NP-Completeness*. W. H. Freeman and Co., 1979.

[2] J. Koomey, "Growth in data center electricity use 2005 to 2010," *Analytics Press*, Aug. 2011.

[3] B. Khemka, R. Friese, L. D. Briceño, H. J. Siegel, A. A. Maciejewski, G. A. Koenig, C. Groer, G. Okonski, M. M. Hilton, R. Rambharos, and S. Poole, "Utility functions and resource management in an oversubscribed heterogeneous computing environment," *IEEE Transactions on Computers*, accepted to appear pending minor revisions.

[4] L. D. Briceño, B. Khemka, H. J. Siegel, A. A. Maciejewski, C. Groer, G. Koenig, G. Okonski, and S. Poole, "Time utility functions for modeling and evaluating resource allocations in a heterogeneous computing systems," in *20th Heterogeneity in Computing Workshop (HCW 2011), in IPDPS 2011*, May 2011, pp. 7–19.

[5] E. Jensen, C. Locke, and H. Tokuda, "A time-driven scheduling model for real-time systems," in *Int'l Real-Time Systems Symp.*, Dec. 1985, pp. 112–122.

[6] B. Ravindran, E. D. Jensen, and P. Li, "On recent advances in time/utility function real-time scheduling and resource management," in *Int'l Symp. on Object-Oriented Real-Time Distributed Computing (ISORC 2005)*, May 2005, pp. 55–60.

[7] K. Chen and P. Muhlethaler, "A scheduling algorithm for tasks described by time value function," *J. of Real-Time Systems*, vol. 10, no. 3, pp. 293–312, May 1996.

[8] M. Kargahi and A. Movaghar, "Performance optimization based on analytical modeling in a real-time system with constrained time/utility functions," *IEEE Trans. on Computers*, vol. 60, no. 8, pp. 1169–1181, Aug. 2011.

[9] C. B. Lee and A. E. Snavely, "Precise and realistic utility functions for user-centric performance analysis of schedulers," in *Int'l Symp. on High Performance Distributed Computing (HPDC '07)*, 2007, pp. 107–116.

[10] J.-K. Kim, H. J. Siegel, A. A. Maciejewski, and R. Eigenmann, "Dynamic resource management in energy constrained heterogeneous computing systems using voltage scaling," *IEEE Trans. on Parallel and Distributed Systems*, vol. 19, no. 11, pp. 1445–1457, Nov. 2008.

[11] M. Maheswaran, S. Ali, H. J. Siegel, D. Hensgen, and R. F. Freund, "Dynamic mapping of a class of independent tasks onto heterogeneous computing systems," *J. of Parallel and Distributed Computing*, vol. 59, no. 2, pp. 107–121, Nov. 1999.

[12] B. D. Young, J. Apodaca, L. D. Briceo, J. Smith, S. Pasricha, A. A. Maciejewski, H. J. Siegel, B. Khemka, S. Bahirat, A. Ramirez, and Y. Zou, "Deadline and energy constrained dynamic resource allocation in a heterogeneous computing environments," *J. of Supercomputing*, vol. 63, no. 2, Feb. 2013.

[13] H. Barada, S. M. Sait, and N. Baig, "Task matching and scheduling in heterogeneous systems using simulated evolution," in *Int'l Heterogeneity in Computing Workshop (HCW 2001), in IPDPS 2001*, Apr. 2001, pp. 875–882.

[14] M. K. Dhodhi, I. Ahmad, and A. Yatama, "An integrated technique for task matching and scheduling onto distributed heterogeneous computing systems," *J. of Parallel and Distributed Computing*, vol. 62, no. 9, pp. 1338–1361, Sep. 2002.

[15] A. Ghafoor and J. Yang, "A distributed heterogeneous supercomputing management system," *IEEE Computer*, vol. 26, no. 6, pp. 78–86, Jun. 1993.

[16] M. Kafil and I. Ahmad, "Optimal task assignment in heterogeneous distributed computing systems," *IEEE Concurrency*, vol. 6, no. 3, pp. 42–51, Jul. 1998.

[17] A. Khokhar, V. K. Prasanna, M. E. Shaaban, and C. Wang, "Heterogeneous computing: Challenges and opportunities," *IEEE Computer*, vol. 26, no. 6, pp. 18–27, Jun. 1993.

[18] D. Xu, K. Nahrstedt, and D. Wichadakul, "QoS and contention-aware multi-resource reservation," *Cluster Computing*, vol. 4, no. 2, pp. 95–107, Apr. 2001.

[19] C. M. Krishna and K. G. Shin, *Real-Time Systems*. McGraw-Hill, 1997.

[20] T. D. Braun, H. J. Siegel, N. Beck, L. Boloni, R. F. Freund, D. Hensgen, M. Maheswaran, A. I. Reuther, J. P. Robertson, M. D. Theys, and B. Yao, "A comparison of eleven static heuristics for mapping a class of independent tasks onto heterogeneous distributed computing systems," *J. of Parallel and Distributed Computing*, vol. 61, no. 6, pp. 810–837, Jun. 2001.

[21] L. D. Briceño, H. J. Siegel, A. A. Maciejewski, M. Oltikar, J. Brateman, J. White, J. Martin, and K. Knapp, "Heuristics for robust resource allocation of satellite weather data processing onto a heterogeneous parallel system," *IEEE Trans. on Parallel and Distributed Systems*, vol. 22, no. 11, pp. 1780–1787, Nov. 2011.

[22] V. Shestak, J. Smith, H. J. Siegel, and A. A. Maciejewski, "Stochastic robustness metric and its use for static resource allocations," *J. of Parallel and Distributed Computing*, vol. 68, no. 8, pp. 1157–1173, Aug. 2008.

[23] P. Sugavanam, H. J. Siegel, A. A. Maciejewski, M. Oltikar, A. Mehta, R. Pichel, A. Horiuchi, V. Shestak, M. Al-Otaibi, Y. Krishnamurthy, S. Ali, J. Zhang, M. Aydin, P. Lee, K. Guru, M. Raskey, and A. Pippin, "Robust static allocation of resources for independent tasks under makespan and dollar cost constraints," *J. of Parallel and Distributed Computing*, vol. 67, no. 4, pp. 400–416, Apr. 2007.

[24] I. Al-Azzoni and D. G. Down, "Linear programming-based affinity scheduling of independent tasks on heterogeneous computing systems," *IEEE Trans. on Parallel and Distributed Systems*, vol. 19, no. 12, pp. 1671–1682, Dec. 2008.

[25] J.-K. Kim, S. Shivle, H. J. Siegel, A. A. Maciejewski, T. Braun, M. Schneider, S. Tideman, R. Chitta, R. B. Dilmaghani, R. Joshi, A. Kaul, A. Sharma, S. Sripada, P. Vangari, and S. S. Yellampalli, "Dynamically mapping tasks with priorities and multiple deadlines in a heterogeneous environment," *J. of Parallel and Distributed Computing*, vol. 67, no. 2, pp. 154–169, Feb 2007.

[26] S. Ghanbari and M. R. Meybodi, "On-line mapping algorithms in highly heterogeneous computational grids: A learning automata approach," in *Int'l Conf. on Information and Knowledge Technology (IKT '05)*, May 2005.

[27] Q. Ding and G. Chen, "A benefit function mapping heuristic for a class of meta-tasks in grid environments," in *Int'l Symp. on Cluster Computing and the Grid (CCGRID '01)*, May 2001, pp. 654–659.

[28] K. Kaya, B. Ucar, and C. Aykanat, "Heuristics for scheduling file-sharing tasks on heterogeneous systems with distributed repositories," *J. of Parallel and Distributed Computing*, vol. 67, no. 3, pp. 271–285, Mar. 2007.

[29] S. Shivle, H. J. Siegel, A. A. Maciejewski, P. Sugavanam, T. Banka, R. Castain, K. Chindam, S. Dussinger, P. Pichumani, P. Satyasekaran, W. Saylor, D. Sendek, J. Sousa, J. Sridharan, and J. Velazco, "Static allocation of resources to communicating subtasks in a heterogeneous ad hoc grid environment," *J. of Parallel and Distributed Computing*, vol. 66, no. 4, pp. 600–611, Apr. 2006.

[30] M. Wu and W. Shu, "Segmented min-min: A static mapping algorithm for meta-tasks on heterogeneous computing systems," in *Int'l Heterogeneity in Computing Workshop (HCW 2000), in IPDPS 2000*, Mar. 2000, pp. 375–385.

[31] F. Berman, R. Wolski, H. Casanova, W. Cirne, H. Dail, M. Faerman, S. Figueira, J. Hayes, G. Obertelli, J. Schopf, G. Shao, S. Smallen, S. Spring, A. Su, and D. Zagorodnov, "Adaptive computing on the grid using AppLeS," *IEEE Trans. on Parallel and Distributed Systems*, vol. 14, no. 4, pp. 369–382, Apr. 2003.

[32] H. Casanova, A. Legrand, D. Zagorodnov, and F. Berman, "Heuristics for scheduling parameter sweep applications in grid environments," in *Int'l Heterogeneity in Computing Workshop (HCW 2000), in IPDPS 2000*, Mar. 2000, pp. 349–363.

[33] M. Snir and D. A. Bader, "A framework for measuring supercomputer productivity," *Int'l J. of High Performance Computing Applications*, vol. 18, no. 4, pp. 417–432, Nov. 2004.

[34] P. Li, B. Ravindran, H. Cho, and E. D. Jensen, "Scheduling distributable real-time threads in Tempus middleware," in *Int'l Conf. on Parallel and Distributed Systems (ICPADS '04)*, 2004, pp. 187–194.

[35] P. Li, B. Ravindran, S. Suhaib, and S. Feizabadi, "A formally verified application-level framework for real-time scheduling on POSIX real-time operating systems," *IEEE Trans. on Software Engineering*, vol. 30, no. 9, pp. 613–629, Sep. 2004.

[36] S. Ali, H. J. Siegel, M. Maheswaran, D. Hensgen, and Sa. Ali, "Representing task and machine heterogeneities for heterogeneous computing systems," *Tamkang J. of Science and Engineering*, vol. 3, no. 3, pp. 195–207, Nov. 2000.

[37] R. Friese, B. Khemka, A. A. Maciejewski, H. J. Siegel, G. A. Koenig, S. Powers, M. Hilton, J. Rambharos, G. Okonski, and S. W. Poole, "An analysis framework for

investigating the trade-offs between system performance and energy consumption in a heterogeneous computing environments," in *22nd Heterogeneity in Computing Workshop (HCW 2013), in the proceedings of the IPDPS 2013 Workshops & PhD Forum (IPDPSW)*, May 2013, pp. 19–30.

[38] Environmental Protection Agency, "Report to congress on server and data center energy efficency," http://www.energystar.gov/ia/partners/prod_development/downloads/EPA_Datacenter_Report_Congress_Final1.pdf, Aug. 2007.

[39] R. Friese, T. Brinks, C. Oliver, H. J. Siegel, and A. A. Maciejewski, "Analyzing the trade-offs between minimizing makespan and minimizing energy consumption in a heterogeneous resource allocation problem," in *The 2nd International Conference on Advanced Communications and Computation (INFOCOMP 2012)*, Oct. 2012, p. 9 pp.

[40] K. Deb, A. Pratap, S. Agarwal, and T. Meyarivan, "A fast and elitist multiobjective genetic algorithm: NSGA-II," *IEEE Transactions on Evolutionary Computation*, vol. 6, no. 2, pp. 182–197, Apr. 2002.

[41] J. J. Dongarra, E. Jeannot, E. Saule, and Z. Shi, "Bi-objective scheduling algorithms for optimizing makespan and reliability on heterogeneous systems," in *The 19th Annual ACM Symposium on Parallel Algorithms and Architectures (SPAA '07)*, 2007, pp. 280–288.

[42] E. Jeannot, E. Saule, and D. Trystram, "Bi-objective approximation scheme for makespan and reliability optimization on uniform parallel machines," in *The 14th International Euro-Par Conference on Parallel Processing (Euro-Par '08)*, vol. 5168, 2008, pp. 877–886.

[43] B. Abbasi, S. Shadrokh, and J. Arkat, "Bi-objective resource-constrained project scheduling with robustness and makespan criteria," *Applied Mathematics and Computation*, vol. 180, no. 1, pp. 146–152, 2006.

[44] J. Pasia, R. Hartl, and K. Doerner, "Solving a bi-objective flowshop scheduling problem by Pareto-ant colony optimization," in *Ant Colony Optimization and Swarm Intelligence*, vol. 4150, 2006, pp. 294–305.

[45] Y. He, F. Liu, H.-j. Cao, and C.-b. Li, "A bi-objective model for job-shop scheduling problem to minimize both energy consumption and makespan," *Journal of Central South University of Technology*, vol. 12, pp. 167–171, Oct. 2005.

[46] J. Apodaca, D. Young, L. Briceno, J. Smith, S. Pasricha, A. A. Maciejewski, H. J. Siegel, S. Bahirat, B. Khemka, A. Ramirez, and Y. Zou, "Stochastically robust static resource allocation for energy minimization with a makespan constraint in a heterogeneous computing environment," in *9th IEEE/ACS International Conference on Computer Systems and Applications (AICCSA '11)*, Dec. 2011, pp. 22–31.

[47] B. D. Young, J. Apodaca, L. D. Briceo, J. Smith, S. Pasricha, A. A. Maciejewski, H. J. Siegel, B. Khemka, S. Bahirat, A. Ramirez, and Y. Zou, "Deadline and energy constrained dynamic resource allocation in a heterogeneous computing environments," *The Journal of Supercomputing*, vol. 63, no. 2, pp. 326–347, Feb. 2013.

[48] J. Teich, "Hardware/software codesign: The past, the present, and predicting the future," *Proceedings of the IEEE*, vol. 100, no. 13, pp. 1411–1430, 2012.

[49] (accessed: 07/24/2012) Intel core i7 3770k power consumption, thermal. [Online]. Available: http://openbenchmarking.org/result/1204229-SU-CPUMONITO81#system_table

[50] A. M. Al-Qawasmeh, A. A. Maciejewski, H. Wang, J. Smith, H. J. Siegel, and J. Potter, "Statistical measures for quantifying task and machine heterogeneities," *J. of Supercomputing*, vol. 57, no. 1, pp. 34–50, July 2011.

[51] M. G. Kendall, *The Advanced Theory of Statistics*. Charles Griffin and Company Limited, 1945, vol. 1.

[52] V. Pareto, *Cours d'economie politique*. Lausanne: F. Rouge, 1896.

[53] O. H. Ibarra and C. E. Kim, "Heuristic algorithms for scheduling independent tasks on non-identical processors," *J. of the ACM*, vol. 24, no. 2, pp. 280–289, Apr. 1977.

[54] B. Khemka, R. Friese, S. Pasricha, A. A. Maciejewski, H. J. Siegel, G. A. Koenig, S. Powers, M. Hilton, R. Rambharos, and S. Poole, "Utility maximizing dynamic resource management in an oversubscribed energy-constrained heterogeneous computing system," *Sustainable Computing (SUSCOM) Special Issue on Energy Aware Resource Management and Scheduling (EARMS)*, accepted to appear pending minor revisions.

[55] ——, "Utility driven dynamic resource management in an oversubscribed energy-constrained heterogeneous system," in *23rd Heterogeneity in Computing Workshop (HCW 2014), in the proceedings of the IPDPS 2014 Workshops & PhD Forum (IPDPSW)*, May 2014, pp. 58–67.

[56] P. Bohrer, E. N. Elnozahy, T. Keller, M. Kistler, C. Lefurgy, C. McDowell, and R. Rajamony, "The case for power management in web servers," in *Power Aware Computing*, ser. Series in Computer Science, R. Graybill and R. Melhem, Eds. Springer US, 2002.

[57] I. Rodero, J. Jaramillo, A. Quiroz, M. Parashar, F. Guim, and S. Poole, "Energy-efficient application-aware online provisioning for virtualized clouds and data centers," in *International Green Computing Conference*, Aug 2010, pp. 31–45.

[58] M. P. Mills. The Cloud Begins With Coal - Big Data, Big Networks, Big Infrastructure, and Big Power. Digital Power Group. [Online]. Available: http://www.tech-pundit.com/wp-content/uploads/2013/07/Cloud_Begins_With_Coal.pdf

[59] 2012 DatacenterDynamics Industry Census. [Online]. Available: http://www.datacenterdynamics.com/blogs/industry-census-2012-emerging-data-center-markets

[60] D. J. Brown and C. Reams, "Toward energy-efficient computing," *Communications of the ACM*, vol. 53, no. 3, pp. 50–58, Mar. 2010.

[61] A. M. Al-Qawasmeh, A. A. Maciejewski, R. G. Roberts, and H. J. Siegel, "Characterizing task-machine affinity in heterogeneous computing environments," in *20th Heterogeneity in Computing Workshop (HCW 2011), in the proceedings of the IPDPS 2011 Workshops & PhD Forum (IPDPSW)*, May 2011, pp. 33–43.

[62] Colorado State University ISTeC Cray High Performance Computing Systems. [Online]. Available: http://istec.colostate.edu/activities/cray

[63] H. Singh and A. Youssef, "Mapping and scheduling heterogeneous task graphs using genetic algorithms," in *Int'l Heterogeneity in Computing Workshop (HCW 1996), in IPDPS 1996*, Apr. 1996, pp. 86–97.

[64] Z. Jinquan, N. Lina, and J. Changjun, "A heuristic scheduling strategy for independent tasks on grid," in *Int'l Conf. on High-Performance Computing in Asia-Pacific Region*, Nov. 2005.

[65] Y. Tian, E. Ekici, and F. Ozguner, "Energy-constrained task mapping and scheduling in wireless sensor networks," in *IEEE Mobile Adhoc and Sensor Systems Conference*, Nov. 2005, p. 8.

[66] K. H. Kim, R. Buyya, and J. Kim, "Power aware scheduling of bag-of-tasks applications with deadline constraints on DVS-enabled clusters," in *IEEE/ACM International Symposium of Cluster Computing and the Grid (CCGrid 2007)*, 2007, pp. 541–548.

[67] R. Friese, T. Brinks, C. Oliver, A. A. Maciejewski, H. J. Siegel, and S. Pasricha, "A machine-by-machine analysis of a bi-objective resource allocation problems," in *The 2013 International Conference on Parallel and Distributed Processing Techniques and Applications (PDPTA 2013)*, July 2013, pp. 3–9.

[68] B. Khemka, A. A. Maciejewski, and H. J. Siegel, "A performance comparison of resource allocation policies in distributed computing environments with random failures," in *2012 International Conference on Parallel and Distributed Processing Techniques and Applications (PDPTA 2012), sponsor: World Academy of Science and Computer Science Research, Education, and Applications (CSREA)*, Jul. 2012, pp. 3–9.

[69] Extreme science and engineering discovery environment (xsede). [Online]. Available: https://www.xsede.org/

[70] V. Shestak, E. K. P. Chong, A. A. Maciejewski, and H. J. Siegel, "Probabilistic resource allocation in heterogeneous distributed systems with random failures," *Journal of Parallel and Distributed Computing*, vol. 72, no. 10, pp. 1186–1194, Oct. 2012.

[71] R. Koo and S. Toueg, "Checkpointing and rollback-recovery for distributed systems," *IEEE Transactions on Software Engineering*, vol. SE-13, no. 1, pp. 23–31, Jan. 1987.

[72] D. Manivannan, "Checkpointing and rollback recovery in distributed systems: existing solutions, open issues and proposed solutions," in *Proceedings of the 12th International Conference on Systems*. World Scientific and Engineering Academy and Society (WSEAS), 2008, pp. 569–574.

[73] B. Nazir, K. Qureshi, and P. Manuel, "Adaptive checkpointing strategy to tolerate faults in economy based grid," *The Journal of Supercomputing*, vol. 50, pp. 1–18, 2009.

[74] Y. Zhang, A. Mandal, C. Koelbel, and K. Cooper, "Combined fault tolerance and scheduling techniques for workflow applications on computational grids," in *Proceedings of the 9th IEEE/ACM International Symposium on Cluster Computing and the Grid (CCGRID '09)*, 2009, pp. 244–251.

[75] B. Schroeder and G. A. Gibson, "A large-scale study of failures in high-performance computing systems," *IEEE Transactions on Dependable and Secure Computing*, vol. 7, no. 4, pp. 337–350, Oct 2010.

[76] P. Garraghan, P. Townend, and J. Xu, "An empirical failure-analysis of a large-scale cloud computing environment," in *2014 IEEE 15th International Symposium on High-Assurance Systems Engineering (HASE)*, Jan 2014, pp. 113–120.

[77] Operational data to support and enable computer science research. Los Alamos National Laboratory. [Online]. Available: http://institutes.lanl.gov/data/fdata/

[78] Google cluster data v2. Google. [Online]. Available: http://code.google.com/p/googleclusterdata/wiki/ClusterData2011_1

[79] C. Derman, G. J. Lieberman, and S. M. Ross, "A sequential stochastic assignment problems," *Management Science*, vol. 18, no. 7, pp. 349–355, Mar. 1972.

[80] J. Abawajy, "Fault-tolerant scheduling policy for grid computing systems," in *Proceedings of the 18th International Parallel and Distributed Processing Symposium (IPDPS'04)*, Apr 2004, pp. 238–244.

[81] C. E. Ebeling, *Introduction to Reliability and Maintainability Engineering.* Waveland Pr Inc, 2005.

[82] M. Rausand and A. Hyland, *System Reliability Theory: Models, Statistical Methods, and Applications*. Wiley-Interscience, 2008.

[83] X. Kong, C. Lin, Y. Jiang, W. Yan, and X. Chu, "Efficient dynamic task scheduling in virtualized data centers with fuzzy prediction," *Journal of Network and Computer Applications*, vol. 34, no. 4, pp. 1068–1077, July 2011, advanced Topics in Cloud Computing. [Online]. Available: http://www.sciencedirect.com/science/article/pii/S1084804510000998

[84] C. Reiss, J. Wilkes, and J. L. Hellerstein, "Google cluster-usage traces: format + schema," *Google Inc., White Paper*, 2011.

[85] Ricoh InfoPrint. [Online]. Available: http://www.infoprint.com/internet/ipww.nsf/vwWebPublished/print-infoprint-5000-en

[86] Y. Oh and S. Son, "Scheduling real-time tasks for dependability," *The Journal of the Operational Research Society*, vol. 48, no. 6, pp. 629–639, Jun. 1997.

[87] A. Litke, D. Skoutas, K. Tserpes, and T. Varvarigou, "Efficient task replication and management for adaptive fault tolerance in mobile grid environments," *Future Generation Computer Systems*, vol. 23, no. 2, pp. 163–178, Feb. 2007.

[88] Q. Zheng, B. Veeravalli, and C.-K. Tham, "On the design of fault-tolerant scheduling strategies using primary-backup approach for computational grids with low replication costs," *IEEE Transactions on Computers*, vol. 58, pp. 380–393, Mar. 2009.

APPENDIX A

Permuting Initial Virtual-Queue Tasks

For the batch-mode heuristics, we experiment with an additional technique to modify the ordering of the tasks that are at the head of the virtual queue of the machines. The motivation for doing this is to take advantage of the following situation: consider that there are two tasks, with one having a utility function that starts at a higher utility value but decays very slowly (marked as "1" in Fig. A.1), whereas the other task's utility function starts at a relatively lower utility, but has a quick decay occurring very soon (marked as "2" in Fig. A.1). The utility maximizing heuristics may schedule task 1 ahead of task 2 when assigning them to a machine. In this scenario, higher overall utility may be earned by switching the execution order because the loss in utility from task 1's delayed execution might be less than the gain in utility from the earlier completion of task 2.

To capture this benefit, once the batch-mode heuristic has made its resource allocation decisions, we try all permutations of the two, three, or five initial tasks within the virtual queue of each machine. For each machine, the ordering that earns the highest utility from the three tasks is chosen. We use a dropping threshold of 0.5 to perform our experiments with the permuting operation because it explicitly does not drop tasks of certain priority levels. There was no significant difference in the performance of the batch-mode heuristics with the permuting operation.

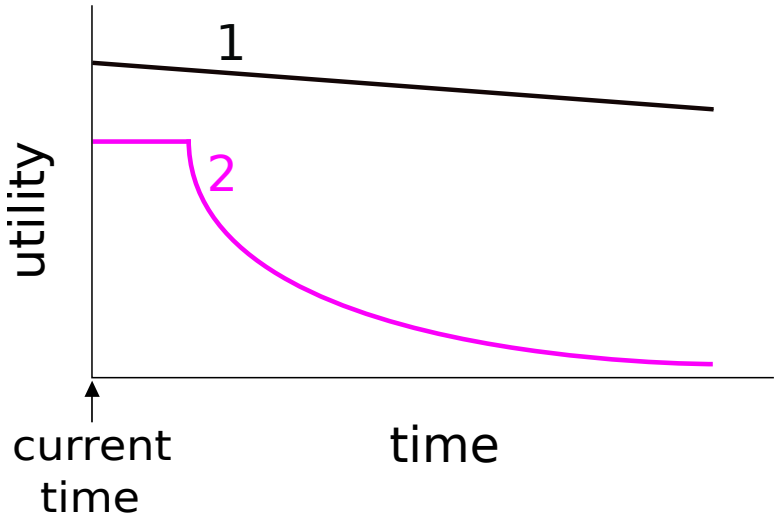

FIGURE A.1. Though task 2 has lower utility than task 1, there might be benefit in scheduling it before task 1.

APPENDIX B

Calculating Duration of the First Interval

To make the starting utility value of each task realizable, this utility value persists for some time before it starts to decay. If this is not done, even if the task starts execution as soon as it arrives on the machine that can complete it the soonest, it will not be possible to obtain the task's maximum utility value. For our simulation studies, the length of time for which the starting utility value of the task persists is dependent on the urgency level of the task and its average execution time across the machine types. We compute for each task the average execution time of that task across the machine types (ignoring machine types that cannot execute it). We scale this average value by a factor dependent on the urgency level of the task. If the task is an *extreme* urgency task, then we scale the average execution time of this task by 80% to obtain the length of its first interval. For *high*, *medium*, and *low* urgency levels, we scale the average value by 90%, 100% (no scaling), and 110%, respectively.

APPENDIX C

Values of the Utility Classes

As mentioned in Sec. 2.2.1.2, a utility class has three parameters associated with each interval (except the first). The values of the three parameters used to create the four utility classes that we model in this study are given Table C.1. The utility of all utility classes drops to zero 10,000 minutes after their first interval has completed.

Table C.1. Values of the three parameters for the different intervals (except the first) of the four utility classes that we model in this study. τ is the arrival time of the task and F is the duration of the first interval.

Utility Class	**Parameter**	$k = 2$	$k = 3$	$k = 4$	$k = 5$	$k = 6$	$k = 7$
A	$t(k, A)$	$\tau + F$	$\tau + F + 5$	$\tau + F + 10$	$\tau + F + 20$	$\tau + F + 30$	$\tau + F + 10000$
	$\psi(k, A)$	100%	60%	30%	20%	10%	0%
	$\delta(k, A)$	1.1	1.15	1.2	1.1	1.2	10
B	$t(k, B)$	$\tau + F$	$\tau + F + 7$	$\tau + F + 15$	$\tau + F + 22.5$	$\tau + F + 30$	$\tau + F + 10000$
	$\psi(k, B)$	100%	50%	25%	12%	5%	0%
	$\delta(k, B)$	0.9	0.9	0.9	0.9	0.9	10
C	$t(k, C)$	$\tau + F$	$\tau + F + 10$	$\tau + F + 20$	$\tau + F + 30$	$\tau + F + 40$	$\tau + F + 10000$
	$\psi(k, C)$	100%	75%	50%	25%	12%	0%
	$\delta(k, C)$	0.9	0.85	0.85	0.8	0.8	10
D	$t(k, D)$	$\tau + F$	$\tau + F + 12.5$	$\tau + F + 25$	$\tau + F + 37$	$\tau + F + 50$	$\tau + F + 10000$
	$\psi(k, D)$	100%	80%	66%	33%	11%	0%
	$\delta(k, D)$	1.2	1.1	1.1	0.9	0.9	10

APPENDIX D

Joint Probability Distribution of Priority and Urgency Levels

To generate the priority and urgency levels for the tasks, we use a joint probability distribution represented by the matrix shown in Table D.1. This table is representative of DOE/DoD environments. The matrix models an environment where the probability of a task having *critical* priority and *low* urgency is zero. Similarly, *extreme* and *high* urgency tasks are unlikely to have *low* priority. Most of the tasks have *medium* and *low* priorities with *medium* and *low* urgencies. A few important tasks have *critical* and *high* priorities with *extreme* and *high* urgencies. The results in Sec. 2.7 show that the timely execution of the *critical* priority tasks (approximately 4% of the tasks) significantly contributes to the total utility earned by the system. For each task, we sample from this joint probability distribution to obtain the task's priority and urgency levels.

Table D.1. The joint probability distribution of tasks having certain priority and urgency levels

priority levels	**urgency levels**			
	extreme	***high***	***medium***	***low***
critical	2%	2%	0.05%	0%
high	3.45%	5%	1.5%	3%
medium	0%	10%	10%	10%
low	0%	0%	20%	33%

APPENDIX E

Simulation Parameters for Generating Estimated Time to Compute (ETC) Matrices

To generate the entries of the ETC matrix, we adopt the Coefficient of Variation (COV) method [36] to our environment. The mean value of execution time on the general-purpose and the special-purpose machine types is set to ten minutes and one minute, respectively. The coefficient of variation along the task types is set to 0.1. The coefficient of variation along the special-purpose machine types is also set to 0.1, whereas the coefficient of variation along the general-purpose machine types is set to 0.25. This models heterogeneity in the ETC matrix [36]. To represent the fact that some task types are incapable of executing on some of the special-purpose machine types, we set the corresponding entries of the matrix to infinity. Table E.1 shows a sample ETC matrix with only four machine types and only four task types. Among the four machine types, machine types A and B are modeled as special-purpose machine types. Each of them has one task type that is special on them.

Across the different simulation trials, the actual number of machines for each machine type is constant, but the properties of the machine types varies. The partitioning of the 100 machines into the 13 machine types is as follows: 2, 2, 3, 3, 5, 5, 5, 10, 10, 10, 10, 15, and 20. The first four machine types in this list are the special-purpose machine types. So, in all we have 10 special-purpose machines. This distribution of the number of machines across the machine types is chosen based on the expectations for future environments of DOE and DoD interest.

TABLE E.1. A sample ETC matrix with only four machine types and only four task types showing the execution times in minutes. Machine types A and B are special-purpose machine types (task types 1 and 2, respectively, are special on them). All other task types are incompatible on the special-purpose machine types. In the table, "spl" is used to denote a special-purpose task/machine type and "gen" is used to denote a general-purpose task/machine type.

	machine type A (spl)	**machine type B (spl)**	**machine type C (gen)**	**machine type D (gen)**
task type 1 (spl)	1.1	∞	13	9
task type 2 (spl)	∞	0.9	8	11
task type 3 (gen)	∞	∞	10	12
task type 4 (gen)	∞	∞	12	9

APPENDIX F

Generation of Task Arrivals for Simulations

The arrival patterns used are based on the expectations for future environments of DOE and DoD interest. For the general-purpose task types, we use a sinusoidal pattern for the arrival rate. We set the frequency of the sinusoidal curve by specifying the number of complete sinusoidal cycles to occur during the 24 hour period. For each general-purpose task type, we randomly select an integer from 1 to 24 with uniform probability to obtain the number of sinusoidal cycles. We do not use fractions because the integers ensure that at the start and end of the 24 hour period (i.e., end of the 2^{nd} and end of the 26^{th} hour), the arrival rates are equal. This is important because the arrival pattern models a day and, the end of the 2^{nd} and the 26^{th} hour correspond to the same time of the day. The phase-shift of the sinusoidal curve is randomly sampled from the range 0 to 2π using uniform probability. The amplitude is calculated by multiplying an amplitude factor and the mean arrival rate. The amplitude factor of the curve is sampled randomly from the range 0.25 to 0.9. Using this technique, each general-purpose task type has its own arrival rate pattern. Fig. F.1 shows example sinusoidal arrival rate patterns (with dashed lines showing their mean arrival rates) for five general-purpose task types.

For the special-purpose task types, we use a "bursty" arrival rate pattern. The pattern consists of two types of alternating intervals for the arrival rate: baseline interval and the burst interval. The baseline intervals have a lower arrival rate and a longer duration than the burst intervals. For each baseline interval, the arrival rate is obtained by multiplying the mean arrival rate (computed as mentioned before) with a number sampled uniformly at random from the range [0.5, 0.75]. In contrast, for the burst interval the range from

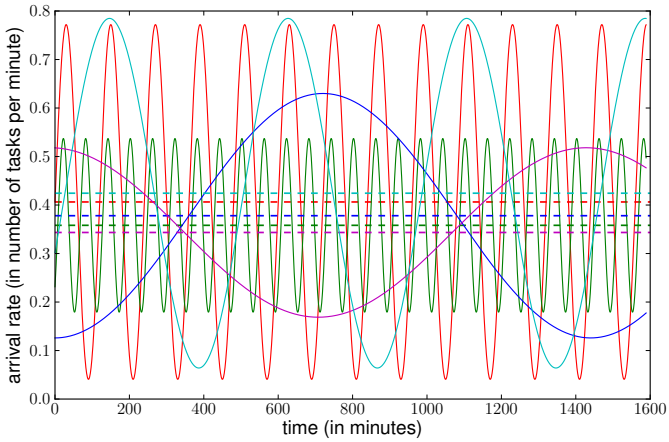

FIGURE F.1. Example sinusoidal curves that model the arrival rate for the general-purpose task types. Curves for five general-purpose task types are shown with dashed lines representing their mean arrival rates.

which the random number is sampled is [1.25, 1.5]. The duration of each baseline interval is obtained by sampling uniformly at random from the range [3, 5] hours, whereas for each burst interval the range is [30, 90] minutes. To ensure that the arrival rate of the 2^{nd} and 26^{th} hour remain the same, we make sure that the duration of the interval that was present just before the end of the 2^{nd} hour is repeated just before the end of the 26^{th} hour. Fig. F.2 shows example arrival rate patterns for five special-purpose task types with their mean arrival rate shown using dashed lines.

Once we have an arrival rate pattern for every task type, we step along the curve to generate the arrival times of the different tasks that will belong to this task type. We start with the arrival rate at the beginning of each curve. We sample an exponential distribution with the rate to get a time duration. We step along the curve based on the sampled time duration value and generate the arrival time of the next task (of this type). We keep repeating the process until the end of the 26^{th} hour. This generates not only the arrival times but also generates the number of tasks that belong to that task type. In regions where the arrival rate is higher, the sampled time from the exponential distribution is lower, and therefore the

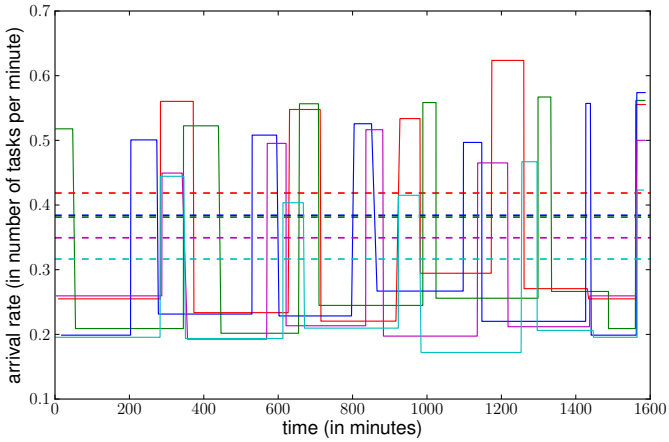

FIGURE F.2. Step-shaped curves that model the baseline and burst periods of arrival rates for the special-purpose task types. Example curves for five special-purpose task types are shown with dashed lines representing their mean arrival rates.

arrival time of the next task is closer to the current task's arrival time. If the arrival rate is very low for some part of the arrival rate curve, then the time value sampled from the exponential distribution might be too long. This may prevent any further sampling for this task type. To avoid such cases, each time we sample from the exponential distribution, if the sampled next arrival time of a task is greater than a pre-set upper limit, then we set the next arrival time to that upper limit value. For our simulations we set the upper limit to $1/50^{th}$ of the 24 hour duration, i.e., $24 \times 60/50 = 28.8$ minutes. Fig. F.3 shows the number of tasks that arrive in a minute (including both general-purpose and special-purpose) from a single simulation trial.

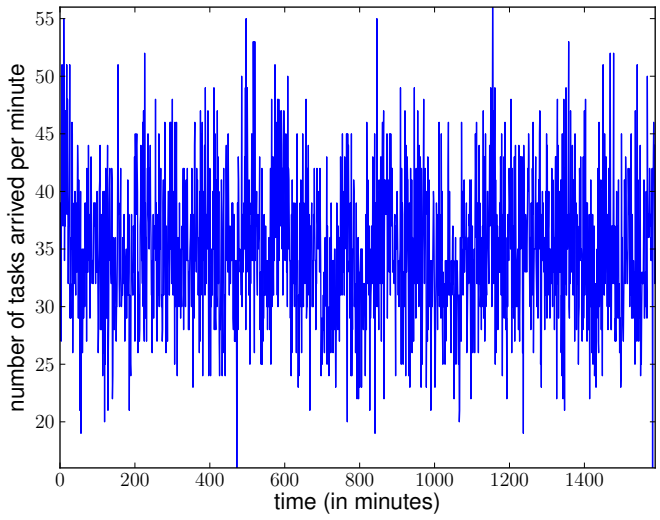

FIGURE F.3. An example trace of the number of tasks (both general-purpose and special-purpose) that arrive per minute as a function of time. We generate the arrival of tasks for a duration of 26 hours.

APPENDIX G

Results from 33,000 Tasks per Day Oversubscription Level

Fig. G.1 shows the results with the dropping operation for all the heuristics when we had 33,000 tasks arrive in the day. The two notable differences between the percentage of maximum utility earned by the heuristics in the 33,000 tasks per day case as opposed to the 50,000 tasks per day case are that all the heuristics are able to earn a higher percentage of maximum utility (because the environment is not as oversubscribed), and the batch-mode heuristics do not have as much of an increase in performance with the dropping operation (because even with the no dropping case, on average only 32% of mapping events were delayed due to excessive heuristic execution times).

Table G.1 gives the average execution time of the mapping events for the heuristics with a dropping threshold of 0.5. These times include the execution time for the heuristic and the dropping operation.

Table G.1. Average execution time of the mapping events for all the heuristics with a dropping threshold of 0.5 for the two levels of oversubscription.

heuristic	**mapping event execution time (in milliseconds)**	
	33,000 tasks per day	**50,000 tasks per day**
Random	0.14	0.15
Round-Robin	0.14	0.15
Max Util	0.20	0.22
Max UPT	0.30	0.33
MET-Random	0.20	0.22
MET-Max Util	0.20	0.22
Min-Min Comp	9.76	46.66
Sufferage	57.32	280.09
Max-Max Util	51.64	316.47
Max-Max UPT	64.2	319.61
MET-Max Util-Max UPT	23.68	66.22

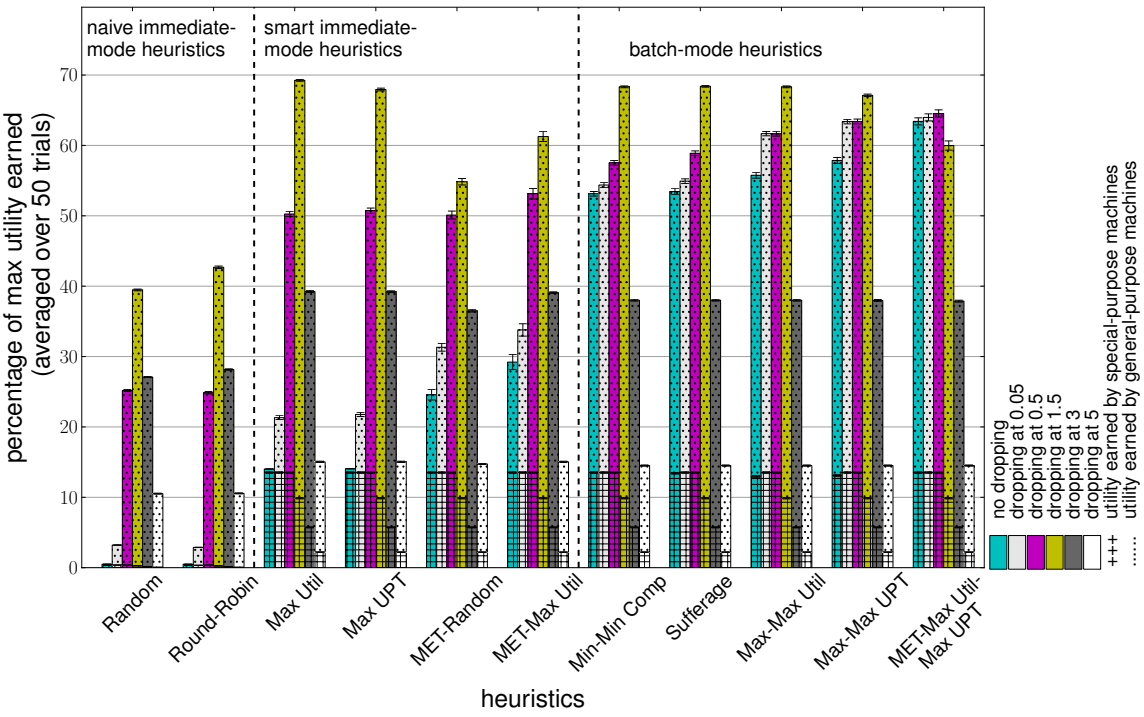

FIGURE G.1. Percentage of maximum utility earned by all the heuristics for the different dropping thresholds with an oversubscription level of 33,000 tasks arriving during the day. The average maximum utility bound for this oversubscription level is 65,051.

APPENDIX H

Discussion of Additional Results

We performed experiments with the maximum utility values for the priority levels set at 1000, 100, 10, and 1 instead of 8, 4, 2, and 1, respectively. The dropping thresholds that we used in that case were: 500, 50, 5, 0.5, 0.05, and 0.005. We observed that the utility being earned in those cases was controlled to a large extent by the timely execution of the *critical* priority tasks. A significant amount of utility could be earned even if all tasks except the *critical* priority tasks were dropped. This is because with the priorities set at 1000, 100, 10, and 1, it takes ten *high* priority tasks to equal the benefit of one *critical* priority task, as opposed to two *high* priority tasks in our current model with priorities set at 8, 4, 2, and 1. These latter priority values better match the intended environment.